

XII-th INTERNATIONAL CONFERENCE

on

ION IMPLANTATION AND OTHER APPLICATIONS OF IONS AND ELECTRONS



**June 18-21, 2018
Kazimierz Dolny, Poland**

Edited by
Janusz Filiks and Jerzy Żuk

The Market Square in Kazimierz Dolny drawn by Artur Orłowski

ISBN: ??????????

CHAIRPERSONS

Jerzy Żuk – chairman, Maria Curie-Skłodowska University

Paweł Żukowski – co-chairman, Lublin University of Technology

Jerzy Zdanowski – co-chairman, Wrocław University of Technology

INTERNATIONAL SCIENTIFIC COMMITTEE

V.M. Anishchik (Belarus)

R.L. Boxman (Israel)

P. Budzyński (Poland)

J. Jagielski (Poland)

F.F. Komarov (Belarus)

Z.W. Kowalski (Poland)

F. Nickel (Germany)

A.D. Pogrebnjak (Ukraine)

W. Skorupa (Germany)

B. Słowiński (Poland)

L. Thomé (France)

A. Tuross (Poland)

Z. Werner (Poland)

K. Wieteska (Poland)

LOCAL ORGANIZING COMMITTEE

J. Filiks (Secretary – Maria Curie-Skłodowska University)

A. Drożdżel (Maria Curie-Skłodowska University)

T. Kołtunowicz (Lublin University of Technology)

K. Pysznik (Maria Curie-Skłodowska University)

V.A. Skuratov (Joint Institute for Nuclear Research)

M. Turek (Maria Curie-Skłodowska University)

CONTENTS

INVITED LECTURE

I-1	<i>Barcz Adam</i> , Ion Irradiation of SiC and GaN: One Technique for Different Purposes	15
I-2	<i>Budzyński P., Kamiński M., Pysznik K., Wiertel M.</i> , Long-range effect of ion-implanted materials in tribological investigations	16
I-3	<i>Fedotov A.K., Fedotova J.A., Streltsov E.A., Żukowski P., Kottunowicz T.N., Kalinin Yu.E., Evtukh A.A.</i> , Development of improved ion-beam technologies for preparation of nanocomposite heterostructures with tunable electric and magnetic properties	18
I-4	<i>Gaiduk P.I.</i> , Self-organized nano-voids in irradiated SiGe/Si hetero-structures for plasmonic application	20
I-5	<i>Jagielski Jacek, Thomé Lionel, Chartier Alain, Mieszczynski Cyprian, Jozwik Iwona, Dorosh Orest.</i> , Damage accumulation studies in irradiated oxides: current status and new perspectives	21
I-6	<i>Komarov F.F., Konstantinov S.V., Pilko V.V., Pogrebnjak A.D.</i> , Structure, tribomechanical properties and radiation tolerance of nanostructured (TiHfZrVNb)N coatings	22
I-7	<i>Krügener Jan, Haase Felix, Peibst Robby, Osten H.-J.</i> , Ion implantation for photovoltaic applications: Review and outlook for silicon solar cells.....	23
I-8	<i>Krzyżanowska Halina, Baydin A., Feldman L.C., Tolk N.H.</i> , Depth dependent optical and elasto-optical effects of ion implantation studied by time-domain Brillouin scattering	24
I-9	<i>Lerch Wilfried, Niess Jürgen</i> , Advancement in Ion Implantation Annealing from Seconds to Milliseconds.....	25
I-10	<i>Horodek P., Khilinov V., Kobets A., Meshkov I., Orlov O., Siemek K., Sidorin A.A.</i> , Development of Positron Annihilation Spectroscopy at Joint Institute for Nuclear Research	26
I-11	<i>Neethling J.H., Janse van Vuuren A., Olivier E.J.</i> , HAADF STEM Imaging of Dislocation Loops in Irradiated GaAs	28
I-12	<i>Prucnal Sławomir</i> , Towards group IV semiconductor laser	29
I-13	<i>Rubel M., Petterson P., Moon S.W., Fortuna E., Krawczynska A., Widdowson A.</i> , Mirrors for plasma plasma diagnosis in reactors of controlled thermonuclear fusion: Ion-induced damage and ion beam analyses.....	30
I-14	<i>Sartowska B., Barlak M., Konarski P.</i> , Ions in materials testing.....	31
I-15	<i>Scheit A., Lenke T., Heinemann B., Rücker H., Wolansky D., Skorupa W., Schumann T., Rebohle L., Häberlein Sven</i> , Millisecond Flash Lamp Annealing and Application for SiGe-HBT.....	32
I-16	<i>Shvetsov V.N.</i> , Neutron Physics at the Joint Institute for Nuclear Research	33
I-17	<i>Skuratov V.A., Dauletbekova A., Kirilkin N., Akylbekov A., Seitbayev A., Teterev Yu.G., Zdorovets M.</i> , High energy ionoluminescence of oxide and alkali halide crystals	34

I-18	<i>Tan Yang</i> , Enhanced out-of-plane charge-transfer on a monolayer TMDCs by controlled defect creation: Optical Evidences in Heterostructure and Application for SERS	35
I-19	<i>Zimek Z.</i> , Radiation processing of polymers and semiconductors by electron beam.....	36

ORAL PRESENTATION

O-1	<i>Alontseva D.L.</i> Microplasma deposition of biocompatible coatings using an intelligent robotic system for plasma processing.....	39
O-2	<i>Horodek P.</i> , The Long Range Effect Detection by Positron Lifetime Experiments.....	40
O-3	<i>Kislitsin S., Ivanov I., Zdorovets M., Larionov A.</i> , Radiation Effects in TiNbN Coatings Induced by Impact of Low-Energy Helium, Krypton and Xenon Ions	41
O-4	<i>Konarski P., Miśnik M., Ażgin J., Zawada A.</i> , Recent developments in SIMS and GD-MS, two analytical techniques used for surface analysis	42
O-5	<i>Kulik M., Kołodyńska D.E., Przewłocki H.M., Hubicki Z., Żuk J., Pyszniak K.</i> , Optical properties and chemical composition of transition layers formed by irradiation of multilayer TiO ₂ /SiO ₂ samples with Ne ⁺ , Ar ⁺ , Kr ⁺ and Xe ⁺ ions	43
O-6	<i>Lee M.E., O'Connell J.H., Skuratov V.A.</i> , Observation of stabilized tetragonal latent tracks induced by single SHI impacts in monoclinic natural zirconia at room temperature	44
O-7	<i>Olejniczak A., Nebogatikova N.A., Kulik M., Skuratov V.A.</i> , Swift Heavy-Ion Irradiation of graphene oxide: localized reduction and formation of sp-hybridized carbon atomic wires	45
O-8	<i>Pelc Andrzej, Pieńkos Tomasz</i> , Low energy electron attachment to PtBr ₂ molecules.....	46
O-9	<i>Słowiński B.</i> , Longitudinal electromagnetic cascades in heavy amorphous segmented materials.....	47
O-10	<i>Szala Mirosław, Dudek Agata, Maruszczuk Andrzej, Walczak Mariusz, Chmiel Jarosław</i> , Effect of TiO ₂ -NiAl plasma sprayed coatings thickness on cavitation erosion, sliding and abrasive wear resistance	48
O-11	<i>Turek Marcin, Drożdźiel Andrzej, Pyszniak Krzysztof, Luchowski Rafał, Grudziński Wojciech</i> , Modification of PET polymer foil by Na ⁺ implantation	49
O-12	<i>Vuuren Arno Janse, Skuratov Vladimir, Ibraeva Anel, Zdorovets Maxim</i> , Microstructural Effects of Al Doping on Si ₃ N ₄ Irradiated with Swift Heavy Ions.....	50
O-13	<i>Yastrubchak O., Gluba L., Żuk J., Tataryn N., Drożdźiel A., Grudziński W., Turek M., Mamykin S., Borkovska L., Kolomys O., Sadowski J.</i> , Optical Properties of Mn and Bi Ion Implanted and Low Temperature MBE – doped GaAs Layers	51

YOUNG SCIENTISTS CONTEST
ORAL PRESENTATIONS

YSC-1	<i>Berencén Y., Prucnal S., Möller W., Hübner R., Rebohle R., Böttger R., Glaser M., Schönherr T., Yuan Y., Wang M., Georgiev Y.M., Erbe A., Lugstein A., Helm M., Zhou S., Skorupa W.,</i> Intermediate-band silicon nanowires realized by ion beam hyperdoping	55
YSC-2	<i>Czarnacka Karolina, Koltunowicz Tomasz N., Makhavikou Maxim, Parkhomenko Irina, Komarov Fadei,</i> Electrical and optical properties of SiO ₂ thin layers implanted with Zn ions	57
YSC-3	<i>Fedotov A.S., Rusak D., Koltunowicz T.N., Zukowski P., Fedotova J.A., Kasiuk J.V., Ronassi Ali Arash,</i> “Negative Capacitance” Effect in Nanogranular Composite Films (Fe ₄₅ Co ₄₅ Zr ₁₀) _x (SiO ₂) _(100-x) Prepared by Ion-Beam Technology in Ar Atmosphere	58
YSC-4	<i>Kozubal M., Barcz A., Pągowska K., Jakiela R., Taube A., Ratajczak J., Wojciechowski T., Celler G.K.,</i> Formation of buried, electrically insulating layer by proton implantation in GaN for vertical leakage current reduction	60
YSC-5	<i>Łatka L., Szala M., Michalak M., Sokołowski P.,</i> Cavitation erosion resistance of plasma sprayed ceramic coatings.....	61
YSC-6	<i>Makhavikou Maksim, Komarov Fadei, Kuchinsky Peter, Milchanin Oleg, Vlasukova Ludmila, Parkhomenko Irina, Romanov Ivan, Żuk Jerzy, Wendler Elke,</i> Structure and optical properties of ZnSe/SiO ₂ -nanocomposite formed by ion implantation	62
YSC-7	<i>Nagy Gy., Kerékgyártó R., Csík A., Rajta I.,</i> Proton beam machining of poly(tetrafluoroethylene).....	63
YSC-8	<i>Nechaev N.S., Komarov F.F., Ivlev G.D., Vlasukova L.A., Parkhomenko I.N., Romanov I.A., Wendler E.,</i> Hyperdoping Si with Se by ion implantation followed by pulsed laser melting.....	64
YSC-9	<i>O’Connell J.H., Skuratov V.A.,</i> Overview of latent track morphology in crystalline insulators from direct observation with TEM.....	65
YSC-10	<i>Phuc T.V., Kulik M., Kolodynska D., Kobzev A.P., Khiem L.H., Żuk J., Turek M.,</i> Investigation of atomic depth distribution and chemical composition in multilayer structures of TiO ₂ /SiO ₂ /Si after ion irradiation	66
YSC-11	<i>Samadov S., Samadov O., Kulik M., Pyszniak K., Olejniczak A., Najafov A., Huseynov N., Huseynov E.,</i> Optical properties of TiGaSe ₂ before and after ion implantation with H ⁺ and He ⁺	67
YSC-12	<i>Tooski Sahib Babaee,</i> Quantum entanglement, and electronic transport in quantum dots system.....	68
YSC-13	<i>Wang Mao, Berencén Y., Prucnal S., García-Hemme E., Hübner R., Yuan Ye, Xu Chi, Rebohle L., Böttger R., Heller R., Schneider H., Skorupa W., Helm M., Zhou Shengqiang,</i> Extended infrared photoresponse in room-temperature Si hyperdoped with Te.....	69

YSC-14	<i>Xu Chi, Yuan Ye, Wang Mao, Böttger R., Helm M., Zhou Shengqiang,</i> <i>p-type co-doping effect in (Ga,Mn)As: Mn lattice location and magnetic phase transition.....</i>	70
--------	------------------------------------------------------------------------------------------------------------------------------------------------------------------------------------	----

POSTER PRESENTATIONS

Po-1	<i>Aldabergenova T., Wieleba W., Kislitsin S.,</i> Influence of the proton irradiation on surface structure and physical mechanical properties of tungsten	73
Po-2	<i>Billewicz P., Węgierek P., Grudniewski T.,</i> Research on multiple excitations probability in ion-implanted silicon structures in the aspect of possible photovoltaic applications	74
Po-3	<i>Billewicz P., Węgierek P., Grudniewski T.,</i> Temperature dependences of resistivity of metal-semiconductor ohmic contacts in silicon structures dedicated to photovoltaic applications	75
Po-4	<i>Boiko O., Fedotov A.K., Fedotova J.,</i> Electrical characterization of ceramic matrix nanocomposites with using of impedance spectroscopy	76
Po-5	<i>Bondarenko G.G., Borovitskaya I.V., Nikulin V.Ya., Mikhailova A.B., Silin P.V., Gaidar A.I., Paramonova V.V., Peregudova E.N.,</i> Investigation of the damage of the surface layers of vanadium irradiated in the Plasma Focus facility.....	78
Po-6	<i>Odnodvoretz L., Bondariev V., Tyschenko K., Shumakova N., Protsenko I.,</i> Strain effect in film materials based on magnetic metals.....	79
Po-7	<i>Cieślak I., Czarnewicz S., Sitek R., Duchna M., Kurpaska E.,</i> Study of strength properties after high temperature crawl conditions in ceramic thermal barrier coatings based on In 740	80
Po-8	<i>Czarnacka Karolina, Koltunowicz Tomasz N., Fedotova Julia A., Fedotov Aleksander K.,</i> AC electrical properties of silicon-on-insulator structures with In and Sb nanocrystals heated at high temperatures.....	81
Po-9	<i>Dosbolayev M.K., Raiymkhanov Zh., Tazhen A.B., Utegenov A.U., Ramazanov T.S.,</i> Impulse plasma deposition of carbon nanoparticles.....	82
Po-10	<i>Drożdździał A., Turek M., Pyszniak K., Żuk J., Prucnal S.,</i> Doping of Ge and GeSn via nonequilibrium processing.....	83
Po-11	<i>Duk M., Kociubiński A., Szypulski M., Zarzeczny D., Lizak T., Muzyka K., Prendecka M., Małecka-Massalska T.,</i> Plasma Sputtering Deposition of Thin Film Cu, Ti and NiCr Capacitors on Biocompatible Substrate	84
Po-12	<i>Fedotov A.S., Ape P., Yurasov D., Novikov A., Svito I., Fedotov A.K., Zukowski P.,</i> Influence of Irradiation by Swift Heavy Ions on Carrier Transport in Si<Sb> Delta-Layer	85
Po-13	<i>Kalinin Yu.E., Sitnikov A.V., Koltunowicz T.N., Zukowski P., Fedotova V.V., Ronassi Ali Arash, Evtukh A.A., Fedotov A.K.,</i> The features of reactive admittance in the nanogranular composites $(\text{Fe}_{45}\text{Co}_{45}\text{Zr}_{10})_x(\text{SiO}_2)_{(100-x)}$ manufactured by Ion-Beam Sputtering Technique with Ar ions	86
Po-14	<i>Kurovets V.V., Fedoriv V.D., Yaremiy S.I., Garpul O.Z.,</i> Structural changes in helium-implanted epitaxial La, Ga: YIG films	87

Po-15	<i>Kobets A.G., Horodek P., Siemek K., Skuratov V.A.,</i> Positron Beam Studies of Radiation Damage Induced by Heavy Ions in Iron.....	88
Po-16	<i>Kociubiński A., Lizak T., Muzyka K., Szypulski M., Zarzeczny D., Duk M., Prendecka M., Malecka-Massalska T.,</i> Technology of Nickel Thin Films Deposited by Magnetron Sputtering for Cell Morphology Monitoring	89
Po-17	<i>Odnodvoretz L., Koltunowicz T.N., Bondariev V., Protsenko S., Tkach O., Shumakova M.,</i> Electrophysical properties of granular film alloys	90
Po-18	<i>Poplavsky V.V., Luhin V.G., Koltunowicz T.N.,</i> Morphology and composition of surface layers prepared by ion beam assisted deposition of platinum and dysprosium on carbon fiber paper catalysts carriers.....	91
Po-19	<i>Komarov Fadei, Ivlev Gennady, Zayats Galina, Komarov Alexander, Nechayev Nikita, Wendler Elke, Miskiewicz Siarhiej,</i> Experimental study and modeling of silicon supersaturated with selenium by ion implantation and nanosecond-laser melting	92
Po-20	<i>Bezdidko O., Świc A., Komsta H., Opielak M., Cheshko I., Protsenko S.,</i> Magneto-Optical Properties of Film Systems Based on Fe and Cr	93
Po-21	<i>Lohvynov A., Cheshko I., Protsenko S., Swic A., Komsta H., Opielak M.,</i> Magnetoresistive properties of synthetic antiferromagnetic spin valves structures on the basis Co and Ru	94
Po-22	<i>Prokopchuk Nikolay, Luhin Valery, Shashok Zhanna, Prishchepenko Dmitry, Komsta Henryk,</i> Electrospinning process technology parameter influence on the properties of Polyamide-6 and Chitosan nanofibrous coatings for air filtration	95
Po-23	<i>Konstantinov S.V., Komarov F.F.,</i> Effects of nitrogen selective sputtering and flecking of nanostructured coating TiN, TiAlN, TiAlYN, TiCrN, (TiHfZrVNb)N under helium ion irradiation	96
Po-24	<i>Kravchenko Ya.O., Bondar O.V., Pogrebnyak A.D., Piotrowska K.,</i> Development of multilayer condensates based on refractory compounds with a variable composition of the second layer in the bilayer.....	97
Po-25	<i>Kravchenko Ya.O., Iatsunskiy I., Maksakova O.V., Pogrebnyak A.D., Kierczynski K., Koltunowicz T.N., Zukowski P.,</i> Structure and phase composition of nanostructured functional coatings (TiAlSiY)N/MoN.....	98
Po-26	<i>Liu Chaoming, Wang Mao, Berencén Yonder, Yang Jianqun, Li Xingji, Zhou Shengqiang,</i> Radiation Effects on Single Crystal β -Ga ₂ O ₃ : Hydrogen vs. Optical Properties	99
Po-27	<i>Maciążek D., Postawa Z.,</i> Soft-landing of organic molecules with mixed argon cluster on a metallic surface.....	100
Po-28	<i>Madadzada Afag I., Kulik M., Kolodynska D., Kobzev A.P., Asgerov E.B.,</i> Influence of noble gases irradiation on the formation of transient layers in multilayer systems	101
Po-29	<i>Majcher J., Boguta A.,</i> The use of piezoelectric phenomena to assess the moisture content of rape seeds	102
Po-30	<i>Andreev Dmitrii V., Bondarenko Gennady G., Andreev Vladimir V., Maslovsky Vladimir M., Stolyarov Alexander A.,</i> Modification of MIS Devices by Radio-Frequency Plasma Treatment	103

Po-31	<i>Andreev D.V., Levin M.N., <u>Maslovsky V.M.</u>, Intrinsic gettering in silicon at complex influence of radiation and pulsed magnetic fields.....</i>	104
Po-32	<i>Galimov A.M., Zebrev G.I., <u>Maslovsky V.M.</u>, Heavy ion induced subthreshold upsets modeling in memory devices.....</i>	105
Po-33	<i>Lagov P.B., Kulevoi T.V., <u>Maslovsky V.M.</u>, <i>Andreev D.V., Volkov A.N.</i>, Lifetime control of silicon devices by proton and carbon implantation.....</i>	106
Po-34	<i>Lagov P.B., <u>Maslovsky V.M.</u>, Pavlov Yu.S., Rogovsky E.S., Drenin A.S., Skryleva E.A., Lednev A.M.</i> , High-rate high-density ICP etching of germanium.....	107
Po-35	<i>Miskiewicz Siarhiej, Komarov Fadei, Komarov Alexander, Yuvchenko Vera, Bozhatkin Vitali, Zayats Galina</i> , Simulation of silicon device structures operating in radiation environment	108
Po-36	<i>Njoroge E., Odutemowo O.S., Mlambo M., Hlatshwayo T., Wendler E., Malherbe J.</i> , Diffusion and structural changes of ion implanted glassy carbon after thermal annealing.....	109
Po-37	<i>Olejniczak K., Apel P.Y.</i> , The influence of PET film morphology on the ion transport properties of asymmetric track-etched single nanopores.....	110
Po-38	<i>Bereznyak Yu., <u>Opielak M.</u>, Poduremne D., Protsenko I., Shabelnyk Yu.</i> , Crystalline structure and physical properties of multicomponent (high-entropy) film alloys	111
Po-39	<i>Komarov F.F., Vlasukova L.A., Milchanin O.V., Makhavikou M.A., Skuratov V.A., Vuuren A. Janse, Neethling J.N., Žuk J., Dauletbekova A.K., <u>Parkhomenko I.N.</u>, Yuvchenko V.N.</i> , Swift heavy ion modification in "Silica+Zn nanocomposite"	112
Po-40	<i>Satpaev D.A., Poltavtseva V.P., Degtyaryova V.P., <u>Partyka J.</u></i> , Changes of Ti-Cr-N coatings structure and hardness under the impact of xenon ions and annealing	113
Po-41	<i>Satpaev D.A., Poltavtseva V.P., <u>Partyka J.</u></i> , Effect of the fluence of high-energy krypton ions irradiation on Ni-Ti alloy hardening	114
Po-42	<i>Pilko Vladimir, Komarov Fadei, Budzyński Piotr</i> , Structure and hardness evolution of silicon carbide epitaxial layers irradiated with He ⁺ ions.....	115
Po-43	<i>Plaipaitė-Nalivaiko Rita, Griškonis Egidijus, Adlienė Diana</i> , Continuous ultrasound assisted sonoelectrochemical synthesis of W-Co alloy nanoparticles.....	116
Po-44	<i>Bondar O.V., <u>Pogrebnyak A.D.</u>, Takeda Y., Zukowski P.</i> , Combined multilayered coatings based on alternative triple nitride and binary metallic layers, their structure and physical-mechanical properties.....	118
Po-45	<i>Pylypiv V.M., Garpul O.Z., Khrushch L.Z.</i> , Comparative analysis of structural disorder of surface layers of Yttrium Iron Garnet Films as a result of implantation by Si ⁺ and P ⁺ ions	119
Po-46	<i>Starosta W., Barlak M., Smolik J., Waliś L., Sartowska B.</i> , Studies on transformation of magnetron sputtered and pulse electron beam melted zirconium silicide coatings deposited on zirconium alloy	120

Po-47	<i>Maksakova O.V., Pogrebnjak A.D., Bondar O.V., Świć A.,</i> Microstructure and physical-mechanical properties of nanosized ZrN/CrN coatings under different deposition conditions.....	121
Po-48	<i>Tetelbaum D.I., Mikhaylov A.N., Belov A.I., Korolev D.S., Okulich E.V., Okulich V.I., Shuisky R.A., Guseinov D.V., Gryaznov E.G., Stepanov A.V., Gorshkov O.N.,</i> Ion Implantation in the Technology of Metal-Oxide Memristive Devices	122
Po-49	<i>Tetelbaum D.I., Nikolskaya A.A., Korolev D.S., Mikhaylov A.N., Belov A.I., Sushkov A.A., Pavlov D.A.,</i> Synthesis of hexagonal silicon by ion implantation	123
Po-50	<i>Turek Marcin, Droździel Andrzej, Pyszniak Krzysztof, Prucnal Sławomir, Żuk Jerzy, Yuschkevich Yuriy, Węgierek Paweł,</i> Thermal desorption of He implanted into Ge	124
Po-51	<i>Turek Marcin,</i> Ion beam emittance for an ion source with a conical hot cavity.....	125
Po-52	<i>Turek Marcin,</i> Negative ion beam production in an ion source with chamfered extraction opening.....	126
Po-53	<i>Walczak M., Pasierbiewicz K.,</i> Properties and scratch resistance of PVD coatings on Ti6Al4V alloy	127
Po-54	<i>Węgierek P., Billewicz P., Pietraszek J.,</i> Analysis of the influence of annealing temperature on mechanisms of charge carrier transfer in GaAs in the aspect of possible applications in photovoltaics	128
Po-55	<i>Żukowski P., Pazukha I., Shuliarenko D., Protsenko S.,</i> Magnetoresistive properties of nanostructured thin film systems based on Ni ₈₀ Fe ₂₀ and Ag.....	129
Po-56	<i>Żukowski Paweł, Rogalski Przemysław,</i> Constant current hopping conductivity in percolation channel	130
Po-57	<i>Pochtenny A., Luhin V., Volobuev V., Shikanov S., Żukowski P.,</i> Electrical conduction properties of DC magnetron sputtered indium oxide thin films	131
	Authors Index	133

INVITED LECTURE

Ion Irradiation of SiC and GaN: One Technique for Different Purposes

Barcz Adam^{1,2)}

¹⁾*Institute of Electronic Technology, Al. Lotników 32/46, 02-668 Warsaw, Poland*

²⁾*Institute of Physics of the Polish Academy of Sciences, Al. Lotników 32/46, 02-668 Warsaw, Poland*

Ion implantation is being routinely used to create doped regions that act as active channel layers or contacts in semiconducting materials. Here, the emphasis is placed on less conventional applications of energetic ion beams. First, a brief survey of the phenomena that may accompany the passage of an ion through matter will be outlined. This will include the emission of electrons, photons and single or cluster atoms leaving the solid surface as well as the process of damaging the crystal, generation of collisional cascades, ion mixing etc. In particular, diffusion and segregation behavior of hydrogen and oxygen in silicon carbide subjected to H implantation and subsequent annealing were studied with a number of analytical techniques [1]. At sufficiently high doses, a well-defined buried planar zone forms in SiC at the maximum of deposited energy, comprising numerous microvoids and platelets that are trapping sites for hydrogen atoms. For gallium nitride, the accelerator beam was used to either n-type doping of a sub-surface layer or to completely isolate a small volume of the semiconductor. Lateral isolation was accomplished by a low-dose implantation of Al⁺ while the vertical electrical separation – through formation of a buried, highly damaged layer created by proton irradiation [2]. Implant isolation retains the planarity of the surface for subsequent resist application and metal step coverage giving a significant advantage over chemical mesa etching.

References

- [1] A. Barcz., Kozubal M., Jakiela R., Ratajczak J., Dyczewski J., Gołaszewska K., Wojciechowski T., Celler G. K.; *J. Appl. Phys.* **115**, p.223710 (2014)
- [2] M. Kozubal, PhD Dissertation, 2018

Long-range effect of ion-implanted materials in tribological investigations

Budzyński P.¹⁾, Kamiński M.¹⁾, Pyszniak K.²⁾, Wiertel M.²⁾

¹⁾*Faculty of Mechanical Engineering, Lublin University of Technology, Nadbystrzycka 36, 20-618 Lublin, Poland*

²⁾*Institute of Physics, Maria Curie-Skłodowska University, Pl. M. Curie-Skłodowskiej 1, 20-031 Lublin, Poland*

Obtained microhardness results and the presence of radiation effects at a depth higher than the predicted range of implanted ions pointed to the presence of a so-called long-range effect. An attempt is made to determine the thickness of a layer with modified tribological properties by measuring the friction and wear factors. The authors of this study decided to explain the mechanism of the long-range effect. Tribological tests were performed on a pin-on-disc stand. The real thickness of a layer with implantation-modified tribological properties can be determined via tribological testing by measuring the wear trace depth when the value of friction factor and/or wear of the implanted sample is close to the value characteristic of the unimplanted sample. The prediction range of implanted ions RSRIM [μm] was estimated by SRIM. The presence of the long-range effect was confirmed for the steel grades AISI 316L, H11, Raex 400, Hardox 450 as well as for the alloys Stellite 6 and Ti6Al4V. The modified layer thickness determined by tribological testing is much higher (by 4.7÷16.7 times) than the initial range of the implanted nitrogen ions. The depth of changes in the tribological properties of the surface layer (due to the long-range effect) agrees with the nanohardness measurement result obtained for the steel grades AISI 316 and H11.

An analysis of the content of elements on the sample surface as well as in its wear trace and wear products was performed by X-ray spectroscopy (EDS and WDXS). Obtained results demonstrate that one of the causes of the long-range effect is the dislocation of nitrogen and carbon atoms in the zone of friction during the tribological test. The long-range effect was also observed in Ti6Al4V alloy implanted with carbon atoms by ion beam assisted deposition (IBAD) using a beam of nitrogen ions with an energy of 120 keV.

The tribological test results demonstrate that the thickness of a layer with lower friction and wear factors is much higher than the initial range of implanted ions (atoms). Apart from the diffusion of radiation effects inside the sample, one can also observe the diffusion of the implanted ions of nitrogen and carbon, the latter being an alloying component of the tested steel. The dislocation of nitrogen and carbon atoms is caused

by accelerated radiation diffusion and a higher diffusion coefficient resulting from a local temperature increase in the friction pair during the tribological test. The thickness of the modified surface layer depends on the applied test conditions such as the load exerted on the sample by the countersample.

References

- [1] Sharkeev Yu.P, Gritsenko B.P, Fortuna S.V, Perry A.J, Vacuum 1999;52:247.
- [2] Sharkeev Yu.P, Gashenko S.A, Pashchenko O.V, Krivobokov V.P, Surf. Coat. Technol. 1997;91:20.
- [3] Tetelbaum D.I, Kurilchik E.V, Latisheva N.D, Nucl. Instr. Meth. 1997;B127/128:153.
- [4] Sharkeev Yu.P, Kozlov E.V, Surf. Coat. Technol. 2002;158-159:219.
- [5] Fischer-Cripps A.C, Vacuum 2000;58:569.
- [6] Budzynski P, Tarkowski P, Jartych E, Kobzev A.P, Vacuum 2001;63:737.
- [7] Budzyński P, Nucl. Instr. Meth. in Phys. Res. B 2015;342:1.
- [8] Budzyński P, Kara L, Küçükömeroğlu T, Kamiński M, Vacuum 2015;122:1.
- [9] Budzyński P, Sielanko J, Acta Phys. Polon. A 2015;128:841.
- [10] Korycki J, Dygo A, Pietrak R, Turos A, Gawlik G, Jagielski J, Nucl. Instr. Meth. in Phys. Res. B 1987;19-20:177.
- [11] Sharkeev Yu.P, Perry A.J, Fortuna S.V, Surf. Coat. Technol. 1998:108-109:419.

Development of improved ion-beam technologies for preparation of nanocomposite heterostructures with tunable electric and magnetic properties

Fedotov A.K.¹⁾, Fedotova J.A.²⁾, Streltsov E.A.¹⁾, Żukowski P.³⁾, Kołodziej T.N.³⁾, Kalinin Yu.E.⁴⁾, Evtukh A.A.⁵⁾

¹⁾Belarusian State University, 4, Nezavisimosti av., 220030 Minsk, Belarus

²⁾Research Institute for Nuclear Problems of Belarusian State University, 11, Bobruiskaya Str., 220030 Minsk, Belarus

³⁾Lublin University of Technology, 38d, Nadbystrzycka Str., 20-618 Lublin, Poland

⁴⁾Voronezh State Technical University, 14, Moscow av., 394026 Voronezh, Russia

⁵⁾Institute of Semiconductor Physics of National Academy of Sciences of Ukraine, 41, Nauka av., 03028 Kiev, Ukraine

This work is devoted to the results of the study of metal-semiconductor-insulator (MSI) nanostructures, produced by ion-beam technologies, which can be used for production of sensors, memory media and micro- and nanosized electric engineering componentry.

MSI film nanocomposites were deposited by ion-beam sputtering of compound targets FeCo-insulator (silica, alumina, fluoride, PZT) in vacuum chamber with argon or argon-oxygen gas atmosphere. As a rule, such nanocomposites contain FeCo-based nanoparticles embedded into insulating matrixes and possess “core-shell” structures. When “shells” around metallic “core” are composed of semiconducting FeCo-based oxides, MSI film nanocomposites show inductive-like contribution into reactive part of impedance in form of the so-called “negative capacitance” effect. We analyze the conditions (concentration of FeCo-base phase, type and state – amorphous or crystalline – of insulating matrix, composition of “core-shell” structure, temperature, frequency range, annealing, etc.) when inductive-like contribution prevails over capacitive one. The domination of inductive-like contribution (approached the values of 10-20 $\mu\text{H}/\mu\text{m}^3$) in some of composite MSI nanostructures allows to use them in future as miniature planar (non-coil-like) inductive elements with the tunable parameters in hybrid ICs or other electric engineering applications. We offer to use this principle to develop planar microinductors replacing the gyrators and Archimedian spirals in hybrid ICs. Some of the composites studied possessed temperature dependences of resistance which are linearized in log-log, Arrheniuse or Mott scales allowing to use them as a low-cost temperature sensors in the wide range of temperatures (2-400 K). Nanocomposites FeCoZr-fluorite have shown perpendicular magnetic anisotropy that can be used for the formation of magnetic memory media.

Ni/SiO₂/Si composite nanostructures contain array of Ni nanorods, distributed in pores of SiO₂ layer, on Si substrate. These structures were sintered by template-assisted deposition using porous SiO₂/Si templates with SiO₂ layer irradiated by swift heavy ions with energies of about 50-400 MeV and the following selective etching of template for the formation of vertical cone-like pores. Using under-potential

electrochemical deposition, these pores were filled with Ni nanoparticles forming the array of Ni nanorod-like Schottky barriers on Si substrate. After preparation of Ni/SiO₂/Si nanostructure, three electrodes, two of which were situated on the top side of nanostructure and the third - on the back side of Si substrate. It was shown that, at the determined combination of operating current between two top probes and also sign and value of transversal bias voltage (applied between top and backside probes) Ni/SiO₂/Si nanostructure display the huge magnetoresistive effect (tuned by both longitudinal and transversal electric fields) in the temperature range 20-30 K (approaching the values up to 35 000% at $H=8$ T) and in the range 200-320 K (up to 500%).

We offer to fabricate such Ni/SiO₂/Si nanostructures in the ordered pores created using micron or submicron lithography and other methods of planar Si technology to form electric probes to every Ni rod. This will allow to manufacture magnetosensitive matrices with Ni rod arrays permitting to show distribution (visualization) of magnetic fields in space in different magnetic systems like superconducting solenoids, transformers and other magnetic systems.

Self-organized nano-voids in irradiated SiGe/Si hetero-structures for plasmonic application

Gaiduk P.I.

Belarusian State University, prosp. Nezavisimosti 4, 220030, Minsk, Belarus

The formation of new Si-based materials with enhanced light absorption is of great importance for the development of high efficient photodetectors and photovoltaic devices. Light scattering and excitation of localized surface plasmons due to interaction with nano-cavities, metallic nano-shells and nano-particles leads to enhanced light absorption. The present study is devoted to strain-assisted formation of 2D array of optically active nano-voids and dots self-organized nearby to p-n junction.

Strained layers of Si/SiGe(Sn)/Si are grown in a solid-source MBE machine. The samples are then irradiated with H⁺ or He⁺ ions followed by high temperature annealing to create the layer of nano-voids and segregation of metallic impurities into the voids. Optical measurements of the Si/SiGe(Sn)/Si samples show a successive increase of the reflectivity in the spectral range of 800-1800 nm after deposition, irradiation and high temperature annealing.

We will briefly review the effects of strain-driven nano-void formation in Si/SiGeSn layers, gettering and segregation of impurities and formation of buried nano-shells and nano-dots of Ge, Sn and Au in Si layers. It will be discussed in the talk that metallic nano-shells possess tuneable optical resonances. By varying the relative core and shell thicknesses, the absorption and scattering properties of metallic nano-shells can be varied in a broad range. Finally, special attention will be devoted to possible plasmonic structures for enhancement of the efficiency of Si-based devices.

Damage accumulation studies in irradiated oxides: current status and new perspectives

Jagielski Jacek^{1,2)}, Thomé Lionel³⁾, Chartier Alain⁴⁾, Mieszczynski Cyprian²⁾, Jozwik Iwona¹⁾, Dorosh Orest¹⁾

¹⁾National Centre for Nuclear Research, A. Soltana 7, 05-400 Otwock/Swierk, Poland

²⁾Institute of Electronic Materials Technology, Wolczynska 133, 01-919 Warsaw, Poland

³⁾Centre de Sciences Nucléaires et de Sciences de la Matière, Université Paris-Saclay, Bat 108, 91405 Orsay Campus

⁴⁾DEN-Service de la Corrosion et du Comportement des Matériaux dans leur Environnement (SCCME), CEA, Université Paris-Saclay, 91191, Gif-sur-Yvette, France

A complete description of damage accumulation process in irradiated solids is one of the key issues of nuclear engineering. Development of predictive models of material behavior in nuclear installations requires detailed understanding of mechanisms leading to structural transformations and, consequently, changes in their functional properties. In general damage accumulation analysis involves three main aspects: (i) identification of kind of defects at various stages of damaging process, (ii) quantitative measurement of the damage level and (iii) modelization of the damage accumulation process.

Various experimental and simulation tools may be used for damage accumulation studies. The method of choice in analysis of defect structure is Transmission Electron Microscopy (TEM), whereas for quantitative analysis of damage level Rutherford Backscattering/Channeling (RBS/C) method is mainly used.

Numerous studies performed in the past allowed to collect a solid database describing the evolution of defects upon irradiation and to build models (mainly phenomenological) of damage accumulation. Current status of the results collected for irradiated oxides will be reviewed in the first part of the presentation.

Critical review of the currently available information points to the missing elements in damage accumulation approach. Among them the need for a method allowing for quantitative assessment of damage level in polycrystals and to close a gap between atomistic simulations (essentially made by using Molecular Dynamics, MD) and results of the experiments performed on irradiated materials appear as the most urgent tasks. The preliminary results of already initiated attempts to answer these needs will be presented in the second part of the talk.

The last part of the presentation will be devoted to the proposition of a more complete approach in the analysis of damage accumulation in irradiated oxides combining several experimental techniques (RBS/C, TEM, XRD) with molecular dynamic simulations and phenomenological modelling.

Structure, tribomechanical properties and radiation tolerance of nanostructured (TiHfZrVNb)N coatings

Komarov F.F.¹⁾, Konstantinov S.V.¹⁾, Pilko V.V.¹⁾, Pogrebnjak A.D.²⁾

¹⁾*A.N. Sevchenko Institute of Applied Physical Problems of Belarusian State University, Kurchatov St., 7, 220045, Minsk, Belarus*

²⁾*Sumy University, R. Korsakov St., 2, 40007, Sumy, Ukraine*

We performed studies of the (TiHfZrVNb)N coatings based on high-entropy alloy (HEA) irradiated with 500 keV He⁺ ions. These high-entropy systems are of great interest due to their unique mechanical properties [1, 2]. Also, these coatings can serve as new radiation resistant materials. The coatings were obtained using cathode vacuum-arc evaporation. Irradiation by He⁺ ions with an energy of 500 keV in the range

of fluences from $5 \cdot 10^{16}$ to $3 \cdot 10^{17}$ ion/sm⁻² was performed. The depth distribution of atomic species in the deposited layers was measured by Rutherford backscattering spectrometry (RBS). Structural properties of coatings were studied by means of scanning electron microscopy (SEM). X-ray diffraction (XRD) was applied in order to study phase composition and to determine the grain size of formed coatings. To find the hardness, friction coefficient and wear resistance, the tribomechanical tests were performed. According to the results obtained, the following conclusions were made. High entropy of the deposited systems can stabilize the formation of a single-phase state in the form of a disordered solid solution and prevent the formation of intermetallic compounds during solidification. Nanostructured (TiHfZrVNb)N coatings are radiation tolerant and perspective for nuclear fuel claddings.

References

- [1] R. Krause-Rechberg, A.D. Pogrebnjak, V.N. Borisyuk, M.V. Kaverin, A.G. Ponomarev, M.A. Belokur, K. Yoshi, Y. Takeda, V.M. Beresnev, O.V. Sobol', *The Physics of Metals and Metallography*. 114 № 8, 672 (2013).
- [2] S.-Ch. Liang, Z.-Ch. Chang, D.-Ch. Tsai, Y.-Ch. Lin, H.-Sh. Sung, M.-J. Deng, F.-Sh. Shieu, *Applied Surface Science*. 257, 7709 (2011).

Ion implantation for photovoltaic applications: Review and outlook for silicon solar cells

Krügenger Jan¹⁾, Haase Felix²⁾, Peibst Robby^{1,2)}, Osten H.-J.¹⁾

¹⁾*Institute of Electronic Materials and Devices, Leibniz Universität Hannover, Schneiderberg 32, D-30167 Hannover, Germany;*

²⁾*Institute of Solar Energy Research Hamelin, Am Ohrberg 1, D-31860 Emmerthal, Germany*

Here we present a brief summary about the use of ion implantation for photovoltaic (PV) applications in the past and present. Furthermore, we highlight how ion implantation might be used in the future within the fast moving field of silicon solar cells. Ion implantation as a doping technique for silicon-based solar cells is already under investigation for several decades [1]. Nevertheless, it took more than 40 years for ion implantation to become a popular research topic for photovoltaic industry [2]. During that time, conventional Al-BSF industrial silicon solar cells featured p-type Czochralski-grown or block-casted multicrystalline base material and a POCl₃ diffused emitter. Thus, the first recent studies of ion implantation in PV focus n-type emitters for p-type solar cells [2-5]. However, the already lean manufacturing process of (local) Al-BSF cells in which p+ doping is induced via the metallization process diminishes major advantages ion implantation. The situation is completely different for n-type cell designs. Here, the use of one-sided doping by ion implantation offers a process simplification, e.g. for the passivated emitter and rear, totally diffused (PERT) concept, compared to diffusion-based approaches. Especially the formation of p-type emitters by implantation of boron or boric molecules is an intensively studied topic [6-8]. Furthermore, ion-implanted PERT solar cells offer the possibility of collecting light from front and rear-side (bifaciality). Very recently bifacial factors of up to 99 % are reported, together with a simplified interconnection scheme for the production of solar cell modules [9,10]. In addition to this possible short term industrial implementation, ion implantation might become an industrial key technology for production of high efficiency silicon solar cells. Especially the combination of state of the art contact schemes, like e.g. passivating contacts [11], and back junction and back contacted (BJBC) solar cells is considered. In this context, we show the latest results of our PERT and BJBC solar cells on n-type silicon, which feature efficiencies of 21.8% and 26.1%, respectively.

References

- [1] J.T. Burrill *et al.*, *IEEE Transactions on Electron Devices*, vol. 14, pp. 10-17, 1967.
- [2] R. Low *et al.*, in *35th IEEE PVSC*, pp. 1440-1445, 2010.
- [3] H. Hieslmair *et al.*, *Energy Procedia*, vol. 27, pp. 122-128, 2012.
- [4] J. Le Perchec *et al.*, in *27th EUPVSEC*, pp. 2090-2093, Frankfurt, Germany, 2012.
- [5] A. Lawrenz *et al.*, in *27th EUPVSEC*, pp. 1553-1557, Frankfurt, Germany, 2012.
- [6] W.S. Ho *et al.*, in *37th IEEE PVSC*, p. 1058, 2011.
- [7] Y.-W. Ok *et al.*, *Solar Energy Materials and Solar Cells*, vol. 123, pp. 92-96, 2014.
- [8] J. Krügenger *et al.*, *IEEE Journal of Photovoltaics*, vol. 5, pp. 166-173, 2015.
- [9] F. Kiefer *et al.*, *Solar Energy Materials & Solar Cells*, vol. 157, pp. 326-330, 2016.
- [10] H. Schulte-Huxel *et al.*, in *32nd EUPVSEC*, Munich, Germany, 2016.
- [11] R. Peibst *et al.*, *IEEE Journal of Photovoltaics*, vol. 4, pp. 841-850, 2014.

Depth dependent optical and elasto-optical effects of ion implantation studied by time-domain Brillouin scattering

Krzyżanowska Halina^{1,2)}, Baydin A.¹⁾, Feldman L.C.³⁾, Tolk N.H.¹⁾

¹⁾*Department of Physics and Astronomy, Vanderbilt University, Nashville, TN, USA*

²⁾*Institute of Physics, Maria Curie-Skłodowska University, Pl. M. Curie-Skłodowskiej 1, 20-031 Lublin, Poland*

³⁾*Institute for Advanced Materials, Devices and Nanotechnology, Rutgers University, Piscataway, NJ, USA*

In semiconductors, defects (vacancies, interstitials) and dopants play a critical role in the performance of electrical devices. Such defects become increasingly important as size scales approach the order of tens of nanometers and the influence of defects may significantly alter the entire device performance. Under these circumstances it is extremely important to identify both the location and concentration of defects as well as their effect on the optoelectronic properties. Traditionally, either optical or ion beam analysis methods have been used to characterize defect distributions. On one hand, while optical methods can deliver information regarding the average electronic structure, depth-dependent information is typically lost in measurement. Ion beam analysis, while providing some depth resolution, creates damage in a sample similar to that which is being studied and, in general, is not sensitive on dopant fluences lower than 10^{16} cm^{-2} .

In this talk, results of time-domain Brillouin scattering from implanted samples will be discussed. We have applied TDBS, also known as coherent acoustic phonon spectroscopy or picosecond ultrasonics, to the characterization of implanted GaAs [1], diamond [2], silicon carbide [3], and GaP specimens. The changes of the optoelectronic properties (refractive index, extinction coefficient, photoelastic coefficients) of these materials as a function of depth as well as defect concentration have been determined.

An ultrafast laser pulse (120 fs) was employed to generate and monitor a picosecond strain wave which transiently modifies the material as it passes through the specimen. The resulting time-resolved optical response is highly sensitive to local changes in a material's photoelastic properties. Our measurements extend over two orders of magnitude in defect concentration, and provide a tabletop method for non-invasive and non-destructive defect characterization, which is two orders of magnitude more sensitive than channeling.

We acknowledge financial support through from the Army Research Office (ARO) under contract W911NF-14-1-0290.

References

- [1] A. Baydin, H. Krzyżanowska, R. Gatamov, J. Garnett, and N. Tolk, *Sci. Rep.* 7, 15150 (2017)
- [2] J. Gregory, A. Steigerwald, H. Takahasi, A. Hmelo, and N. Tolk, *Applied Physics Letters* 101, 181904 (2012)
- [3] A. Baydin, H. Krzyżanowska, M. Dhanunjaya, SVS Nageswara Rao, J.L Davidson, L.C. Feldman, N.H. Tolk, *Appl. Phys. Lett. Photonics*, 1, 036102 (2016)

Advancement in Ion Implantation Annealing from Seconds to Milliseconds

Lerch Wilfried¹⁾, Niess Jürgen²⁾

¹⁾SkyLark.Solutions – Technology Consulting, Dornstadt-Tomerdingen, Germany

²⁾HQ-Dielectrics GmbH, Dornstadt, Germany

Thermal processes are some of the key steps in semiconductor manufacturing. A critical issue associated with the continuous reduction of dimensions of CMOS transistors is the realization of highly conductive, ultra-shallow junctions for source/drain extensions. The temperature-time cycle has changed radically over the past 10 years. Halogen lamp-based thermal annealing, for a period of seconds, evolved to spike anneals of one second and then to flash-lamp annealing or laser annealing. These provide an ultra-sharp temperature peak of the order of milli-seconds and are favored for this kind of activation anneals. Other processes that have historically been thermally driven such as oxidation of silicon have migrated to process solutions using other drivers such as plasma activation. This contribution reviews various annealing equipment types and their annealing schemes (temperature-time cycles and gaseous ambient) and investigates the formation of ultra-shallow, highly-electrically-activated and custom-shaped junctions by discussing various annealing strategies like e.g. combinations

of milli-second and halogen-lamp based rapid thermal annealing. Furthermore activities like the “re-invention” of solid phase epitaxy is discussed including the thermal stability of these junctions. Moreover, annealing of defects is always linked to the activation anneal. Therefore the deactivation of highly-activated junctions will also be shortly reviewed. Finally for silicon the co-implantation of carbon and fluorine to reduce the dopant junction depth is noted exemplarily and some latest advancements in predictive simulation of leading edge junctions are shortly summarized.

Development of Positron Annihilation Spectroscopy at Joint Institute for Nuclear Research

Horodek P.^{1,2)}, Khilinov V.¹⁾, Kobets A.^{1,3)}, Meshkov I.^{1,4)}, Orlov O.¹⁾, Siemek K.^{1,2)}, Sidorin A.A.¹⁾*

¹⁾*Joint Institute for Nuclear Research, Dubna, Russia*

²⁾*Institute of Nuclear Physics of PAS, Krakow, Poland*

³⁾*Institute of Electrophysics and Radiation Technology of NAS of Ukraine, Kharkov, Ukraine*

⁴⁾*St.Petersburg State University, St.Petersburg, Russia*

The method of positron annihilation spectroscopy (PAS) is sensitive to point defects in a solid material and is a well-known and used in material science. It allows one to study the concentration of defects with dimensions less than 10 nm on different depths depending of the energy of the positrons. In JINR this method is under development and application since 2012 when the first experimental station for PAS has been created at the LEPTA facility at Dzhelepov Laboratory of Nuclear Problems of JINR.

The PAS at the LEPTA is based on the slow positron injector that has two unique features:

- High monochromaticity of a positron flux – spectral width (FWHM) at the exit of the positron source is of 1.5-2 eV;

- Positron energy can be varied in the range of 50 eV – 35 keV (90 keV in the nearest future) with an accuracy of not less than 1% on target.

The construction of the slow positron injector was completed in mid-2011, and the group have focused on the development of the PAS method. These works were continued during the next years, and creating a special transportation channel of monochromatic positrons and experimental stations for PAS application, equipped with instrumentation for spectroscopy has been constructed. The first version of PAS – so called Doppler PAS – was developed and used up to now performing about 30 experiment runs per year for studying different kinds of materials:

- 1) Metals and alloys: steel embrittlement in reactor pressure vessel, fatigue effects in aircraft wings and different power units (screw propellers), corrosion of metallic structures;
- 2) Ultra fine-grained metals – studies of structure;
- 3) Semiconductors: studies of atomic defects in semiconductors (independent of its doping and conductivity).

(The polymers and porous materials and different plastic materials are not aloud due to vacuum restriction).

The most effective version of PAS – Positron Annihilation Lifetime spectroscopy (PALS) is under development presently. PALS has a specific sensitivity to vacancy-type defects which makes their identification straightforward and can be applied to any material. The PALS version under development at LEPTA is based on the original

* Corresponding author: Igor Meshkov meshkov@jinr.ru

scheme of formation of an ordered positron flux proposed by the authors. Special beam transfer channel has been designed and commissioned this year.

The project has attractive features due to possibility of application of slow monochromatic positron beam with variable and well controlled positron energy. All this makes the project attractive for potential cooperation.

HAADF STEM Imaging of Dislocation Loops in Irradiated GaAs

Neethling J.H., Janse van Vuuren A. and Olivier E.J.

Centre for HRTEM, Nelson Mandela University, Port Elizabeth, South Africa

GaAs based space solar cells have a higher conversion efficiency and better radiation resistance than Si solar cells [1]. Solar cells used in space are exposed to severe radiation and the lattice defects induced by high-energy electron and proton irradiations cause a decrease in the power output of the solar cells [1]. Radiation damage and the formation and growth of dislocation loops in GaAs have been studied in detail over many years [2-4]. In this paper, atomic resolution images of small dislocation loops in irradiated GaAs are presented. The images were recorded by using a double Cs-corrected TEM. The high resolution images together with earlier conventional TEM results of proton, electron and neutron irradiated and annealed GaAs are used to correct the earlier faulty identification of the nature and habit planes of small dislocation loops on {110} and {111} planes and hydrogen platelets on {111} planes of GaAs [2-3].

Small dislocation loops on {110} and {111} planes in both 1MeV electron and neutron irradiated GaAs became visible after annealing at 500°C. Atomic resolution HAADF STEM analyses of the loops revealed that the small loops on {111} planes consist of an interstitial layer of GaAs atoms with two layers of GaAs atoms in twin orientation. HAADF STEM indicated that the small loops on {110} planes are pure-edge interstitial dislocations consisting of two layers of GaAs atoms. A thorough understanding of the mobility and agglomeration behavior of irradiation induced point defects in GaAs is important for its widespread use in space missions where higher conversion efficiencies and radiation resistance are required.

References

- [1] Yamaguchi M, *Solar Energy Materials & Solar Cells* 2001; 68: 31.
- [2] Neethling JH, Snyman HC, *J. Appl. Phys.* 1986; 60: 941.
- [3] Neethling JH, *Physics B* 1991; 170: 285.
- [4] Neethling JH, *Proc. 13th Internat. Congress on Electron Microsc.*, Paris, 1994: 101.

Towards group IV semiconductor laser

Prucnal Sławomir^{1,2)}

¹⁾Helmholtz-Zentrum Dresden-Rossendorf, Institute of Ion Beam Physics and Materials Research,
P.O. Box 510119, 01314 Dresden, Germany

²⁾Maria Curie-Skłodowska University, Pl. M. Curie-Skłodowskiej 1, 20-035 Lublin, Poland

The main drawback of group IV semiconductors is the indirect band gap which makes them poor light emitters. Ge with a quasi-direct band gap can be created by strain engineering, formation of binary (GeSn) and ternary (SiGeSn) alloys, quantum dots or ultra-high n-type doping. This can be realized only utilizing strongly non-equilibrium processing like ion implantation and molecular beam epitaxy followed by the ultra-short annealing.

Here an overview of different doping and alloying techniques (*in-situ* and *ex-situ*) will be presented. Special attention will be focused on the use of ion implantation followed by flash-lamp (FLA) annealing for the fabrication of heavily doped Ge, GeSn and SiGeSn. In contrast to conventional annealing procedures, rear-side FLA leads to full recrystallization of Ge and dopant activation independently of pre-treatment. The maximum carrier concentration is well above 10^{20} cm^{-3} for n-type and above 10^{21} cm^{-3} for p-type doping. The recrystallization mechanism and the dopant distribution during rear-side FLA are discussed in detail. In this work, we report on the strong mid-IR plasmon absorption from heavily n-doped Ge and GeSn thin films and the room temperature photoluminescence observed from the direct band gap in Ge.

Acknowledgement: This work was partially supported by the German Academic Exchange Service (DAAD, Project-ID:57216326) and the National Science Centre, Poland, under Grant No. 2016/23/B/ST7/03451.

Mirrors for plasma diagnosis in reactors of controlled thermonuclear fusion: Ion-induced damage and ion beam analyses

Rubel M.¹⁾, Petterson P.¹⁾, Moon S.W.¹⁾, Fortuna E.²⁾, Krawczynska A.²⁾, Widdowson A.³⁾

¹⁾Royal Institute of Technology (KTH), 100 44 Stockholm, Sweden

²⁾Warsaw University of Technology, Warsaw, Poland

³⁾Culham Science Centre, Abingdon, OX14 3DB, United Kingdom

Optical spectroscopy and imaging diagnostics in next-step fusion devices, ITER and DEMO, will rely on metallic mirrors. The performance of mirrors is studied in present-day tokamaks and in laboratory systems. This work deals with comprehensive tests of mirrors: (a) exposed in JET with the ITER-Like Wall (JET-ILW); (b) irradiation by H^+ , He^+ (1-2 keV) and $^{98}Mo^+$, $^{93}Zr^+$, $^{90}Nb^+$ (30 keV) to simulate transmutation effects and damage which may be induced by neutrons under reactor conditions in the optically active layer of mirrors: 15-30 nm.

Material studies performed with a wide range of ion beam (standard and μ -beam NRA with $^3He^+$, PIXE, RBS and HIERDA with $^{127}I^{9+}$), microscopy methods (including STEM, FIB) and spectro-photometry techniques have led to results summarised briefly in the following.

First Mirror Test at JET for ITER has been for Mo mirrors placed in the main chamber wall and in the divertor during a single campaign and during all three ILW campaigns, ~62 h of fusion plasma operation:

- In the main chamber only mirrors located at the entrance to the cassette lost reflectivity (Be deposition from the eroded limiters), while those in the channels were only lightly affected.
- The performance of all divertor mirrors was strongly degraded by deposition of beryllium, tungsten and other species.
- Splashing of metal droplets from molten limiters on mirrors also occurred. It should be stressed, that solid Mo test mirrors were not damaged by arcing.

Work towards DEMO: radiation damage in mirrors: To induce changes predominantly in the optically active layer the conditions for the irradiation were based on SRIM simulations. The selection of ion type and dose was based on the FISPACT-II and TENDL-2014 predictions. Studies were done both for mirrors irradiated with a single species and with several types of ions, e.g. H^+ , He^+ and Zr^+ .

- The stepwise irradiation up to 30 dpa by heavy ions (Mo, Zr or Nb) caused only small changes in the optical performance. In some cases even improving even reflectivity due to the removal of surface layer with Mo oxides.
- Much stronger effects have been produced by helium because of bubble formation which led to the reflectivity decrease by more than 20%. Helium retention studies revealed that only 7-9% of the implanted He was retained mainly in two types of bubbles as detected by STEM. Helium residence time in Mo mirrors is long, as proven by HIERDA immediately after the irradiation and one year later.

Ions in materials testing

Sartowska B.¹⁾, Barlak M.²⁾, Konarski P.³⁾

¹⁾*Institute of Nuclear Chemistry and Technology, Dorodna 16, 03-195 Warsaw, Poland*

²⁾*National Centre for Nuclear Studies, Andrzeja Sołtana 7, 05-400 Otwock, Świerk, Poland*

³⁾*Tele & Radio Research Institute, Ratuszowa 11, 03-450 Warsaw, Poland*

Materials testing is always present in scientific investigations as well as in practical applications of different materials.

We have to know and be able to determine materials properties in situations as for example: (i) properties changes as the result of applied treatments or work in different environments, (ii) define requirements for special application and develop new material with tailored properties.

There is a lot of methods for materials investigations and testing. Methods on the base of ions application can deliver new and more detailed information about structure, composition and others. Techniques mainly differ by what is sent in versus what is collected out.

Examples of testing techniques used ions beams like: Rutherford Backscattered Spectroscopy (RBS), Secondary Ion Mass Spectrometry (SIMS), Ion Beam Induced Charge (IBIC) for example and other applications: ion cleaning and Ion beam etching for example will be presented.

Millisecond Flash Lamp Annealing and Application for SiGe-HBT

Scheit A.¹⁾, Lenke T.¹⁾, Heinemann B.¹⁾, Rücker H.¹⁾, Wolansky D.¹⁾, Skorupa W.²⁾, Schumann T.²⁾, Rebohle L.²⁾, Häberlein Sven³⁾

¹⁾ IHP, Im Technologiepark 25, 15236 Frankfurt (Oder), Germany

²⁾HZDR, Bautzner Landstraße 400, 01328 Dresden, Germany

³⁾FHR Anlagenbau GmbH, Am Huegel 2, 01458 Ottendorf-Okrilla, Germany

A 200 mm flash lamp annealing (FLA) prototype was developed beside the EU project DOTSEVEN, named after the f_{\max} target of 0.7 THz. Among different experiments n-type Si (100) wafers (8-12 Ωcm) were implanted with Germanium ($5 \cdot 10^{14}/\text{cm}^2$; 15 keV) followed by Boron (B) ($2 \cdot 10^{15}/\text{cm}^2$; 1 keV) [1]. FLA with 20 J/cm² results in a suppressed B diffusion (Fig.1a) with concurrent higher activation ($R_s = 174 \Omega/\text{sq}$) compared to spike annealing (SPA) at 1020°C ($R_s = 348 \Omega/\text{sq}$). The second experiment is based on a model HBT with B base prepared by LPCVD. A FLA with 27 J/cm² reduces the profile broadening by a factor of four compared to SPA at 1020°C (Fig.1b). The combination of the high activation and low dopant diffusion of the FLA process and the low deactivation of a backend with low thermal budget allowed us finally to meet the project targets. An experimental SiGe HBT technology featuring $f_T / f_{\max} / BV_{\text{CEO}} = 505 \text{ GHz} / 720 \text{ GHz} / 1.6 \text{ V}$ and a minimum CML ring oscillator gate delay of 1.34 ps was developed [2].

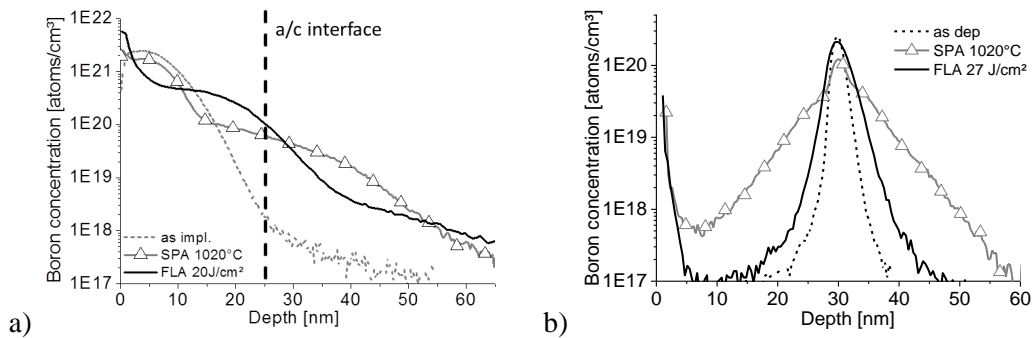


Figure 1: Comparison of Boron SIMS depth profiles after SPA and FLA of a) implanted Boron and b) model HBT structure with Boron base

References

[1] A. Scheit et al. (IIT 2014), pp. 1-4

[2] B. Heinemann et al. (IEDM 2016), pp. 3.1. (2016)

Neutron Physics at the Joint Institute for Nuclear Research

*Shvetsov V.N.**

Joint Institute for Nuclear Research, Joliot-Curie 6, Dubna, Russia

Frank Laboratory of Neutron Physics is one of the laboratories of the Joint Institute for Nuclear Research that investigates the neutron as an elementary particle, and employs the neutron as an instrument to investigate the structure and dynamics of condensed matter, including crystals and nanosystems, functional materials, complex liquids and polymers, rocks, etc. so that our findings could find application in molecular biology and pharmacology, engineering diagnostics and in other fields of science and technology.

Major directions of the FLNP research program are: neutron-nuclear investigations, condensed matter physics and applied research.

The main objectives of the FLNP research in the framework of the condensed matter physics involved the application of neutron scattering techniques and complementary methods such as RBS and PIXE to investigate the structure, dynamics and microscopic properties of nanosystems and novel materials, modern condensed matter physics and interdisciplinary sciences.

In the field of neutron nuclear physics researches are carried out in investigations of time and space parity violation processes in neutron-nuclear interactions; studies of the fission process; experimental investigations of fundamental properties of the neutron; gamma-spectroscopy of neutron-nuclear interactions; nuclear data for reactor applications and nuclear astrophysics; experiments with ultracold neutrons.

* shv@nf.jinr.ru

High energy ionoluminescence of oxide and alkali halide crystals

*Skuratov V.A., Dauletbekova A., Kirilkin N., Akyzbekov A., Seitbayev A.,
Teterev Yu.G., Zdorovets M.*

*Flerov Laboratory of Nuclear Research, Joint Institute for Nuclear Research, Dubna, Russia
L.N. Gumilyov Eurasian National University, Astana, Kazakhstan
Astana Branch of Institute of Nuclear Physics, Astana, Kazakhstan*

The spectral content and emission intensities of the ion-beam induced luminescence in insulators are strongly affected by accumulated radiation damage and associated mechanical stresses. In this report we review the results of recent high energy (1.2-3 MeV/amu) ionoluminescence (IL) characterization of Al_2O_3 , $\text{Al}_2\text{O}_3:\text{Cr}$, MgO and LiF using experimental set-up at FLNR JINR and INF cyclotrons. To evaluate the stress level the well-known piezospectroscopic method, utilizing the relationship between the stress and changes in optical spectra have been used.

Dose dependence of the IL spectra measured from Al_2O_3 during swift Kr, Xe and Bi ion irradiation clear evidences different stages in damage and stress accumulation at fluences before and after ion track overlapping. Contrary, real-time examination of MgO at the same experimental conditions did not reveal the changes in the IL spectra which could be ascribed to mechanical stresses in the irradiating crystals. In-situ studies of of F-type color centers luminescence in LiF followed by postradiation measurements of depth-resolved luminescence demonstrated that the luminescence yield is defined by radiation defects formed in elastic collisions in the end-of-range region.

Enhanced out-of-plane charge-transfer on a monolayer TMDCs by controlled defect creation: Optical Evidences in Heterostructure and Application for SERS

Tan Yang

School of Physics, State Key Laboratory of Crystal Materials, Shandong University, Shandong, Jinan, 250100, China

Two-dimensional transition metal dichalcogenides (TMDCs) has attracted an increasing attention due to its novel and intriguing material properties. The charge transfer in/out the plane of TMDCs has a crucial role for functions of the TMDCs. Compared with graphene, the TMDCs has a relative low formation energy, therefore point defects are more easily generated in the monolayer of TMDCs. It has been reported that point defects block the charge transfer in the plane of TMDCs. On the contrary, we demonstrate, in this work, the charge transfer out of the plane of TMDCs is enhanced by the controllable formation of point defects, benefiting its application as a Raman enhancement platform. Point defects were generated on the monolayer of TMDCs with the controllable density of point defects via the ion irradiation. The fs optical probe-pump measurements prove that point defects do not hamper the charge-transfer out of the plane of TMDCs monolayers, and the electron transition probability rate between TMDCs and neighbored materials is increased. Besides, point defects with a specific density can significantly enhance the surface enhanced Raman scattering (SERS) effect of TMDCs for 20 times at 680 cm^{-1} . Our work shows a methodology to tailor the charge-transfer out of TMDCs for the desired functions, and promotes the application of TMDCs in SERS for the molecular detection.

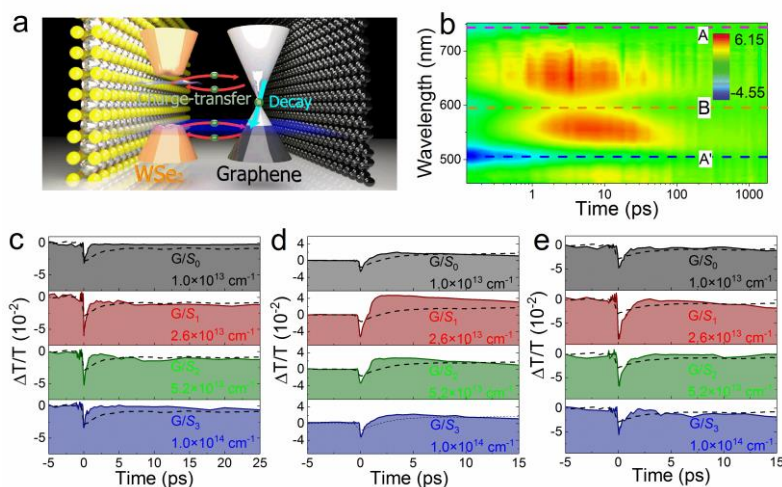


Figure 1. (a) Schematic diagram showing electronic transitions between graphene and the WSe₂ monolayer. (b) The fs optical pump-probe spectroscopy of the as-prepared WSe₂ monolayer. The intensity of $\Delta T/T_0$ at exciton resonances of A' (c), B (d) and A (e). The dashed lines are the spectroscopy of S₀ for comparisons

Radiation processing of polymers and semiconductors by electron beam

Zimek Z.

Institute of Nuclear Chemistry and Technology, Dorodna 16 Str., 03-95 Warsaw, Poland

Electron beam treatment process has been successfully applied for modification of gas, liquid and solid phase of the matter. Radiation processing can be recognized as one of Advanced Oxidation Technology, where chemical, physical or biological transformations may occur when materials are exposed to high energy radiation (electron beam in particular case). The advantages of radiation processing are connected to the unique capability for material modifications, its high efficiency and possibility to transfer high amount of energy directly into the irradiated object. The first electron accelerator applied in the field of radiation chemistry and radiation processing was installed in Poland in 1971 when multipurpose facility was completed at the Institute of Nuclear Chemistry and Technology (INCT) in Warsaw. Since than nearly 30 electron accelerators have been installed in Poland as laboratory instruments, pilot plant installations and industrial facilities.

R&D studies in the field of radiation technology in Poland are mostly concentrated at the Institute of Nuclear Chemistry and Technology. The results INCT works on polymers and semiconductors modification have been implemented in various branches of national economy, particularly in industry and medicine starting from middle of 70-ties. Among others, the processes of irradiation and heat shrinkable products expansion were developed and transferred to the industry. The study on formulation of new PE composites better suited to new generation of heat shrinkable products, hot-melt adhesives, electrical wire and cables have been developed to meet specific requirements of customers. Modified polypropylene (PP-M) has been formulated at INCT to provide material suitable for medical application and radiation sterilization process.

Modification of the semiconductors devices by e-beam was applied on industrial scale since 1978 when INCT and LAMINA (semiconductor factory) successfully adopted that technology to improve quality of high power semiconductor devices. This activity is continued on commercial basis where INCT facility are being served as contract irradiation of certain semiconductor devices according to manufacturing program of LAMINA factory and customer from abroad.

ORAL PRESENTATIONS

Microplasma deposition of biocompatible coatings using an intelligent robotic system for plasma processing

Alontseva D.L.

D. Serikbayev East Kazakhstan State Technical University, Protozanov Street 69, 070004, Ust-Kamenogorsk, Kazakhstan

The paper presents the method of microplasma deposition of biocompatible coatings using an intelligent robotic system for plasma processing. The two-layer coatings from biocompatible materials, namely from titanium wire and hydroxyapatite powders are sprayed on the surface of titanium substrates. The porosity of coatings is controlled by changing the spraying regime. The use of the intelligent robotic system for plasma processing allows movement of a robot arm along a given 3D-trajectory and accurate maintaining plasma spraying parameters: the trajectory and travel speed of the plasma source, an angle between the sprayed surface and the plasma jet and the distance from the plasma source to the surface of substrates.

The coatings deposition has been carried out on microplasma processing areas based on the industrial robot Kawasaki RS-010LA (Kawasaki Robotics, Japan) at D.Serikbayev East Kazakhstan State Technical University with the use of microplasmatron MPN-004 manufactured by E.O. Paton Electric Welding Institute (Ukraine). X-ray structure phase analysis, transmission and scanning electron microscopy have been used to study the structure-phase composition of coatings and substrates. The influence of the main parameters of microplasma spraying on morphology and structure-phase transformations in coatings have been studied.

The composition and regimes of microplasma spraying of the two-layer coatings with a sub-layer of a porous titanium coating and an upper layer of hydroxyapatite have been developed. Technological guidelines and software have been developed enabling to implement the method of microplasma deposition of biocompatible coatings using an intelligent robotic system for plasma processing.

Acknowledgment. The study has been conducted with the financial support of the Science Committee of RK MES by the project AP05130525 “The intelligent robotic system for plasma processing and cutting of large-size products of complex shape”.

The Long Range Effect Detection by Positron Lifetime Experiments

Horodek P.^{1,2)}

¹⁾*Institute of Nuclear Physics, Polish Academy of Science, Krakow 31-342, Poland*

²⁾*Joint Institute for Nuclear Research, Dubna 141980, Russia*

Ion implantation is a tool to evaluate the tolerance of materials to extreme radiation environments and to modify properties of surfaces. It is known that the ion distribution demonstrates the existence of three theoretical regions. The zone, where ions slow down because of electronic energy loss processes is located on depths between the surface and Bragg peak. Second region appears in the surroundings of the peak where heavy ions interact with lattice atoms via nuclear collisions and stop in the solid. At the depths behind only non-implanted region extends.

According to theoretical calculations the depth occupied by the radiation-induced defects should be comparable with the implanted one. However, there are papers reporting the existence of “the long range effect” (LRE) [1,2]. According to this effect defects, especially dislocations appear at the depths of a few times deeper as the implanted area. The nature of LRE and reasons of its existence have not been explained so far.

Within this presentation results of positron lifetime studies of LRE will be shown. This technique is not a commonly used method in this topic. We are going to report experimental investigations of pure metals exposed to heavy ion irradiation. The positron lifetimes measured in etching experiment give information about kind of defects, their distribution and existence of LRE.

References

[1] Lu Ch, et al., *Sci. Rep.* 2016;6:19994.

[2] Mazzoldi P, et al., *J. Phys. D* 2009;42:115418.

Radiation Effects in TiNbN Coatings Induced by Impact of Low-Energy Helium, Krypton and Xenon Ions

Kislitsin S.^{1,2)}, Ivanov I.¹⁾, Zdorovets M.^{1,2)}, Larionov A.¹⁾

¹⁾*Institute of Nuclear Physics, Ibragimov street, 1, 050032 Almaty, Kazakhstan*

²⁾*NRNU "MEPhI", Kashirskoe Avenue, 31, 119409 Moscow, Russia*

For study of the effect of irradiation with low-energy noble gas ions on structure and properties of TiNbN coatings we used scanning electron and atomic force microscopy, Rutherford backscattering, X-ray diffraction, measurements of nanohardness and corrosion resistance. Coatings of ~ 600 nm thick were synthesized by magnetron sputtering from two magnetrons in nitrogen atmosphere on a 12Cr18Ni10Ti steel substrate. Irradiation with ${}^4\text{He}^{2+}$, ${}^{84}\text{Kr}^{14+}$ and ${}^{132}\text{Xe}^{18+}$ ions was carried out on the low-energy channel of the accelerator DC-60 with an energy of 20 keV/charge up to fluence 10^{17} cm^{-2} , the ion energy was 40 keV (He), 280 keV (Kr), and 360 keV (Xe), respectively,. The projected range of the He, Kr, and Xe ions with the indicated energies was practically the same ~ 100 nm (SRIM calculations) and does not exceed thickness of coating.

The main research results are following:

- The crystalline structure of the TiNbN coating consisting of a mixture of two nitride phases (TiN and NbN) changes slightly after ion irradiation;
- Irradiation with alpha-particles does not lead to a significant change in the structure of the coating surface, in contrast to steel, where blistering is observed under the same conditions of irradiation;
- Irradiation with heavy ions Kr and Xe leads to strong sputtering and ion etching of the surface, coral-like structure of the surface is formed;
- The nanohardness of the unirradiated TiNbN is in ~ 2.5 times higher than in steel. Irradiation with He ions leads to hardening of the coating surface by factor of ~ 4, irradiation with Kr and Xe ions leads to hardening of the surface by a factor of ~ 2. An increase in the irradiation fluence leads to a softening of the TiNbN coating.
- Corrosion resistance of TiNbN coatings irradiated with He, Cr and Xe ions substantially exceeds the corrosion resistance of even unirradiated stainless steel.

Recent developments in SIMS and GD-MS, two analytical techniques used for surface analysis

Konarski P.¹⁾, Miśnik M.^{1,2)}, Ażgin J.^{1,3)}, Zawada A.^{1,3)}

¹⁾*Instytut Tele- i Radiotechniczny, Ratuszowa 11, 03-450 Warszawa, Poland*

²⁾*Faculty of Technical Physics and Applied Mathematics, Gdańsk University of Technology, Narutowicza 11/12, 80-233 Gdańsk, Poland*

³⁾*Military University of Technology, Kaliskiego 2, 00-908 Warszawa, Poland*

We present our recent modifications of two established analytical techniques: secondary ion mass spectrometry (SIMS) and glow discharge mass spectrometry (GD-MS).

In the case of SIMS, a “storing matter” procedure was developed in order to reduce the so-called matrix effect and enable quantitative analysis. In this procedure we sputter analysed sample and deposit sputtered flux onto the substrate (collector). Subsequently, we analyse the formed deposit by SIMS, using titanium oxide or molybdenum oxide as the collector [1]. These two oxides have a high dielectric constant, significantly increasing the sticking coefficients of metals [2]. In addition, oxides also enhance sensitivity of detection, since the ionization coefficient of deposited metals increases due to a red-ox reaction: $\text{Me}^I + \text{Me}^{II}\text{O}_x = \text{Me}^I\text{O}_y + \text{Me}^{II}\text{O}_{x-y}$, where Me^I is the deposited metal and Me^{II}O_x is the substrate oxide [3].

In case of GD-MS we present the development of a stepper motor controlled mechanical system that allows for surface mapping [4]. We compare the results of GD-MS and SIMS maps of the same samples.

All of the presented results were obtained using quadrupole mass analysers: SIMS model SAJW-05 equipped with the Ar^+ ion gun, Hiden Analytical SIMS Workstation equipped with O^+ ion gun and GD-MS model SMWJ-01 analyser with DC glow discharge source.

References

[1] Miśnik, M., Konarski, P., & Zawada, A. *Nucl.Instr.Meth.B*, 2016;371:199.

[2] Stoneham, A. M. *Appl.Surf.Sci.*, 1983;14(3-4):249.

[3] Fu, Q., & Wagner, T. *Surf.Sci.Rep.*, 2007;62(11):431.

[4] Konarski, P., Miśnik, M., Zawada, A. *J.Anal.Atom.Spectr.*, 2016;31(11):2192.

Optical properties and chemical composition of transition layers formed by irradiation of multilayer TiO₂/SiO₂ samples with Ne⁺, Ar⁺, Kr⁺ and Xe⁺ ions

Kulik M.^{1,2)}, Kołodyńska D.E.³⁾, Przewłocki H.M.⁴⁾, Hubicki Z.³⁾, Żuk J.²⁾ and Pyszniak K.²⁾

¹⁾Joint Institute for Nuclear Research, Dubna, Moscow reg., Russia, 141980;

²⁾Institute of Physics, Maria Curie-Skłodowska University, 20-031, Lublin Poland;

³⁾Faculty of Chemistry, Maria Curie-Skłodowska University, 20-031, Lublin Poland;

⁴⁾Institute of Electron Technology, 02-668, Warszawa Poland

Four groups of TiO₂/SiO₂/TiO₂/Si have been irradiated with the same fluence $3 \times 10^{16} \text{cm}^{-2}$ of different ions Ne⁺, Ar⁺, Kr⁺ and Xe⁺. Each of these groups was divided into four subgroups containing samples implanted with the same ion but at different energy of incidence. The energies were 100 keV, 150 keV, 200 keV and 250 keV. The implantation process was carried out at room temperature. Spectra of dielectric function and chemical compositions were obtained for the all samples, before and after irradiations. Measurements of these quantities were made with the help of the spectroscopic ellipsometry (SE) and X-ray photoelectron spectroscopy (XPS) methods.

The results of the conducted research indicate that there are transitional layers between the homogeneous layers of TiO₂ and SiO₂. It has been noticed that the thickness and chemical composition of these layers change with the energy and mass of implanted ions.

The spectra of refraction and extinction coefficient for the all layers of the studied samples were obtained for wavelengths in the range from 250 nm to 1000 nm. It was found that those spectra of the transition layers can be described using the approximation of effective medium approximations (EMA).

It was found using ion sputtering of the TiO₂ surface layers and the measurement of the XPS Ti2p and Ti3p lines that concentration of Ti, TiO, TiO₂ and Ti₂O₃ changes as the depth increases from the irradiated surface.

Based on the SRIM code on computer simulations, it was found that the above changes can be attributed to the process of formation of vacancies and displacements of atoms in this layer.

Observation of stabilized tetragonal latent tracks induced by single SHI impacts in monoclinic natural zirconia at room temperature

Lee M.E.¹⁾, O'Connell J.H.¹⁾ and Skuratov V.A.²⁾

¹⁾*Centre for HRTEM, Nelson Mandela University, Port Elizabeth, South Africa*

²⁾*Flerov Laboratory for Nuclear Research, Joint Institute for Nuclear Research, Dubna, Russia*

Zirconia (ZrO_2) is a polymorphic oxide that exists in three different crystal structures below its melting point namely, the high temperature phases cubic and tetragonal as well as the low temperature monoclinic phase [1]. The tetragonal to monoclinic transformation mechanism has received considerable attention and there have been a number of modeling approaches which have been adopted in the interpretation of the phase transformation namely the thermodynamic-based models and crystallographic-based models and more recently the phase field model [2]. Monoclinic to tetragonal transformation has been reported for SHI irradiated monoclinic single and polycrystalline bulk zirconia. It was reported that the transformation required fluences in excess of 5×10^{12} ions. cm^{-2} for heavy ions such as Pb and U [3].

In this paper, we describe the crystalline nature of single latent tracks in monocrystalline bulk monoclinic zirconia irradiated with 167 MeV Xe to a fluence of 2×10^{10} cm^{-2} at room temperature. The observed tetragonal nature of the tracks in the monoclinic matrix as demonstrated by high resolution transmission electron microscopy will be described. To our knowledge, this is the first direct observation of such

a transformation in a single ion track. It was shown that the tetragonal tracks transform to the monoclinic phase containing a line of residual defect loops on annealing at about 400°C. The results obtained in this investigation are compared to the predictions of the various models for the phase transformation mechanisms.

References

- [1] Sickafus K.E., et al., J. Nucl. Mater. 1999; 274: 66.
- [2] Mamivand M., et al., Acta Mat. 2013; 61: 5223.
- [3] Shuster B., et al., Nucl. Inst. Meth. 2009; B267: 964.

Swift Heavy-Ion Irradiation of graphene oxide: localized reduction and formation of sp-hybridized carbon atomic wires

Olejniczak A.^{1,2)*}, *Nebogatikova N.A.*^{3,4)}, *Kulik M.*^{1,5)}, *Skuratov V.A.*¹⁾

¹⁾*Joint Institute for Nuclear Research, Joliot-Curie 6, Dubna 141980, Russia*

²⁾*Faculty of Chemistry, Nicolaus Copernicus University, 87-100 Toruń, Poland*

³⁾*Rzhanov Institute of Semiconductor Physics, Novosibirsk 630090, Russia*

⁴⁾*Novosibirsk State University, Novosibirsk 630090, Russia*

⁵⁾*Institute of Physics, Maria Curie-Skłodowska University, 20-031 Lublin, Poland*

We report the fabrication of nanometer-sized reduced graphene oxide (rGO) spots by swift heavy-ion (SHI) bombardment. Such structures can be considered graphene quantum dots (QDs) embedded in a non-conducting matrix. Both the number density and the diameter of the rGO spots can be tailored by a suitable choice of irradiation parameters (i.e., ion type, fluence, and energy). The degree of GO defunctionalization by SHIs with different energies scaled well with the deposited electronic energy density. The resistance of the samples decreased nonlinearly with increasing ion dose, and, at fluences above 10^{13} cm^{-2} , was three orders of magnitude lower than the initial value. An increase in the electronic stopping power of the ion resulted in: (i) suppression of the structural ordering at low fluences, (ii) increased amorphization efficiency and formation of sp-hybridized carbon chains of both polyynes and polycumulenes at high fluences.

A hypothesis suggesting that the sp-C chains are bridges joining opposite sides of nanoholes created inside the track core and thus assuming the formation of a coupled QD-antidot system is presented. The electronic structure and vibrational properties of these carbon-chain molecular junctions were investigated using density functional theory calculations. It is shown that the configuration of the terminal C atoms has a determining effect on π -conjugation, whereas the geometric constraint results in a blue-shift of the longitudinal optical Raman mode.

The phenomena reported above, i.e., the localized reduction of GO and formation of sp-hybridized carbon chains, occurred only in the electronic stopping regime and were not observed for keV energy range ions. In this case, however, irradiation under appropriately selected conditions can lead to the formation of an undersurface layer of higher conductivity.

* aolejnic@chem.umk.pl

Low energy electron attachment to PtBr₂ molecules

Pelc Andrzej, Pieńkos Tomasz

Maria Curie-Skłodowska University, Pl. M. Curie-Skłodowskiej 1, 20-031 Lublin, Poland

The interaction of an electron with a molecule in the gas phase under low pressure condition (when the multiple collisions between molecules do not proceed) may be divided into (i) direct scattering and (ii) resonant scattering. The resonant scattering occurs when the incoming electron is trapped in the vicinity of the molecule for a time considerably longer than the electron flying time over the distance comparable with the molecule diameter. In this case the electron and molecule system may be treated as excited negatively charged system – temporary negative ion (TNI). The energy of the TNI is higher than the ground state of the molecule and electron in the continuum state, so the temporary negative ion is unstable in respect to the following processes: collision with other molecule, radiative stabilization, dissociative electron attachment or autodetachment.

In the following contribution we will present the results of the investigations of the low energy (from zero up to 10 eV) electron interactions with molecules of platinum dibromide. The experiments were carried out using an electron monochromator coupled with a quadrupole mass spectrometer and pulse counting acquisition system. The only anion observed was Br⁻. This ion is formed at three resonance electron energies: 0.4 eV, 1.2 eV and 7 eV. Additionally, the thermodynamic thresholds for dissociative electron attachment reactions for platinum(II) bromide were calculated and compared with the experimental results.

Longitudinal electromagnetic cascades in heavy amorphous segmented materials

Słowiński B.^{1,2)}

¹⁾National Centre for Nuclear Research, Świerk, Poland

²⁾Faculty of Physics, Warsaw University of Technology, Warsaw, Poland

The process of electromagnetic cascades (EMC) created by high enough energy ($E_\gamma \gtrsim 100$ MeV) gamma quanta (GQ) in heavy amorphous media is known for a long time (for example, [1]). Nevertheless, even at present it is reasonable, mostly from the practical viewpoint, to better its so far prevailing simple model description [2] and to investigate the problem of optimal segmentation of EMC registration media as the most favorable for energy reconstruction of primary GQ producing EMC. In the work a five parameter model of longitudinal EMC profile (1) in liquid Xe, BGO and PWO has been introduced and the values of its parameters as a function of E_γ determined in the E_γ range of 200-3500 MeV for three cut-off energy values of cascades electrons: 0.5, 1.2 and 2.0 MeV. For this purpose GEANT4 code was used and 10^4 events for each case were modeled, i.e. in general $3 \times 3 \times 6 \times 10^4$ histories [3].

$$\left(-\frac{dE}{dt}\right) = \alpha(t - \varepsilon)^\beta \exp(-\gamma t^\delta) \quad (1)$$

It has been found that our model approximate satisfactorily all our calculated data (Fig.1) and available experimental results too. Moreover, it was also found that the optimal segmentation of materials registering EMC in the form of layers along the direction of primary GQ is when the layer thickness is equal to $\Delta t = 0.5$ r.l. (radiation length).

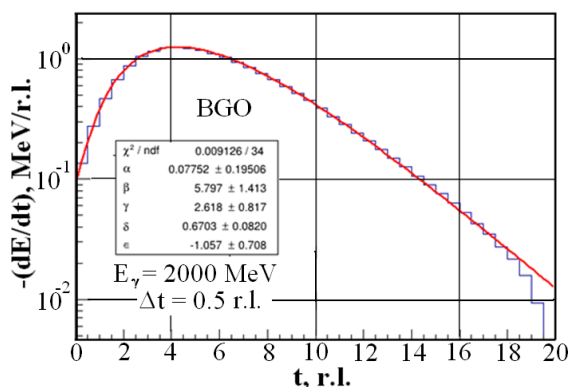


Fig.1. Longitudinal profile of EMC created in BGO by GQ of energy $E_\gamma = 2000$ MeV. BGO is segmented with a layer of $\Delta t = 0.5$ r.l. Solid curve demonstrates the approximation function (1). In inset shown are the corresponding values of its parameters and χ^2/nof

References

- [1] B. Słowiński. Phys. Part. Nucl. 25 (2) March-April 1994, pp.173-209; Radiat.Phys.Chem. V.49, No.3, pp.327-329, 1997.
- [2] Konrad Kleinknecht. Detectors for particle radiation. Cambridge University Press. London-New York-New Rochelle-Melbourne-Sydney, 1986; C.Grupen. Particle detectors. Cambridge University Press. 1996; Dan Green. The Physics of Particle Detectors. Cambridge University Press.2000; Review of Particle Physics. W.-M. Yao, et al., Journal of Physics G33, 1 (2006).
- [3] D.Głazek. Engineer thesis (in progress under scientific leader of B. Słowiński). WF PW. Warsaw, 2018.

Effect of TiO₂-NiAl plasma sprayed coatings thickness on cavitation erosion, sliding and abrasive wear resistance

Szala Mirosław^{1)}, Dudek Agata²⁾, Maruszczuk Andrzej³⁾, Walczak Mariusz⁴⁾, Chmiel Jarosław⁵⁾*

¹⁾*Department of Materials Engineering, Mechanical Engineering Faculty, Lublin University of Technology, 36D Nadbystrzycka Street, 20-618 Lublin, Poland, email: m.szala@pollub.pl*

²⁾*Institute of Materials Engineering, Faculty of Production Engineering and Materials Technology, Częstochowa University of Technology, Armii Krajowej 19, 42-200 Częstochowa, Poland*

³⁾*Faculty of Mechanical Engineering and Computer Science, Częstochowa University of Technology, Armii Krajowej 19, 42-200 Częstochowa*

⁴⁾*Department of Materials Engineering, Mechanical Engineering Faculty, Lublin University of Technology, 36D Nadbystrzycka Street, 20-618 Lublin, Poland*

⁵⁾*Faculty of Engineering and Economics of Transport, Maritime University of Szczecin, H. Pobożnego 11, 70-507 Szczecin, Poland*

Titania (TiO₂) based coatings are ceramic products with unique properties that make them widely applicable (e.g. in automotive industry, optoelectronics, chemical processing or medicine). Atmospheric plasma sprayed process enables to deposit TiO₂ with addition of NiAl feedstock material which has an influence on coating cohesion and adhesion to substrate. The aim of the work was to investigate the influence of TiO₂-10 wt.% NiAl plasma sprayed coatings thickness on cavitation wear and sliding wear.

Titania based coatings were deposited by means of atmospheric plasma sprayed on steel substrate using TiO₂-10 wt.% NiAl feedstock powders. Coatings thickness equals 50 μm, 100 μm, and 200 μm. Morphology and microstructure were examined using profilometric methods, light optical microscope and scanning electron microscope. Coating surface topography and hardness were determined. Porosity and thickness were evaluated by using quantities image analysis programme.

Cavitation erosion tests were performed according to ASTM G32 (vibratory apparatus) and ASTM G134 (cavitating liquid jet). Abrasive and sliding wear test were conducted using three body abrasive tester and ball-on-disc apparatus, respectively. Results indicate that plasma deposited coating thickness effects on wear resistance.

* m.szala@pollub.pl

Modification of PET polymer foil by Na⁺ implantation

*Turek Marcin, Drożdżiel Andrzej, Pyszniak Krzysztof, Luchowski Rafał,
Grudziński Wojciech*

Institute of Physics, Maria Curie Skłodowska University in Lublin

Ion implantation is a popular method for modifying properties of insulating polymers in order to enhance their electrical conductivity and also to change their optical properties. Ions of noble gases, e.g. Ar⁺ [1], are typical projectiles, as they do not form chemical bonds with host molecules, inducing C-H, C-O and C=O bond scission. This effect is also observed in the case of metallic ion irradiation. Bond scission leads to formation of vast carbon-carbon bond based networks as well as carbon cluster formation, resulting in dramatical resistance decrease. A 3 μm thick PET foil samples were irradiated using 150 keV Na⁺ beam with fluences 10¹⁴ cm⁻², 10¹⁵ and 10¹⁶ cm⁻². UV-VIS absorbance spectra were measured, showing significant lowering of band gap energy from ~4 eV to 0.75 eV for maximal fluences. Reduction of PET resistance by several orders of magnitude was observed. FTIR measurements point at increasing bond breaking with implantation fluence, giving opportunity of carbon based structures formation, as confirmed by Raman spectroscopy (carbon D and G bands). Sheet resistance reduction is observed.

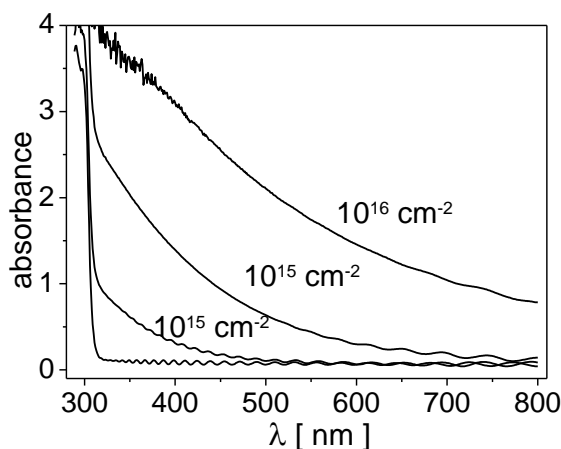


Fig 1. Changes of UV-VIS absorbance spectra due to Na⁺ irradiation

References

- [1] R. Kumar AIP Conf. Proc. 2015;1661:110010

Microstructural Effects of Al Doping on Si₃N₄ Irradiated with Swift Heavy Ions

Vuuren Arno Janse¹⁾, Skuratov Vladimir²⁾, Ibraeva Anel³⁾, Zdorovets Maxim³⁾

¹⁾Centre for HRTEM, Nelson Mandela University, Port Elizabeth, South Africa

²⁾Flerov Laboratory for Nuclear Research, Joint Institute for Nuclear Research, Dubna, Russia

³⁾Institute of Nuclear Physics, Astana, Kazakhstan

Inert matrix (IM) fuel hosts have been suggested as a means of processing transuranic waste products resulting from the nuclear fuel cycle [1]. These materials will be subjected to irradiation by high energy fission fragments in the nuclear reactor environment [1]. Si₃N₄ is part of a larger group of nitride ceramics currently considered as candidate materials for IMs [2, 3]. Its physical properties make it well suited to reactor conditions [3, 4]. However, to prove the viability for nuclear applications the radiation stability must be tested. In this investigation, swift heavy ions (SHIs) are therefore used to simulate the effects of fission fragments (FFs) on the microstructure of Al doped Si₃N₄. In addition to the analysis of the radiation stability the microstructure of latent ion tracks is studied. The mechanisms involved in the process of latent track formation, through electronic energy deposition, in radiation resistant materials are still unconfirmed and it is therefore important, from a fundamental point of view, to obtain experimental data materials with varying properties to determine the true mechanisms involved in track formation. To simulate the effects of SHIs the samples were irradiated with Xe and Bi ions, with energies ranging from 167 MeV to 2.6 GeV and temperatures ranging from LNT to 700°C at the INF and FLNR, JINR cyclotrons. These irradiation parameters allow the determination of electronic energy deposition effects. The microstructure of the irradiated material was studied using Transmission Electron Microscopy Techniques.

References

- [1] Lee Y.-W. et al., Metals and Materials International; 2001; 7:159.
- [2] Nappé, J.C. et al., Nucl. Instr. and Meth. in Phys. Res. B: 2011; 269:100
- [3] Yamane, J. et al., Progress in Nuclear Energy; 2008; 50:621.
- [4] Zinkle, S.J. et al.; Nucl. Instr. and Meth. in Phys. Res. B; 2002, 191:758.

Optical Properties of Mn and Bi Ion Implanted and Low Temperature MBE – doped GaAs Layers

Yastrubchak O.^{1,2)}, Gluba L.^{2,3}, Żuk J.²⁾, Tataryn N.⁴⁾, Drożdźiel A.²⁾, Grudziński W.²⁾, Turek M.²⁾, Mamykin S.¹⁾, Borkovska L.¹⁾, Kolomys O.¹⁾, and Sadowski J.^{5,6,7)}*

¹⁾*V.E. Lashkaryov Institute of Semiconductor Physics, National Academy of Sciences of Ukraine, 03028 Kyiv, Ukraine*

²⁾*Maria Curie-Skłodowska University, Maria Curie-Skłodowska Sq.1, 20-031, Lublin Poland*

³⁾*Institute of Agrophysics, Polish Academy of Sciences, Doświadczalna 4, 20-290 Lublin, Poland*

⁴⁾*National Technical University of Ukraine “Igor Sikorsky Kyiv Polytechnic Institute”, Kyiv 03056, Ukraine*

⁵⁾*Institute of Physics, Polish Academy of Sciences, Aleja Lotników 32/46, PL-02668 Warsaw, Poland*

⁶⁾*MAX-IV laboratory, Lund University, P.O. Box.118, 22100 Lund, Sweden*

⁷⁾*Department of Physics and Electrical Engineering, Linnaeus University, SE-391 82 Kalmar, Sweden*

The multicomponent alloys: (Ga,Mn)As, Ga(Bi,As) and (Ga,Mn)(Bi,As) are promising materials for optoelectronic and spintronic device applications. Ga(Bi,As) is operating in infrared due to shrinkage of its bandgap towards the important in telecommunication 1100-1600 nm region, depending on the Bi content. In the (Ga,Mn)As alloys the semiconducting and ferromagnetic properties are combined. (Ga,Mn)(Bi,As) is potentially important in spintronic because of a large value of spin-orbit splitting energy.

We report the investigation results of Mn and Bi ion implanted GaAs subsequently annealed at temperatures from 200 to 550 °C. The 100 nm thick (Ga,Mn)As, Ga(Bi,As) and (Ga,Mn)(Bi,As) layers for this study have been prepared at approximately 230°C on semi-insulating (001) GaAs substrates with the low temperature MBE growth technique. Micro-Raman and photorefectance spectroscopy as well as spectroscopic ellipsometry have been utilized to characterize the synthesized (Ga,Mn)As, Ga(Bi,As) and (Ga,Mn)(Bi,As) crystalline layers.

Micro-Raman spectroscopy show GaBi – related mode at 185 cm⁻¹ which is present for the ion implanted samples annealed at all temperatures and in the LT-MBE epitaxial layers. The position of GaAs LO phonon peak and its half-width indicate a very good recovery of post-implantation radiation damage. In (Ga,Mn)As and (Ga,Mn)(Bi,As) additionally coupled free hole plasmon-LO phonon related mode (CPPM) is observed. With further increase of Mn concentration the CPPM mode starts to dominate the spectra, simultaneously with its energy shifted towards the TO-phonon-line wavenumber. This is the direct indication of an increasing holes density, which can be quantified from the full line-shape fitting, performed using generalization of Drude theory.

The advanced optical investigations of the described above set of the GaAs/(Ga,Mn)As and GaAs/(Ga,Mn)(Bi,As) heterostructures with the combined photorefectance and spectroscopic ellipsometry methods in a wide range of wavelengths (from 2000 nm to 150 nm) will be presented. Comparing the evolution of the optical transitions at E_0 , E_{SO} with those at E_1 and $E_1 + \Delta_1$ optical-transition spectral areas allows for better understanding the band structure modification in (Ga,Mn)As and (Ga,Mn)(Bi,As).

YOUNG SCIENTISTS CONTEST
ORAL PRESENTATIONS

Intermediate-band silicon nanowires realized by ion beam hyperdoping

Berencén Y.¹⁾, Prucnal S.¹⁾, Möller W.¹⁾, Hübner R.¹⁾, Rebohle R.¹⁾, Böttger R.¹⁾, Glaser M.²⁾, Schönherr T.¹⁾, Yuan Y.¹⁾, Wang M.¹⁾, Georgiev Y.M.¹⁾, Erbe A.¹⁾, Lugstein A.²⁾, Helm M.¹⁾, Zhou S.¹⁾ and Skorupa W.¹⁾

¹⁾*Helmholtz-Zentrum Dresden-Rossendorf, Institute of Ion Beam Physics and Materials Research, Bautzner Landstraße 400, D-01328 Dresden, Germany*

²⁾*Institute for Solid State Electronics, Vienna University of Technology, Floragasse 7, A-1040 Vienna, Austria*

The intentional introduction of deep-level dopants into a semiconductor in excess of equilibrium concentrations causes a broadening of dopant energy levels into an intermediate band between the valence and conduction bands.^[1,2] This phenomenon is referred to as hyperdoping. As intermediate-band material, bulk Si hyperdoped with chalcogens or transition metals holds promises for Si-based short-wavelength infrared photodetectors and solar cells.^[3,4] Intermediate-band nanowires could potentially be used instead of bulk materials to overcome the Shockley-Queisser limit and to improve efficiency in solar cells.^[5,6]

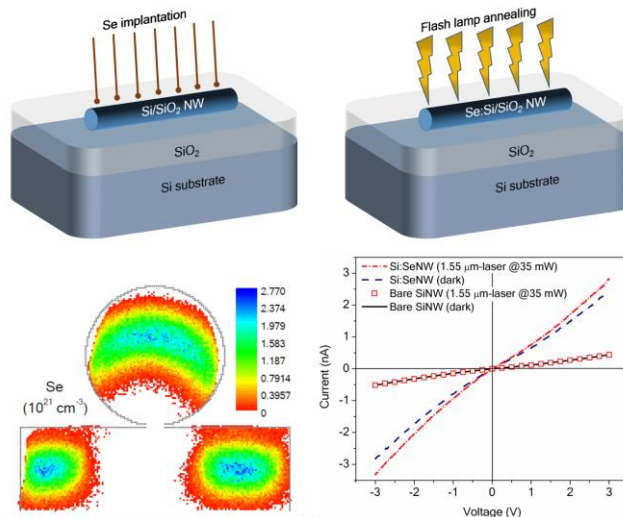


Figure 1: Hyperdoping process and sub-bandgap photoresponse of individual Si nanowires

Here, we show a CMOS-compatible method based on non-equilibrium processing for the controlled doping of Si at the nanoscale with dopant concentrations several orders of magnitude above the equilibrium solid solubility. The approach relies on using ion implantation followed by flash lamp annealing for hyperdoping Si/SiO₂ core/shell nanowires. We induce, by millisecond-flash lamp annealing, a bottom-up template-assisted solid-phase epitaxy recrystallization of the nanowires. This results in the formation of intermediate-band Se-hyperdoped nanowires which exhibit room-

temperature sub-band gap optoelectronic photoresponse when configured as a photoconductor device.

References

- [1] Sher M J, Mazur E, Appl. Phys. Lett. 2014;105:032103.
- [2] Ertekin E, Winkler M, T, Recht D, Said A J, Aziz M J, Buonassisi T, Grossman J C, Phys. Rev. Lett. 2012;108:026401.
- [3] Berencén Y, Prucnal S, Liu F, Skorupa I, Hübner R, Rebohle L, Zhou S, Schneider H, Helm M, Skorupa W, Sci. Rep. 2017;7:43688.
- [4] Mailoa J P, Akey A J, Simmons C B, Hutchinson D, Mathews J, Sullivan J T, Recht D, Winkler M T, Williams J S, Warrender J M, Persans P D, Aziz M J, Buonassisi T, Nat. Commun. 2014;5:3011.
- [5] Beard M C, Luther J M, Nozik A J, Nat. Nanotech. 2014;9:951.
- [6] Tian B, Zheng X, Kempa T J, Fang Y, Yu N, Yu G, Huang J, Lieber C M, Nature 2007;449:885.

Electrical and optical properties of SiO₂ thin layers implanted with Zn ions

*Czarnacka Karolina¹⁾, Koltunowicz Tomasz N.²⁾, Makhavikou Maxim³⁾,
Parkhomenko Irina³⁾, Komarov Fadei³⁾*

¹⁾University of Life Sciences in Lublin, Akademicka 13, 20-950 Lublin, Poland

²⁾Lublin University of Technology, Nadbystrzycka 38D, 20-618 Lublin, Poland

³⁾Belarusian State University, Praspjyekt Nyezalyezhnasti 4, Minsk, Belarus

The paper presents the results of electrical and optical measurements of thin silicon oxide layers to which zinc ions have been implanted. The 600 nm thick layers were deposited on a silicon substrate and then were annealed in air at 1023 K during 2 hours. The depth distribution of the impurity and the size of the obtained zinc nanocrystals were determined by electron microscopy.

For samples immediately after preparation and annealed, AC measurements of resistivity R_p , phase angle θ , capacity C_p and dielectric loss factor were made in function of frequency (measurement range 50 Hz-5 MHz) and measurement temperature (20 K-375 K). On this basis, the frequency-temperature dependence of conductivity σ was prepared. The strong frequency dependence of conductivity indicates that in the Zn/SiO₂ layer the conductivity takes place by hopping exchange (tunneling) of electrons between nanoparticles of the metallic phase. Moreover, after annealing, there is a clear change in the nature of conductivity at high frequencies.

The PL spectra of the as-implanted Zn/SiO₂-nanocomposite exhibit a blue-green band. This band is caused by the formation of oxygen vacancies in silicon dioxide. The intensity of this peak is observed to grow with increasing annealing temperature. Besides, a strong orange-red band was revealed in the PL spectra of the annealed sample. This emission may be attributed to the presence of oxygen interstitial/antisites. The effect of thermal annealing on light-emitting properties has been discussed.

This research was partially supported from the Polish Ministry of Science and Higher Education as a statute tasks of the Lublin University of Technology, at the Faculty of Electrical Engineering and Computer Science, 8620/E-361/S/2017 (S-28/E/2017).

“Negative Capacitance” Effect in Nanogranular Composite Films
 $(\text{Fe}_{45}\text{Co}_{45}\text{Zr}_{10})_x(\text{SiO}_2)_{(100-x)}$ Prepared by Ion-Beam Technology
 in Ar Atmosphere

*Fedotov A.S.¹⁾, Rusak D.¹⁾, Koltunowicz T.N.²⁾, Zukowski P.²⁾, Fedotova J.A.³⁾,
 Kasiuk J.V.³⁾, Ronassi Ali Arash⁴⁾*

¹⁾Belarusian State University, 4, Nezavisimosti av., 220030 Minsk, Belarus

²⁾Lublin University of Technology, 38a, Nadbystrzycka Str., 20-618 Lublin, Poland

³⁾Reserch Institute for Nuclear Problems of Belarusian State University, 11, Bobruiskaya Str., 220030 Minsk, Belarus

⁴⁾Department of Physics, Payame Noor University, The Islamic Republic of Iran

One of the problems of modern integrated microelectronics is the formation of electrical elements that perform the role of inductance and capacitance, which have micron and submicron sizes and can be used in hybrid (HICs) and conventional (ICs) integrated circuits. The main methods for creating IC elements with inductive admittance are their imitation with the help of various kinds of circuitry techniques (for example, by creating phase shifters – gyrators) or the formation of Archimedian spirals [1]. Because of the limitation of the IC size, the inductance of such inductors is usually less than $15 \mu\text{H}/\text{cm}^2$ [1]. Simulation of inductances by circuitry also leads to an inefficient use of the chip area and relatively small values of equivalent inductances. In this connection, there arises the actual task of forming small-size non-coil-like (planar) elements with the properties of inductances based on metal-dielectric nanogranular composite materials in the framework of the technology for fabricating silicon-based ICs and HICs. The “negative capacitance” effect described in such systems [1-3] directly indicates the formation of an inductive contribution to the reactive part of the admittance under certain conditions.

In this work, we established the conditions under which the inductive component of the admittance prevails over capacitive. To achieve this purpose, we performed complex analysis of the chemical and structural-phase composition, as well as the frequency and temperature dependences of admittance. It is shown that these films in the range $20 < x < 79$ at.% have a nanogranular structure containing metal nanoparticles with an average diameter of 2-7 nm, which are homogeneously distributed in the SiO_2 dielectric matrix. Structural disordering of and is established. The Mössbauer spectroscopy and XRD method have revealed that composite films consist of crystalline CoFeZr nanosized “core” with FCC structure which are embedded into an amorphous dielectric matrix SiO_2 and covered with FeCo -based native oxide “shells”. This leads to a shift of the percolation threshold to values of $x_c \sim 70$ at.% and possessing of “negative capacitance” effect. Based on the investigation of the frequency dependences of the reactive part of the admittance at different temperatures,

equivalent circuits of this type films have been developed and the temperature dependences of their capacitive, inductive and resistive contributions have been extracted using special fitting procedure.

References

- [1] N.A. Poklonski, et al., *Semiconductors* 40 (2006) 803-807
- [2] G.B. Parravicini, et al., *Appl. Phys. Lett.*, 85 (2004) 302-309
- [3] A.M. Saad, et al., *Reviews on Advanced Materials Science*, 8 (2004) 34-40

Formation of buried, electrically insulating layer by proton implantation in GaN for vertical leakage current reduction

Kozubal M.¹⁾, Barcz A.^{1,2)}, Pągowska K.¹⁾, Jakiela R.²⁾, Taube A.¹⁾, Ratajczak J.¹⁾, Wojciechowski T.²⁾, Celler G.K.³⁾

¹⁾*Institute of Electronic Technology, Al. Lotników 32/46, 02-668 Warsaw, Poland*

²⁾*Institute of Physics, PAS, Al. Lotników 32/46, 02-668 Warsaw, Poland*

³⁾*Institute for Advanced Materials, Devices, and Nanotechnology, Rutgers University, Piscataway, NJ 08854, USA*

Epitaxial AlGaIn/GaN HEMT structure can be manufactured on different substrates like Al₂O₃, SiC, Si or bulk monocrystalline GaN. For the application in the microwave electronics, the HEMT structures must be grown on the semi-insulating substrate. On the other hand, HEMTs for the power electronics can be produced on the n-type substrate which is cheap, easily available and exhibits good thermal conductivity. In this case, though, the buffer layer is required to increase the breakdown voltage but problems with increased time and cost of production as well as stress in the layer arise. One of the alternative solutions is the use of ion implantation to produce buried, electrically isolating layer to reduce the vertical leakage current.

The aim of this study was the formation of a buried, highly damaged, planar layer by proton implantation with doses of $\sim 10^{17}$ cm⁻² to GaN, followed by subsequent two-step annealing. The crucial issue was to reduce damage population and resistivity in the near-surface regions, above the buried layer, as they would potentially serve as active regions of active devices. This goal was achievable due to a characteristic of light H⁺ implantation, where defects in the material are produced predominantly near the ion projected range, whereas in the region above the ions lose energy mainly in electronic collisions.

Investigation of the proton-implanted gallium nitride concerned the structural and electrical properties of both the near-surface region and buried layer. The analytical methods employed TEM, RBS/c, SIMS and electrical characterization. The process results in the formation of a localized layer, consisting mainly of cavities or bubbles filled with hydrogen. Post-implantation annealing was found to promote accumulation of defects into a narrow band, forming buried layer, rich in defects. The vertical resistance of GaN containing such layer was found to be four orders of magnitude higher than that for the as-grown GaN. Furthermore, in the near-surface region, the reduction of defects to nearly the level of as-grown material was observed, as well as lowering of sheet resistivity and restoration of both the initial carrier concentration and mobility.

The research conducted confirmed the possibility of a buried, insulating layer formation while maintaining the initial electrical parameters of the sub-surface region. This electrical isolation can potentially be applied in the construction of power electronic devices on AlGaIn/GaN HEMT structures in order to reduce the vertical leakage current.

Cavitation erosion resistance of plasma sprayed ceramic coatings

Łatka L.^{1}, Szala M.², Michalak M.¹, Sokołowski P.¹*

¹Department of Materials Science, Strength and Welding, Faculty of Mechanical Engineering, Wrocław University of Science and Technology, 5 Łukasiewicza Street, 50-371 Wrocław, Poland

²Department of Materials Engineering, Mechanical Engineering Faculty, Lublin University of Technology, 36D Nadbystrzycka Street, 20-618 Lublin, Poland

In the paper results of cavitation erosion test of ceramic coatings were presented. The coatings were manufactured by powder plasma spraying. The plasma spray experimental parameters included two variables: (i) spray distance varying from 80 to 100 mm and (ii) torch linear speed varying from 300 to 500 mm/s. Microhardness measurements were carried out, as well as, indentation fracture toughness using Vickers penetrator.

Cavitation tests were conducted on vibratory test rig according do ASTM G-32 standard. The influence of coatings' microstructure and microhardness on cavitation erosion resistance was investigated. The cavitation erosion mechanism was examined by using macroscopic and SEM microscopy. Observations were conducted in specified areas of coatings in defined times of exposition.

* leszek.latka@pwr.edu.pl

Structure and optical properties of ZnSe/SiO₂-nanocomposite formed by ion implantation

Makhavikou Maksim¹⁾, Komarov Fadei¹⁾, Kuchinsky Peter¹⁾, Milchanin Oleg¹⁾, Vlasukova Ludmila²⁾, Parkhomenko Irina²⁾, Romanov Ivan²⁾, Żuk Jerzy³⁾ and Wendler Elke⁴⁾

¹⁾A.N.Sevchenko Institute of Applied Physics Problems, Kurchatov Str. 7, 220045 Minsk, Belarus

²⁾Belarusian State University, Independence Ave. 4, 220030 Minsk, Belarus

³⁾Maria Curie-Skłodowska University, Pl. M. Curie-Skłodowskiej 1, 20-031 Lublin, Poland

⁴⁾Friedrich-Schiller University Jena, Max-Wien-Platz 1, D-07743 Jena, Germany

Selenide-based nanostructural materials, such as wide-band gap A₂B₆ semiconductors, have been studied intensively due to their wide application in the fields of light-emitting devices, solar cells, sensors, and optical recording materials.

In this study, thin layers of SiO₂ (600 nm) were implanted at 500°C with Zn⁺ (150 keV, 4×10¹⁶ cm⁻²) and Se⁺ (170 keV, 4×10¹⁶ cm⁻²) ions. For a part of samples the order of Zn and Se ions implantation was inverted. After implantation these samples were annealed at 1000°C for 3 min in Ar atmosphere. The combination of elemental analysis (RBS), structural (XTEM) and optical (RS and PL) techniques have been used to identify the phases formed and to correlate the optical behaviour of the ZnSe/SiO₂ nano-composite.

Using RBS and TEM techniques it was shown that the sequence of implantation affects elemental composition and structural properties of synthesized clusters. Based on RS and PL data, the silicon oxide films for which Zn ions implanted first exhibited higher crystalline quality of the precipitated ZnSe nanoclusters. Blue (ZnSe band edge emission), green and red (ZnSe deep defect level emission) bands were revealed in the PL spectra of the as-implanted and annealed composites. The PL spectral features observed in the blue region are due to quantum-size effects in the ZnSe nanocrystals embedded into silicon dioxide matrix. The intensity ratio of the deep defect band to the near band edge band of ZnSe is higher for the Se implantation at first. The effect of rapid thermal annealing on structural and light-emitting properties has been discussed.

Proton beam machining of poly(tetrafluoroethylene)

Nagy Gy.^{1,2)}, Kerékgyártó R.²⁾, Csik A.¹⁾ and Rajta I.¹⁾

¹⁾*Institute for Nuclear Research (Atomki), Hungarian Academy of Sciences, Debrecen, Hungary*

²⁾*University of Debrecen, Institute of Physics, Debrecen, Hungary*

Poly(tetrafluoroethylene) (PTFE) has many desirable physical and chemical properties, thus it is a widely used material in industry. Because of this, its responses given to different kinds of radiations are intensively researched fields of science for a long time. It is known from the literature, that few MeV proton irradiation can cause either indentations or protrusions, depending on the irradiation circumstances. Both can be potentially applied in micro- or nanofluidical and -electromechanical systems.

In the present work we have investigated the morphological changes of PTFE surface caused by low current density proton beam irradiation in vacuum. The 1 MeV proton beam was supplied by the 5 MV Van de Graaff accelerator of Atomki. With the help of the slit system and focusing quadrupole lenses of the scanning nuclear microprobe beamline, the current density of the incident beam was varied between 10-100 000 pA/mm². According to model calculations the macroscopic temperature of the target material increases only a few degrees even in case of the highest current density. The applied ion fluence was between 0.1-2 500 nC/mm² for each current density. The changes of the surface morphology were investigated by interference contrast microscopy, surface profilometry and scanning electron microscopy.

The results show that at each current density the surface can be etched, and the etching depth is increasing with increasing ion fluence up to a certain point. However, in each case there is a threshold value, where the process turns back. First, the etching depth starts to decrease. Later, by further increasing the delivered ion fluence, an opposite process begins and the surface becomes humped. In the presentation, the quantitative results and the explanations will be presented, and comparison with a high current density (focused beam) irradiation will be given. Finally, a possible application in proton beam writing will be shown.

Hyperdoping Si with Se by ion implantation followed by pulsed laser melting

Nechaev N.S.¹⁾, Komarov F.F.²⁾, Ivlev G.D.²⁾, Vlasukova L.A.¹⁾, Parkhomenko I.N.¹⁾, Romanov I.A., Wendler E.³⁾

¹⁾Belarusian State University, Independence Ave. 4, Minsk, Belarus

²⁾A.N. Sevchenko Institute of Applied Physical Problems, Belarusian State University, Kurchatova st. 5, Minsk, Belarus,

³⁾Friedrich-Schiller-Universität Jena, Max-Wien-Platz 1, Jena, Germany

Silicon is widely used for fabricating optoelectronic devices, but silicon's indirect 1.12 eV bandgap limits its applications in the infrared (IR) field. Silicon hyperdoped with Se is a promising candidate for IR photodetectors and efficient solar cells because of its sub-band gap absorption [1].

In this work silicon was hyperdoped with selenium by ion implantation ($E = 125$ keV, $D = 1 \times 10^{16}$ cm⁻²) with subsequent pulsed laser melting (PLM). Pulsed laser melting was performed by ruby laser (690 nm, 70 ns FWHM) in conditions described in [2]. Pulse energy density W was set at 1.5, 2 and 2.5 J/cm². For each W two specimens were irradiated by one and three laser shots respectively. Rutherford backscattering with channeling (RBS/C) was performed to obtain impurity depth distributions along with silicon crystallinity profiles and substitutional part of implanted species. Photoluminescence spectra (Fig. 1), Raman scattering spectra, SEM, TEM and optical microscopy images of near-surface region were obtained.

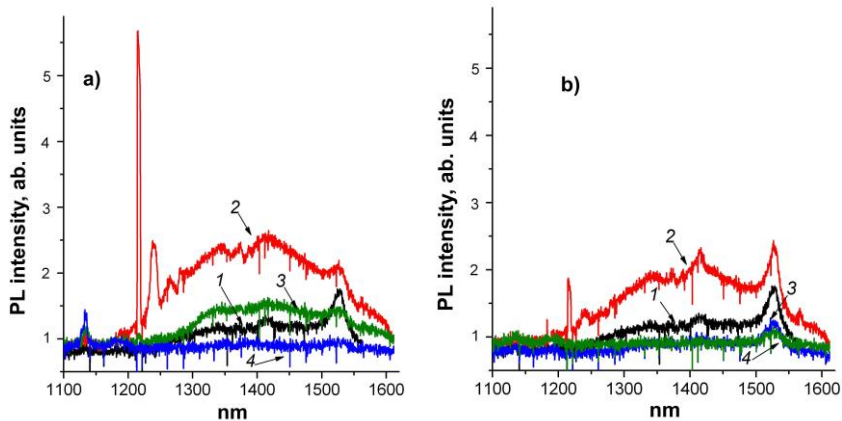


Figure. 1: Photoluminescence spectra of Se-implanted silicon before (1) and after PLM with one (a) and three (b) pulses at energy densities W of 1.5 (2), 2 (3), 2.5 J/cm² (4)

References

- [1] I. Umezu. et al, J. Appl. Phys. 2013, 113:213501.
 [2] G.D. Ivlev et al, Appl. Surf. Sci. 1999, 143:265.

Overview of latent track morphology in crystalline insulators from direct observation with TEM

O'Connell J.H.¹⁾ and Skuratov V.A.²⁾

¹⁾*Centre for HRTEM, Nelson Mandela University, Port Elizabeth, South Africa*

²⁾*Flerov Laboratory for Nuclear Research, Joint Institute for Nuclear Research, Dubna, Russia.*

Swift heavy ion (SHI) induced crystal damage is usually associated with so-called latent tracks. These consist of lines of disordered material which was exposed to high levels of energy deposition during passage of a SHI. The material response during such interactions is typically described by a temperature spike model [1] which is dependent on the thermomechanical properties of the target material as well as the electronic energy loss (S_e) of the ion in question. This model depends strongly on electron-phonon coupling coefficients which are not trivial to obtain. Measurements of experimental track diameters can be fed back into models in order to estimate these coefficients but this in turn depends on a robust, reliable diameter measurement which itself is not well defined for certain materials as will be shown.

In this paper, we describe the general morphology of latent tracks in crystalline insulators of varying crystalline structure and composition as observed by transmission electron microscopy (TEM) in order to elucidate structure/composition dependent trends. Irradiations were performed using various ions, fluences and stopping powers on bulk targets with subsequent thinning to electron transparency in both cross sectional and plan view geometry.

It was found that multi-component, complex structures tend to form mostly continuous, cylindrical, amorphous tracks of relatively large diameter together with amorphous surface hillocks. On the other hand, simpler structures tend to form discontinuous tracks composed of strained crystalline regions subtending more continuous near-surface, amorphous zones which subtend crystalline hillocks.

[1] Toulemonde, M. et al. Nucl. Instr. Meth. B 166–167 (2000) 903-912.

Investigation of atomic depth distribution and chemical composition in multilayer structures of TiO₂/SiO₂/Si after ion irradiation

Phuc T.V.^{1,2)}, Kulik M.^{2,3)}, Kolodynska D.⁴⁾, Kobzev A.P.²⁾, Khiem L.H.¹⁾, Žuk J.³⁾, Turek M.²⁾

¹⁾*Institute of Physics, 10 Dao Tan, Ba Dinh, Ha Noi, Viet Nam*

²⁾*Frank Laboratory of Neutron Physics, Joint Institute for Nuclear Research, 141980 Dubna, Russia*

³⁾*Institute of Physics, Maria Curie-Skłodowska University, pl. M. Curie-Skłodowskiej 1, 20-031 Lublin, Poland*

⁴⁾*Chemical Department, Maria Curie-Skłodowska University, pl. M. Curie-Skłodowskiej 2, 20-031, Lublin, Poland*

In this study the changes in depth distributions of atomic compositions in multilayer structures TiO₂/SiO₂/Si were investigated after ion implantation. The samples were irradiated by Ne⁺ and Xe⁺ ions with the same energy (150 keV) and fluence (3×10^{16} ions/cm²). The irradiation was performed on the UNIMAS ion implanter at Maria Curie - Skłodowska University, Lublin. This process was carried out at the room temperature. The depth profiles of elements in the samples were analyzed by the Rutherford Backscattering Spectrometry (RBS) method. The RBS experiment was performed on the EG-5 accelerator in the Frank Laboratory of Neutron Physics, JINR, Dubna. With a help of the RBS method, the changes of atomic concentration as a result of implantation with different masses of ions were investigated using the SIMNRA code. It was found the existence of the transition layer between the TiO₂ and SiO₂ layers.

The thickness of the transition layer grows with the increasing mass of the implanted ions. In addition, the chemical composition of the near-surface layers was investigated using the X-ray photoelectron spectroscopy (XPS) method. Based on the XPS study for the virgin and implanted samples, it was found that the concentration of TiO increases with the decreasing of TiO₂ concentration as a results of implantation with Ne⁺ and Xe⁺ ions. It was found that the content of atomic Ti decreases because the Ti atoms form the chemical bonds with oxygen atoms from the air. The surface layer is more damaged

by ions of larger mass. The changes of chemical composition can be explained by formation of disorder in the implanted samples. The distribution of different kinds of disorder like atomic displacements and vacancies was obtained by means of the computer code Stopping and Range of Ions in Matter (SRIM)-2008. Changes of atomic contents and depth distribution of the displacement atoms were observed in the near-interface area of the layers after implantation. It was found that after ion implantation the target atoms were displaced not only within the layer that contains them but also displaced into the contiguous layer across the interface. This effect explained the formation of the transition layers.

Optical properties of TlGaSe₂ before and after ion implantation with H⁺ and He⁺

Samadov S.^{1,2*}, *Samadov O.*¹⁾, *Kulik M.*^{2,3)}, *Pysznik K.*³⁾, *Olejniczak A.*^{2,4)},
*Najafov A.*¹⁾, *Huseynov N.*¹⁾, *Huseynov E.*¹⁾

¹⁾*Institute of Radiation Problems, ANAS, Baku, Azerbaijan,*

²⁾*Joint Institute for Nuclear Research, Dubna, Russia,*

³⁾*Institute of Physics, Maria Curie-Skłodowska University, Lublin, Poland,*

⁴⁾*Faculty of Chemistry, Nicolaus Copernicus University, 87-100 Torun, Poland,*

The optical properties and chemical composition of the TlGaSe₂ crystals were investigated before and after ion irradiation using Raman spectroscopy, X-ray photoelectron spectroscopy (XPS) and scanning electron microscopy (SEM). The surfaces of TlGaSe₂ were implanted with He⁺ and H⁺ ions. The energy of the ion beam was 150 keV.

The impact of the ions interaction with the atoms in crystallographic structure of TlGaSe₂ on changes its optical properties was investigated by the Raman spectroscopy at the room temperature. The spectra were collected in the range of 50 to 2000 cm⁻¹. It was observed that the lines corresponding to the vibrations of atoms in the virgin crystals broadened upon ion implantation. Additionally, the relative intensities of these lines have changed and some of them disappeared. These effects depended on the mass of ions with which the samples were irradiated. The chemical composition of the near surface layers was examined by XPS. At a fluency of 10¹⁶ cm⁻² a significant reduction in the surface Tl content was observed. For 150 keV He⁺ ion-irradiation the effect was more pronounced and was accompanied by elimination of Se atoms from the surface. He⁺ ion-irradiated specimens have also demonstrated more significant broadening of Ga 3d and Tl 4f spectral features what can be related to higher efficiency of both irradiation-induced build-in of oxygen (gallium oxide formation) and structural disordering.

* Samirsamedov.rpi@gmail.com

Quantum entanglement, and electronic transport in quantum dots system

Tooski Sahib Babaee

Iran Elite Young Researcher Club, Azad University, Malayer, Iran

We present studies of three electrons confined in a triple quantum dot with one of the dots connected to metallic electrodes which is modeled by a three-impurity Anderson Hamiltonian. It is focused on the pairwise quantum entanglement of a three-spin system and its relation to the thermodynamic and transport properties. It is shown that two many-body phenomena compete with each others, the Kondo effect and the inter-dot exchange interactions. In fact, coupling triple quantum dots to the electrodes results a formation of the Kondo singlet which can switch the entanglement due to the interplay between the interdot spin-spin correlations and various Kondo-like ground states. The quantum phase transition between unentangled and entangled states is studied quantitatively and the corresponding phase diagram is explained by exactly solvable four spin model. Although the work concentrates on the system of quantum dots, the model is more general and can be applied to the Kondo physics in molecules with a triangular symmetry [1].

References

- [1] S. B. Tooski, A. Ramšak, B. R. Bułka, *Physica E* 2016; 75:345-352.

Extended infrared photoresponse in room-temperature Si hyperdoped with Te

Wang Mao^{1,2}, Berencén Y.¹, Prucnal S.¹, García-Hemme E.³, Hübner R.¹, Yuan Ye^{1,2}, Xu Chi^{1,2}, Rebohle L.¹, Böttger R.¹, Heller R.¹, Schneider H.¹, Skorupa W.¹, Helm M.^{1,2} and Zhou Shengqiang¹

¹*Helmholtz-Zentrum Dresden-Rossendorf, Institute of Ion Beam Physics and Materials Research, Bautzner Landstr. 400, 01328 Dresden, Germany*

²*Technische Universität Dresden, 01062 Dresden, Germany*

³*Univ. Complutense de Madrid, Departamento de Física Aplicada III (Electricidad y Electrónica), 28040 Madrid, Spain*

Presently, room-temperature infrared sub-band-gap photoresponse in Si is of great interest for the development of on-chip complementary-metal-oxide-semiconductor (CMOS)-compatible photonic platforms [1]. One of the most promising approaches to further extend the photoresponse of Si to the mid- and far-infrared (MIR/FIR) ranges consists of introducing deep-level dopants into the Si band gap at concentrations in excess of the solid solubility limit [2]. In this work, we demonstrate strong room-temperature sub-band-gap photoresponse of photodiodes based on Si hyperdoped with tellurium [3]. A CMOS-compatible approach of combining ion implantation with pulsed laser melting was applied to synthesize single-crystalline and epitaxial Te-hyperdoped Si layers with a Te concentration five orders of magnitude above the solid solubility limit. Driven by increasing Te concentration, both the insulator-to-metal transition and a band-gap renormalization are observed. The sub-band optical absorption in the resulting Te-hyperdoped Si layers is found to increase monotonically with increasing Te concentration and extends well into the MIR/FIR ranges (1.4 to 25 μm). Importantly, the MIR/FIR optoelectronic response from Te-hyperdoped Si photodiodes is demonstrated to be related with known Te deep-energy levels into the Si band-gap. This work contributes to pave the way towards establishing a Si-based broadband infrared photonic system operating at room temperature.

References

- [1] R. Soref, Nat. Photonics **9**, 358 (2015).
- [2] Y. Berencén, et al. Sci. Rep. **7**, 43688 (2017).
- [3] M. Wang, et al. Phys. Rev. Appl. submitted (2018).

p-type co-doping effect in (Ga,Mn)As: Mn lattice location and magnetic phase transition

Xu Chi^{1,2)}, Yuan Ye^{1,2)}, Wang Mao^{1,2)}, Böttger R.¹⁾, Helm M.^{1,2)} and Zhou Shengqiang¹⁾

¹⁾*Helmholtz-Zentrum Dresden Rossendorf, Institute of Ion Beam Physics and Materials Research, Bautzner Landstrasse 400, D-01328 Dresden, Germany*

²⁾*Technische Universität Dresden, D-01062 Dresden, Germany*

III-Mn-V based diluted magnetic semiconductors offer an opportunity to explore various aspects of carrier transport in the presence of cooperative phenomena [1]. In this work, we demonstrate the efficiency of an alternative approach to control the carrier state through involving one magnetic impurity Mn and one electrically active dopant Zn. Mn-doped and Zn co-doped GaAs films have been prepared by combining ion implantation and pulsed laser melting, followed by a systematic investigation on the magnetic and transport properties of (Ga,Mn)As by varying Mn concentration as well as by Zn co-doping. Changes of electrical, magnetic and magneto-transport behavior of the investigated (Ga,Mn)As were observed after co-doping with Zn. The changes are caused by interstitial Mn atoms which are transferred from substitutional sites or formation of Mn-Zn dimers.

Reference

[1] T. Dietl, *Semicond. Sci. Technol.* **17**(2002)377.

POSTER PRESENTATIONS

Influence of the proton irradiation on surface structure and physical mechanical properties of tungsten

Aldabergenova T.¹⁾, Wieleba W.²⁾, Kislitsin S.³⁾

¹⁾*Al-Farabi Kazakh National University, Almaty, Kazakhstan*

²⁾*Wroclaw University of Technology, Wroclaw, Poland*

³⁾*Institute of Nuclear Physics ME RK, Almaty, Kazakhstan*

Tungsten is considered as a promising plasma face material for divertor and first wall of the thermonuclear reactor due to its properties such as high melting point and thermal conductivity, low surface sputtering coefficient and other characteristics [1]. Irradiation with thermonuclear plasma ions, and especially helium ions, leads to degradation

of tungsten properties caused by changes in surface structure, such as the appearance of blisters and flaking of the surface. This work is aimed at the study of changes in the properties of the surface of tungsten irradiated with protons and of comparing to effects of irradiation with low-energy alpha-particles.

Irradiation of W samples with 1 MeV protons to $5 \cdot 10^{16}$ and 10^{17} cm⁻² fluences at room temperature was carried out at the UKP-2-1 INP accelerator in Almaty. According to SRIM calculations, the projective range of protons with an energy of 1 MeV in tungsten is ~ 6 μm , straggling is ~ 0.65 μm , i.e. hydrogen lies at a sufficiently large distance from the irradiated surface.

Studies carried out by scanning electron, atomic-force microscopy and measurements of microhardness have shown that irradiation to a fluence of 5×10^{16} cm⁻² has little effect on the surface structure, microhardness value also remains practically unchanged also. At an irradiation fluence of 10^{17} cm⁻², chaotically distributed hillocks appear on the surface and microhardness increased by 22%.

The comparison with alpha-particles irradiation show that alpha-particles causes significantly larger changes in surface structure and mechanical properties.

References

[1] Bolt H., Barabash V., Krauss W., et al, J. Nucl. Mater. 2004; 329-333, 66.

Research on multiple excitations probability in ion-implanted silicon structures in the aspect of possible photovoltaic applications

Billewicz P.¹⁾, Węgierek P.¹⁾, Grudniewski T.²⁾

¹⁾Lublin University of Technology, Nadbystrzycka 38 D, 20-618 Lublin, Poland

²⁾Pope John Paul II State School of Higher Vocational Education, Sidorska 95/97, 21-500 Biala Podlaska, Poland

In the papers [1,2] some mathematical models of carrier charge transfer mechanisms in impurity photovoltaic (IPV) structures have been proposed. It has been suggested that some defects allow electrons to be excited from the valence band to the conduction band via the mid-gap defect level through the absorption of previously lost sub-band gap photons.

The aim of this work is to investigate the probability of multiple excitation in silicon structures defected by ion implantation. Conducted experiment included samples of silicon with an initial resistivity changing from 0,01 $\Omega\cdot\text{cm}$ to 10 $\Omega\cdot\text{cm}$, doped with boron, phosphorus and antimony. Tested samples were exposed to the implantation of Ne^+ ions of energy 100 keV and fluences ranging from 10^{13} cm^{-2} to $4\cdot 10^{14} \text{ cm}^{-2}$, followed by isochronous thermal annealing in the temperature ranging from 373 K to 873 K. Stated conclusions concern the possibility of applications of ion implantation in order to introduce particular defects of crystal lattice to improve silicon solar cell absorption rate.

References

- [1] Brown A.S., Green M.A., Journal of Applied Physics 2002;92:1329.
- [2] Hai Huang, Jianghua Li, Modern Physics Letters B 2013;27:1350116-1.

Temperature dependences of resistivity of metal-semiconductor ohmic contacts in silicon structures dedicated to photovoltaic applications

Billewicz P.¹⁾, Węgierek P.¹⁾, Grudniewski T.²⁾

¹⁾Lublin University of Technology, Nadbystrzycka 38 D, 20-618 Lublin, Poland

²⁾Pope John Paul II State School of Higher Vocational Education, Sidorska 95/97, 21-500 Biała Podlaska, Poland

In our previous works [1, 2] it was shown that in boron-doped silicon it is possible to observe the state of thermal stability of resistivity, after being subjected to the ion implantation of specific parameters and subsequent isochronous thermal annealing. Therefore, it is reasonable to conduct further research aimed at determination of the effect of ion implantation conditions on the electrical parameters of silicon in terms of evaluation of the applicability of formed structures in the process of PV cells production.

The superiority of application of ion implantation over diffusion in order to form $n-n^+$ structures has been already confirmed in [3]. The main purpose of this article is to present results of the research directed into influence of ambient temperature on the resistivity of metal-semiconductor ohmic contacts. As it is known, such structures are commonly used in silicon solar cells, where it is significantly important to minimize contact resistance due to the internal resistive losses in the solar cell, which deteriorate photoconversion efficiency. In the scope of this work we investigated the way which ion implantation could affect the resistivity of metal-semiconductor ohmic contacts in the aspect of photovoltaic applications.

References

- [1] Węgierek P., Billewicz P., *Acta Physica Polonica A* 2015;128:943.
- [2] Węgierek P., Billewicz P., *Acta Physica Polonica A* 2015;128:875.
- [3] Sachenko A.V., Belyaev A.E., Boltovets N.S., Vinogradov A.O., Pilipenko V.A., Peilitskaya T.V., Anischik V.M., Konakova R.V., Korostinskaya T.V., Kostilyov V.P., Kudryk Ya.Ya., Lyapin V.G., Romanets P.N., Sheremet V.N., *Semiconductor Physics, Quantum Electronics & Optoelectronics* 2014;17:1.

Electrical characterization of ceramic matrix nanocomposites with using of impedance spectroscopy

Boiko O.^{1}, Fedotov A.K.²⁾, Fedotova J.³⁾*

¹⁾ Lublin University of Technology, 20-618 Lublin, Poland

²⁾ Belarusian State University, 220030 Minsk, Belarus

³⁾ NC PHEP Belarusian State University, 220040 Minsk, Belarus

The objective of the present paper have been to perform electrical characterization of ferromagnetic alloy-ferroelectric ceramic $(\text{FeCoZr})_x(\text{PbZrTiO}_3)_{(100-x)}$ nanocomposites using impedance spectroscopy approach. Tested materials were obtained by using ion-beam sputtering method. The synthesis atmosphere included argon and oxygen technological gases with different partial pressures. Nanomaterials demonstrate granular structure, FeCoZr metallic alloy nanoparticles (parameter x is the metallic phase concentration) disorderly surrounded by PbZrTiO₃ ceramic matrix.

The AC electrical parameters measurements, such as conductivity σ (fig. 1a), real Z' and imaginary part Z'' of complex impedance (fig.1b), were obtained for ambient temperature range of 81K-238K and measuring frequencies ranging from 50 Hz to 5 MHz. Sample x_2 was subdued to thermal treatment in tubular furnace at temperature of $T_a = 398$ K.

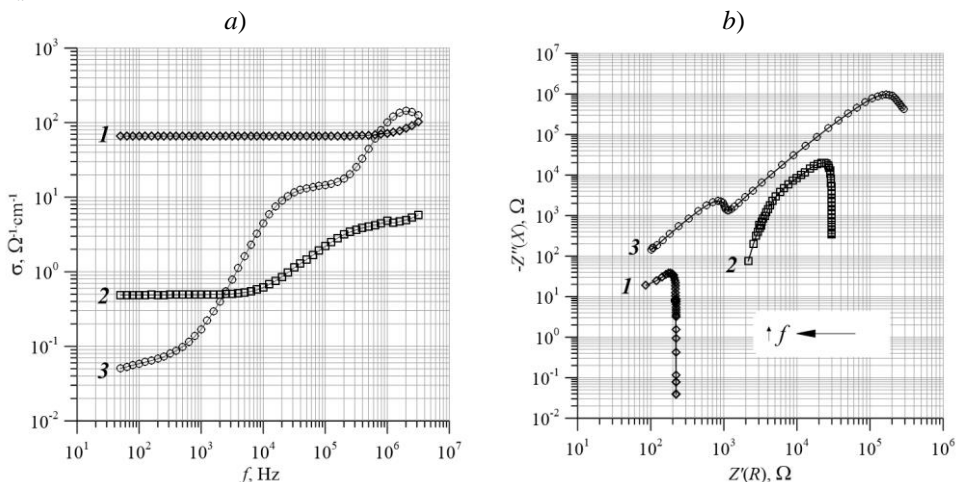


Figure 1. Conductivity versus frequency (a) and Cole-Cole's impedance plots (b) for $(\text{FeCoZr})_x(\text{PbZrTiO}_3)_{(100-x)}$ nanocomposites: 1 – $x_1 = 67.6$ at.% ($T_p = 81$ K, nonannealed), 2 – $x_2 = 73.2$ at.% ($T_p = 178$ K, $T_a = 398$ K) and 3 – $x_3 = 90.0$ at.% ($T_p = 238$ K, nonannealed)

The $\sigma(f)$ and $Z''(Z')$ characteristics are strongly related and demonstrate different behaviors: in case of sample x_1 conductivity doesn't depend on f and Z'' shows similar situation (excluding $f > 10^6$ Hz). Sample x_2 demonstrates nonlinear behavior of conductivity (one step) and $Z''(Z')$ (one hill) which can indicate hopping conduction

* oleksandr.boiko@pollub.edu.pl

in the material with one relaxation time τ . On the other hand, sample x_3 exhibits also hopping mechanism of charge carriers with two different values of parameter τ . It could be related to dynamic electrons hops (between metallic nanoparticles FeCoZr) on different distances through the ceramic matrix PbZrTiO_3 . Paper includes explanation and calculation of relaxation processes during hopping conduction in tested materials.

Investigation of the damage of the surface layers of vanadium irradiated in the Plasma Focus facility

Bondarenko G.G.¹⁾, Borovitskaya I.V.²⁾, Nikulin V.Ya.³⁾, Mikhailova A.B.²⁾, Silin P.V.³⁾, Gaidar A.I.⁴⁾, Paramonova V.V.²⁾ and Peregudova E.N.³⁾

¹⁾National Research University Higher School of Economics, Myasnitskaya ul., 20 Moscow, 101000 Russia

²⁾A.A.Baikov Institute of Metallurgy & Materials Science of the Russian Academy of Sciences (IMET RAS), Leninskii pr., 49 Moscow, 119334 Russia

³⁾P.N.Lebedev Physical Institute of the Russian Academy of Sciences (LPI RAS), Leninskii pr. 53, Moscow, 119991 Russia

⁴⁾Research Institute of Advanced Materials and Technologies, Malaya Pionerskaya ul.,12, Moscow, 115054 Russia

Plasma focus devices are currently actively used to simulate the behavior of materials of the working chamber during plasma disruptions in thermonuclear reactors [1,2]. These devices generate the flows of pulsed high-temperature plasma with a particle flow density of 10^{18} - 10^{19} cm⁻³, a plasma energy flow density of 10^8 - 10^{10} W/cm²; the pressure of the shock wave arising in the solid reaches a value of the order of several megabars. The report is devoted to the results of the investigation of the influence of high-temperature dense plasma pulses generated in the "Plasma focus" facility on structural changes in polycrystalline vanadium. A close interest in research of the high-temperature plasma effect on vanadium is currently due to the fact that vanadium alloys are promising low-activating structural materials of the first wall of a thermonuclear reactor [3]. In our work it is established that as a result of irradiation a fine-grained structure with grain size of 100-200 nm is formed in the surface layer of vanadium. The "destructive" irradiation regimes under which the formation of cracks occurs in the structure of vanadium are determined. In these cases, the cracks in the irradiated samples propagate to a depth of 5 to 20 μ m.

References

- [1] Chernyshova M et al., Fusion Engineering and Design 2016;113:118.
- [2] Gribkov V.A., Plasma Physics and Controlled Fusion 2015;57:065010
- [3] Chen J.M. et al., Journal of Nuclear Materials 2011;417:289.

Strain effect in film materials based on magnetic metals

Odnodvorets L.¹⁾, Bondariev V.²⁾, Tyschenko K.¹⁾, Shumakova N.¹⁾, Protsenko I.¹⁾

¹⁾Sumy State University, 2, Rymyski-Korsakov Str., 40007 Sumy, Ukraine

²⁾Lublin University of Technology, 38 D, Nadbystrzycka Str., 20-618 Lublin, Poland

The studies of the strain effect in Fe, Ni and permalloy $\text{Fe}_x\text{Ni}_{1-x}$ films with a total thickness up to 100 nm were performed. The interval of the longitudinal deformation ε_l was 0-3%, which completely covers the ranges of elastic, quasi-elastic and plastic deformation. Electron-microscopic and diffraction studies indicate that the phase composition of Fe, Ni and permalloy films corresponds to BCC-(α -Fe), FCC-Ni and FCC- FeNi_3 + α -Fe (at concentration c_{Fe} up to 50 at.%), FCC- FeNi + α -phase of the Fe-Ni alloy (at c_{Fe} up to 75 at.%) and the α -phase of the Fe-Ni alloy (at $c_{\text{Fe}} \geq 75$ at.%) (Fig.1).

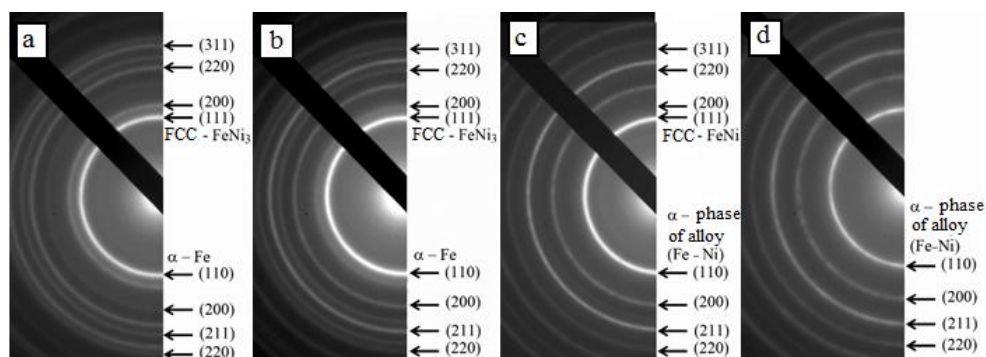


Fig. 1. Diffraction picture from permalloy films with concentration c_{Fe} , at. %: 25 (a), 50 (b), 65 (c) and 75 (d).

It was first observed the anomalous increase effect of differential coefficient of longitudinal strain coefficient $(\gamma_l)_{\text{dif}}$, that appears as a local maximum on the dependence $(\gamma_l)_{\text{dif}}$ versus ε_l . The nature of the effect is related to the nonlinear dependence of the resistivity versus deformation during the transition from elastic to plastic deformation [1]. The physical nature of observation in some cases of abnormally small (< 3 unit) of the integral strain coefficient $(\gamma_l)_{\text{int}}$ was explained.

References

[1] Tyschenko K., Odnodvorets L., Panchal C., Protsenko I., J.Nano- Electron. Phys. 2012; 4(4): 04014.

Study of strength properties after high temperature crawl conditions in ceramic thermal barrier coatings based on In 740

Cieślik I.^{1)}, Czarnewicz S.²⁾, Sitek R.³⁾, Duchna M.¹⁾, Kurpaska Ł.¹⁾*

¹⁾*Material Physics Department, National Center for Nuclear Research A. Soltana 7, 05-400 Otwock, Poland*

²⁾*Institute of Aviation, al. Krakowska 110/114, 02-256, Warsaw, Poland*

³⁾*Warsaw University of Technology, Faculty of Materials Science and Engineering, Warsaw University of Technology, Wołoska 141, 02-507 Warsaw, Poland*

Thermal barrier coatings are one of the group of advantageous materials widely used as insulation to protect the underlying metallic structure [1]. High temperature coats require high thermal conductivity, thermal stability, high coefficient of thermal expansion, resistance to environmental conditions during service. It is extremely difficult task to find all these features in the previously studied ceramic materials. Therefore, with increasing technical progress, it is necessary to develop new solutions or to modify existing ones. Chemical Vapor Deposition (CVD) is one of the most widely used technique in this area. The process yields a high-quality connection of a layer and a core and ensures remarkable oxidation resistance [2].

The aim of this work was to obtain a layer containing β -NiAl intermetallic phase and Ni-Al-Zr elements by the Chemical Vapor Deposition technique on the Inconel 740 and to investigate the creep resistance. Aluminizing process was carried on for 10 h in $\text{AlCl}_3 + \text{H}_2$ vapors, while zirconizing – for 1 h in $\text{ZrCl}_3 + \text{H}_2$ vapors.

Obtained thermal barrier coatings based on Inconel 740 were creep tested at high temperatures. Creep rates are used in evaluating materials primarily for elements used in energy industry, in an aviation or any application that involves high temperatures under load. Understanding high temperature behavior of ceramic coatings is necessary in designing failure resistant systems.

References

- [1] N. Nayeypashae, Silulation of the effect of sub-micron interface roughness n the stress distribution in functionally, *Advanced Ceramic Progress*, 2015, 1, 40-47
- [2] S. Hamadi, Oxidation resistance of a Zr-doped NiAl coating thermochemically deposited on a nickel-based superalloy, *Surface & Coatings Tech.* 2009, 204, 756-760.

* iwona.cieslik@ncbj.gov.pl

AC electrical properties of silicon-on-insulator structures with In and Sb nanocrystals heated at high temperatures

*Czarnacka Karolina*¹⁾, *Kołtunowicz Tomasz N.*¹⁾, *Fedotova Julia A.*²⁾,
*Fedotov Aleksander K.*³⁾

¹⁾Lublin University of Technology, Nadbystrzycka 38D, 20-618 Lublin, Poland

²⁾Reserch Institute for Nuclear Problems of Belarusian State University, 11, Bobruiskaya Str., 220030 Minsk, Belarus

³⁾Belarusian State University, 4, Nezavisimosti av., 220030 Minsk, Belarus

The tested material was obtained by the implantation of In⁺ and Sb⁺ ions into a thin (300 nm) silica film, which was prepared by heating a p-type silicon wafer of orientation (100) and a diameter of 100 mm. The Sb⁺ and In⁺ ions with energy of 200 keV were implanted with a fluence of 8×10^{15} cm⁻². Then, silicon layers were applied to the surface of the material, which resulted in the silicon-on-insulator structure. Finally, the samples were subjected to 30 minutes of heating at selected temperatures.

AC measurements were carried out on materials obtained in the previously described manner. Measured parameters were resistivity R_p , phase angle θ , capacity C_p and loss tangent $\text{tg}\delta$ as a function of frequency and temperature. Based on mathematical and physical calculations, frequency and Arrhenius dependences of conductivity σ were established. This made it possible to determine the activation energy of electrons for selected measurement frequencies.

The obtained results allowed to discuss the electrical properties of the tested material, such as the charge transfer mechanism or dielectric parameters.

Impulse plasma deposition of carbon nanoparticles

Dosbolayev M.K.^{*}, *Raiymkhanov Zh.*, *Tazhen A.B.*, *Utegenov A.U.*, *Ramazanov T.S.*

IETP, Al-Farabi Kazakh National University, Almaty, Kazakhstan

In this paper we present results on the deposition of carbon nanoparticles on the metal surface by the method of impulse plasma deposition (IPD) [1].

Experiments were carried out on the setup of a pulsed plasma accelerator IPU-30 [2].

Carbon nanoparticles are a product of erosion that appears when a plasma stream flows through a graphite grid system. Such interaction of a pulsed plasma with the material surface is accompanied by instantaneous heating (Figure 1b) and pulling out followed by a scatter of particles from the surface of the plates (Figure 1c), where the emerging particles follow the plasma, creating a moving dusty plasma (Figure 1c).

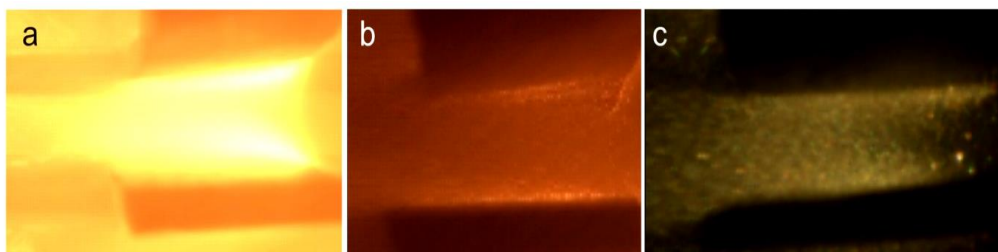


Figure 1: Passing of plasma through the carbon grid (a), heating of the surface of carbon plates due to the friction with the plasma (b) and the ejection of particles from the surface (c)

References

- [1] K. Zdunek, K. Nowakowska-Langier, R. Chodun, S. Okrasa, M. Rabinski, J. Dora, P. Domanowski and J. Halarowicz. *Journal of Physics: Conference Series* 564 (2014) 012007.
- [2] M.K. Dosbolayev, A.U. Utegenov, A.B. Tazhen, T.S. Ramazanov. *Laser and Particle Beams*, 35 (2017) pp. 741-749.

* merlan@physics.kz

Doping of Ge and GeSn via nonequilibrium processing

Drożdżiel A.¹⁾, Turek M.¹⁾, Pyszniak K.¹⁾, Żuk J.¹⁾ and Prucnal S.^{1,2)}

¹⁾*Maria Curie-Skłodowska University, Pl. M. Curie-Skłodowskiej 1, 20-035 Lublin, Poland*

²⁾*Institute of Ion Beam Physics and Materials Research, Helmholtz-Zentrum Dresden-Rossendorf*

The n-type doping of Ge is realized by incorporation into the lattice the group V elements like P, As or Sb. Using conventional doping technique, the maximum carrier concentration is in the range of $2\text{-}5 \times 10^{19} \text{ cm}^{-3}$ and it is limited by the solid solubility of dopants in Ge and point defects e.g. Ge vacancies. To achieve the electron concentration in Ge and GeSn higher than $5 \times 10^{19} \text{ cm}^{-3}$ is possible only using strongly nonequilibrium processing. Here we present the formation of highly doped n-type Ge and GeSn using ion implantation followed by millisecond range flash lamp annealing (FLA). The electrical properties of P, As and Sb doped Ge and GeSn and the carrier concentration is investigated using temperature dependent Hall Effect and FTIR. Rutherford backscattering spectrometry confirms full recrystallization of the implanted layer and the location of dopant in the substitutional position. The maximum carrier concentration is well above 10^{20} cm^{-3} for P doped layers which converts Ge to quasi-direct band gap semiconductor.

Acknowledgement: This work was partially supported by the National Science Centre, Poland, under Grant No. 2016/23/B/ST7/03451.

Plasma Sputtering Deposition of Thin Film Cu, Ti and NiCr Capacitors on Biocompatible Substrate

Duk M.¹⁾, Kociubiński A.¹⁾, Szyplski M.¹⁾, Zarzeczny D.¹⁾, Lizak T.¹⁾, Muzyka K.¹⁾, Predecka M.²⁾ and Małecka-Massalska T.²⁾

¹⁾Lublin University of Technology, Nadbystrzycka 38a, 20-618 Lublin, Poland

²⁾Medical University of Lublin, Al. Raławickie 1, 20-059 Lublin, Poland

This paper presents the technology of the metallization layers on biocompatible substrates for animal cells *in vitro* testing by electrical impedance measurement. By using different materials, it will be possible to obtain more information about the behavior of the animal cells. Copper, titanium and nichrome were deposited by magnetron sputtering on polycarbonate substrates. The materials have been chosen due to their various properties: Cu – bactericidal; Ti – biocompatibility; NiCr – thermal properties. After finishing the manufacturing process, cultureware was delivered to Medical University of Lublin, where electrical parameters were measured during cell growth.

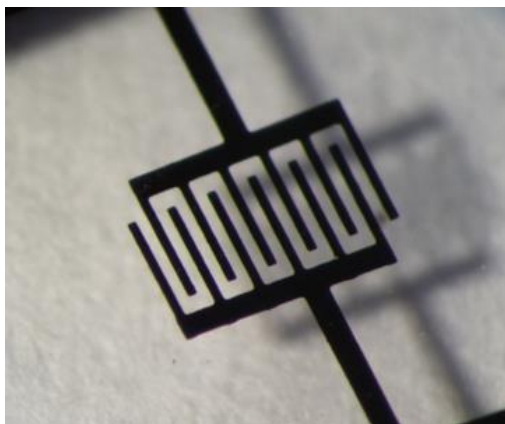


Figure 1: The electrodes made of copper comb (width 100 μ m) capacitors on a polycarbonate substrate

Influence of Irradiation by Swift Heavy Ions on Carrier Transport in Si<Sb> Delta-Layer

Fedotov A.S.¹⁾, Ape P.²⁾, Yurasov D.³⁾, Novikov A.³⁾, Svito I.¹⁾, Fedotov A.K.¹⁾ and Zukowski P.⁴⁾

¹⁾Belarusian State University, 220030 Minsk, Belarus

²⁾Joint Institute for Nuclear Research, Dubna, Russia

³⁾Institute for Physics of Microstructures Russian Academy of Sciences, 603950 Nizhny Novgorod, Russia

⁴⁾Lublin University of Technology, 20-618 Lublin, Poland

Samples with antimony delta-layer of 2-5 nm thick in the epitaxial Si grown on the p-type Si(001) substrate with resistivity $12 \Omega \times \text{cm}$ have been manufactured. We studied influence of irradiation by Ar ions with $0 < D < 1 \cdot 10^9$ ion/cm² and energy 50 MeV on temperature ($2 < T < 300$ K) and magnetic field ($0 < B < 8$ T) dependences of the DC resistance R and Hall coefficient. The study has shown that below 15 K the carrier transport via the delta-layer prevails. For these temperatures the transition from the Arrhenius $\text{Lg}R(1/T)$ to a logarithmic $R \sim \text{Lg}(T)$ temperature dependences of the resistivity was observed. Additionally, transition from positive (PMR) to the negative (NMR) magnetoresistance (MR) was exhibited that is typical for hopping and/or weak localization carrier transport in heavy doped or disordered semiconductors. The progress to the saturation of $R(T)$ curve at $T < 2$ K indicates a possible transition to the so-called limit of minimal metallic conductivity.

Irradiation of the sample by Ar ions led to an increase of electrical resistivity and the Hall coefficient as well as a decrease both PMR and NMR contributions to MR modulo. The calculation of the appropriate Thouless lengths L_{TH} at different temperatures indicated their approximately three-fold decrease after ion exposure. At the same time, the $L_{\text{TH}}(T)$ is approximated well by a power function $L_{\text{TH}} \approx A \cdot T^{p/2}$, where p and A are constant with p depending on the scattering mechanism of charge carriers [1-3]. The best agreement with the experimental data was achieved with p values ~ 0.76 for non-irradiated and $\sim 0.70-0.73$ for irradiated sample, that is close to the theoretical value of $p=1$, for the two-dimensional (2D) quantum corrections to the DC conductivity in the case of weak localization regime excluding the electron-electron interaction. This is also evidenced by the field dependence of the Hall constant and, in particular, the relationship of this value to the relative MR, which at $T < 10$ K had amounts between 1 and 2. The latter is probably indicative of the need for taking into account the electron-electron interaction in the 2D quantum corrections regime to the conductivity of the Si<Sb> delta-layer [3].

References

- [1] B.L. Al'tshuler and A.G. Aronov, in *Electron-Electron Interaction in Disordered Systems*, edited by A. L. Efros and M. Pollak, North-Holland, Amsterdam, 1987.
- [2] P.A. Lee and T.V. Ramakrishnan, *Rev. Mod. Phys.* 57, 287, 1985.
- [3] G. Bergmann, *Phys. Rep.* 107, 1 (1984).

The features of reactive admittance in the nanogranular composites $(\text{Fe}_{45}\text{Co}_{45}\text{Zr}_{10})_x(\text{SiO}_2)_{(100-x)}$ manufactured by Ion-Beam Sputtering Technique with Ar ions

Kalinin Yu.E.¹⁾, Sitnikov A.V.¹⁾, Koltunowicz T.N.²⁾, Zukowski P.²⁾, Fedotova V.V.³⁾, Ronassi Ali Arash⁴⁾, Evtukh A.A.⁵⁾ and Fedotov A.K.⁶⁾

¹⁾Voronezh State Technical University, 14, Moscow av., 394026 Voronezh, Russia

²⁾Lublin University of Technology, 38d, Nadbystrzycka Str., 20-618 Lublin, Poland

³⁾Scientific-Practical Material Research Centre NAS of Belarus, 19, P. Brovki Str., 220072 Minsk, Belarus

⁴⁾Department of Physics, Payame Noor University, The Islamic Republic of Iran

⁵⁾Institute of Semiconductor Physics of National Academy of Sciences of Ukraine, 41, Nauka av., 03028 Kiev, Ukraine

⁶⁾Belarusian State University, 4, Nezavisimosti av., 220030 Minsk, Belarus

Granular composite materials consisting of an insulating matrix mixed with the FeCo-based soft ferromagnetic nanoparticles are used in various electromagnetic applications. Depending on the concentration of a metallic filler x , the electric properties of such nanocomposites may be varied between those of the matrix (dielectric phase) and those of the filler (metallic phase). In the present work we investigate the effect of “negative capacitance” in AC conductance beyond the percolation threshold in nanogranular composites consisting of the $\text{Fe}_{45}\text{Co}_{45}\text{Zr}_{10}$ nanoparticles embedded into amorphous dielectric silica matrix.

The films of 3-6 μm thickness were deposited on ceramic glass substrate using Ar ion-beam sputtering of a complex target containing 10 mm silica stripes covered $\text{Fe}_{45}\text{Co}_{45}\text{Zr}_{10}$ alloy plate with the changing distances. The films were prepared in a chamber evacuated with pure argon under the pressure $P_{\text{Ar}}=0.7\div 0.8$ mPa. Frequency dependences of active $\sigma'(f)$ and reactive $\sigma''(f)$ parts of admittance at 300 K in the frequency range $(5\cdot 10^1-1\cdot 10^6)$ Hz in $(\text{Fe}_{45}\text{Co}_{45}\text{Zr}_{10})_x(\text{SiO}_2)_{100-x}$ nanocomposite films with 57 at.% $<x<79$ at.% have been studied.

In $(\text{Fe}_{45}\text{Co}_{45}\text{Zr}_{10})_x(\text{Al}_2\text{O}_3)_{100-x}$ and $(\text{Fe}_{45}\text{Co}_{45}\text{Zr}_{10})_x(\text{PZT})_{100-x}$ nanocomposite films the effect of “negative capacitance” was observed only in the films deposited in Ar+O₂ atmosphere and after annealing of the air. The behavior of $\sigma'(f)$ and $\sigma''(f)$ dependences at 300 K in $(\text{Fe}_{45}\text{Co}_{45}\text{Zr}_{10})_x(\text{SiO}_2)_{100-x}$ nanocomposite films has displayed the competition between capacitive and inductive-like contributions even in the samples deposited in the pure argon atmosphere. This was confirmed by the change of the phase shift angle sign between current and voltage applied with the increase of frequency. As follows from our experiments, the prevailing of inductive-like contribution (delay of current from voltage) depends both on frequency (it increases with f) and the filler concentration (growing with the x increase). We connect this effect with the so-called “core-shell” structure of $\text{Fe}_{45}\text{Co}_{45}\text{Zr}_{10}$ nanoparticles containing FCC alloy “core” covered with the “shells” from FeO and Fe₂O₃ compounds. As was shown by Mossbauer spectroscopy measurements, the metallic nanoparticles in the studied samples the volume of Fe₂O₃ compound in the “shell”, possessing by semiconducting properties, increases with the growth of the $\text{Fe}_{45}\text{Co}_{45}\text{Zr}_{10}$ filler concentration x and results in “negative capacitance” effect.

Structural changes in helium-implanted epitaxial La, Ga: YIG films

Kurovets V.V., Fedoriv V.D., Yaremiy S.I., Garpul O.Z.*

Vasyl Stefanyk Precarpathian National University, 57 Shevchenko Str., Ivano-Frankivsk, 76018, Ukraine

The present study analyzes the structural changes in epitaxial La, Ga: YIG films implanted by helium ions ($E = 100$ keV, $D = 1 \cdot 10^{15} \text{cm}^{-2} \div 1 \cdot 10^{16} \text{cm}^{-2}$) based on the X-ray structural investigations. The film with thickness $6,06 \mu\text{m}$ have been grown by liquid-phase epitaxy method on the non-magnetic GGG (111) substrate. Calculated from Blenck-Nielsen coefficients, the predicted composition has the formula $\text{Y}_{2.88}\text{La}_{0.12}\text{Fe}_{4.55}\text{Ga}_{0.45}\text{O}_{12}$.

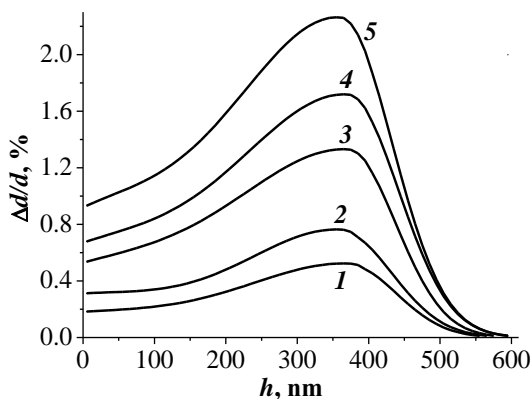


Figure 1: Strain profiles in the near-surface layers of helium-implanted (100 keV) epitaxial La, Ga: YIG films: 1 – $1 \cdot 10^{15} \text{cm}^{-2}$; 2 – $2 \cdot 10^{15} \text{cm}^{-2}$; 3 – $4 \cdot 10^{15} \text{cm}^{-2}$; 4 – $6 \cdot 10^{15} \text{cm}^{-2}$; 5 – $1 \cdot 10^{16} \text{cm}^{-2}$

From the experimental rocking curves, strain profiles of the films were theoretically calculated (Fig. 1) by means of the statistical dynamic theory of X-ray scattering. The value of the relative maximum deformation of the disturbed layer increases linearly to the irradiation dose $4 \cdot 10^{15} \text{cm}^{-2}$. Violation of the indicated linearity at higher doses indicates the beginning of the radiation defects interaction. Calculations showed that in the films the dislocation loops concentration increased and their radius reduced with irradiation dose increasing: the dislocation loops radius varies from 5 nm for dose $1 \cdot 10^{15} \text{He}^+/\text{cm}^2$ to 2 nm for dose

$1 \cdot 10^{16} \text{He}^+/\text{cm}^2$.

Analysis of the strain profiles and the radiation defects distribution profiles (obtained on the basis of the defect formation process simulation using the SRIM-2008 application) indicates that the relative deformation is mainly caused by displaced matrix ions during the elastic collisions of the helium ions with target atoms. In this case, the anion sublattice is destroyed vastly, whereas the energy from helium ions is most effectively transmitted to the anions.

* ogarpul@gmail.com

Positron Beam Studies of Radiation Damage Induced by Heavy Ions in Iron

Kobets A.G.^{1,2)}, Horodek P.^{1,3)}, Siemek K.^{1,3)}, Skuratov V.A.¹⁾

¹⁾Joint Institute for Nuclear Research, Dubna 141980, Russia

²⁾Institute of Electrophysics and Radiation Technologies NAS of Ukraine, Chernyshevsky St. 28, 61002 Kharkov, Ukraine

³⁾Institute of Nuclear Physics, Polish Academy of Science, Krakow 31-342, Poland

The interaction of materials with radiation is interesting from theoretical and experimental points of view. The changes induced by irradiation are irreversible at the atomic level and affect significantly material properties. Due to the fact that during irradiation a great number of point defects is created, the positron annihilation techniques are suitable for studies of such irradiated materials.

We report experimental studies of pure iron exposed to Xe²⁶⁺ irradiation. Implantations with the dose of 5×10^{13} ions/cm² using 167 MeV ions moderated to 122.5, 77 and 44.5 MeV were performed at IC-100 cyclotron at FLNR, JINR. Radiation damages were investigated with variable energy positron beam (VEP). Doppler broadening spectroscopy (DB) was applied and the line shape S parameter of annihilation line was extracted. The analysis of S parameter profiles gives information about the presence of open volume defects in irradiated samples. The positron diffusion lengths extracted from the profile strongly defected two layers on the depth up to 1.4 mm. Similar kind of defects was observed. However, their concentration depends on ion energy. The positron lifetime spectra measured directly on the implanted surface point at the presence of huge vacancy clusters.

Technology of Nickel Thin Films Deposited by Magnetron Sputtering for Cell Morphology Monitoring

Kociubiński A.¹⁾, Lizak T.¹⁾, Muzyka K.¹⁾, Szypulski M.¹⁾, Zarzeczny D.¹⁾, Duk M.¹⁾, Predecka M.²⁾ and Małecka-Massalska T.²⁾

¹⁾Lublin University of Technology, Nadbystrzycka 38a, 20-618 Lublin, Poland

¹⁾Medical University of Lublin, Al. Raławickie 1, 20-059 Lublin, Poland

This paper presents the construction and technology of resistors and comb capacitors on a polycarbonate substrate. The structures have been designed for monitoring the activity of the examined cells by analyzing the changing electrical parameters (impedance, resistance and capacitance) in real time. The nickel layer was embedded by sputtering method. Next, unique circuit pattern was designed in CAD software and printed on the thin transparent foil making it a photomask. Mapping of the desired shape of the electric circuit was made during photolithography process. To get rid of the unnecessary metallization uncovered by photoresist, wet etching was made. The last step was gluing of containers, where medium with cells are dosed, and UV sterilization was made (Fig. 1).

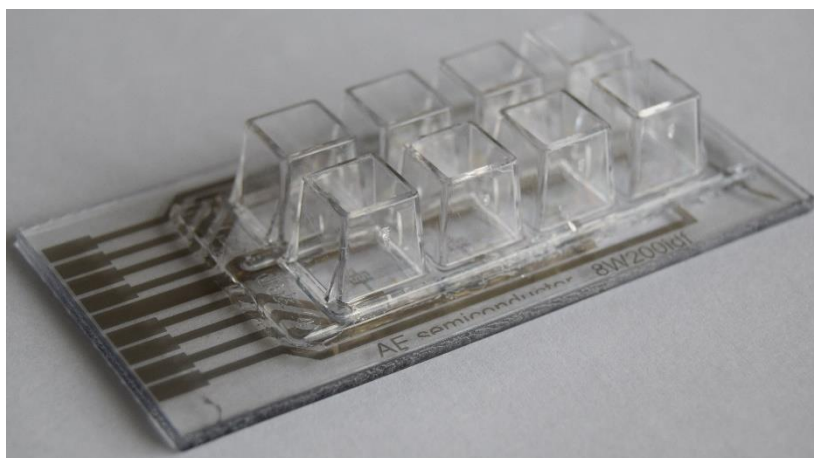


Figure 1: Polycarbonate substrate with nickel electrodes designed to monitor electrical parameters during cell culture

Electrophysical properties of granular film alloys

Odnodvoretz L.¹⁾, Kołtunowicz T.N.²⁾, Bondariiev V.²⁾, Protsenko S.¹⁾, Tkach O.¹⁾, Shumakova M.¹⁾

¹⁾ *Sumy State University, 2, Rymyski-Korsakov Str., 40007 Sumy, Ukraine*

²⁾ *Lublin University of Technology, 38 D, Nadbystrzycka Str., 20-618 Lublin, Poland*

A new type of film materials – granular solid solutions (s.s.) – have unique electrophysical and other physical properties. In particular, we are talking about the relatively high value of the thermal coefficient of resistance (TCR) and the realization of the effect of a giant magnetic resistance as a result of spin-dependent scattering of electrons (SDSE) on magnetic granules.

Granular film alloys are formed by methods of simultaneously or layered condensation of magnetic (Fe, Co) and non-magnetic (Cu, Ag, Au, etc.) metals. Since the components are selected in such a way that their mutual solubility is limited, after the annealing of the film samples limited s.s. are formed. At the excess of the magnetic component, granules of size from 2 to 10 nm are formed. Diffraction studies allow fixing those concentrations of the magnetic component when the transition from diluted to granular solid solutions take place.

On the basis of the experimental dependences of the resistivity the two-layer films Ag/Fe/S and Ag/Co/S or films (total thickness up to 60 nm, and the concentration of the magnetic component from 20 to 80 at.%) versus temperature (interval 300-800 K) were calculated temperature and concentration dependencies for TCR.

At the indicated temperatures and concentrations of the magnetic component, TCR has a value $(1-3) \cdot 10^{-3} \text{K}^{-1}$ in both dilute and granulated alloys. Based on theoretical representations [1] on the additive contribution of SDSE on granules, we performed based on ratio [1] to calculate the magnetic moment (spin) S in the case of $\text{TCR} = 3 \cdot 10^{-3} \text{K}^{-1}$ and the average radius of the granules $r = 10 \text{ nm}$. It turned out that $S = 27.5 \mu_B$ in the temperature range 300-700 K.

References

[1] Csontos M., Balogh J., Kaptas D., et al., Phys. Rev. B 2006; 73: 184412.

Morphology and composition of surface layers prepared by ion beam assisted deposition of platinum and dysprosium on carbon fiber paper catalysts carriers

Poplavsky V.V.¹⁾, Lulin V.G.¹⁾ and Koltunowicz T.N.²⁾

¹⁾*Belarusian State Technological University, 13a, Sverdlov Str., 220006 Minsk, Belarus*

²⁾*Lublin University of Technology, 38d, Nadbystrzycka Str., 20-618 Lublin, Poland*

Surface layers were prepared by ion beam assisted deposition (IBAD) of main catalytic metal – platinum and dysprosium as activating additive on the carbon based Toray Carbon Fiber Paper TGP-H-060 T (TorayCFP) and AVCarb[®] Carbon Fiber Paper P50 (AVCarbCFP) catalysts carriers in order to obtain electrocatalysts for direct methanol and ethanol fuel cells. The basis of both carriers is fibers of polyacrylonitrile, which undergoes thermo oxidative stabilization and subsequent carbonization. The carrier TorayCFP is hydrophobized with polytetrafluoroethylene, the carrier AVCarbCFP is not hydrophobized. They have an irregular porous structure.

The applied method of metal deposition is characterized by the use of deposited-metal ions as assisting ions. Deposition of metal and mixing of the deposited layer with the substrate surface by accelerated ($U = 5$ kV) ions of the same metal have been carried in the experimental unit, respectively, from neutral fraction of metal vapor and ionized plasma of vacuum pulsed electric arc.

Investigation of the morphology and composition of prepared layers was carried out by SEM, EDX and XRF methods. Morphology of the surface of TorayCFP and AVCarbCFP carriers is different, and does not undergo changes in the formation of layers. According to results of investigations with use of EDX and XRF into the composition of layers enter atoms of deposited metals and carriers, and oxygen as impurity. Concentration of deposited metals equals about a few weight percent. At the same time, the surfaces contain deposited metals (Pt, Dy) inclusions with sizes of several micrometers, which arise from the precipitation of metal droplets from the arc discharge of the ion source. We investigated the content of the elements on the average over the surface of the samples, as well as in the drop inclusions of platinum and dysprosium.

Experimental study and modeling of silicon supersaturated with selenium by ion implantation and nanosecond-laser melting

*Komarov Fadei¹⁾, Ivlev Gennady¹⁾, Zayats Galina²⁾, Komarov Alexander¹⁾,
Nechayev Nikita¹⁾, Wendler Elke³⁾, Miskiewicz Siarhiej*

¹⁾*Institute of Applied Physics Problems, BSU, Minsk, Belarus*

²⁾*Academy of Sciences of Belarus, Minsk, Belarus*

³⁾*F. Schiller University, Jena, Germany*

The field of supersaturated Si has recently attracted much attention due to the unusual and interesting properties of these materials, with practical applications in photovoltaic devices and infrared (IR) detection. High absorption coefficient and photoresponse in the IR range could place silicon in the market as an option for imaging or security [1-2]. Once the impurity (Se, S, Te, V, Ti) concentration surpasses the insulator-metal transition, deep levels associated to the impurities could form an intermediate band inside the band gap. It is of utmost relevance for photovoltaic cells and Si-based IR detectors.

B-doped (111) silicon samples with resistivity of 10 Ωcm were implanted at RT with Se^+ at 150 keV with the fluence of 10^{16}cm^{-2} and then 70 ns laser melted at 1.5, 2 and 2.5 j/cm^2 energy density (one, two or three pulses). Atomic Se depth concentrations were measured by RBS examination in random and channeling regimes. Besides that, absorption data in a spectral range of 300 nm to 35 μm were measured as well as photoluminescence spectra in a range of 700 to 1600 nm.

To understand the evolution of the Se concentration profile during laser melting and solidification, we used a numerical solution of the 1D diffusion equation with segregation at a moving boundary. A comparison of experimental and theoretical data for the impurity depth distributions is presented.

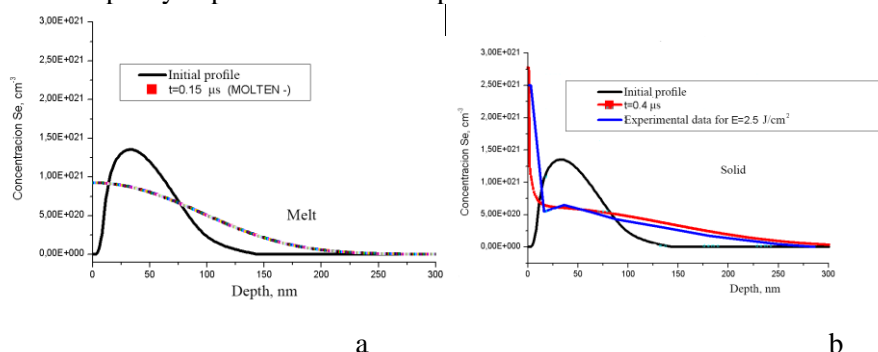


Figure 1. Simulated depth concentrations of implanted and annealed Se in Si (a) and its comparison with the experimental data (b).

References

- [1] Si H. Pan et al. Appl. Phys. Letters 98, 12913 (2011)
- [2] D. Pastor et al. Solar Energy Mater. and Solar Cells 104, 159 (2012)

Magneto-Optical Properties of Film Systems Based on Fe and Cr

Bezdidko O.¹⁾, Swic A.²⁾, Komsta H.³⁾, Opielak M.³⁾, Cheshko I.¹⁾ and Protsenko S.¹⁾

¹⁾Sumy State University, Rymyski-Korsakov Str 2, 40007 Sumy, Ukraine

²⁾Institute of Technological Systems of Information, Lublin University of Technology, Nadbystrzycka 36, 20-618 Lublin, Poland

³⁾Institute of Transport, Combustion Engines and Ecology, Lublin University of Technology, Nadbystrzycka 36, 20-618 Lublin, Poland

Film structures based on ferromagnetic and paramagnetic metals are the main materials for the creation of functional elements of spintronics. In our work, we investigated the dependence of the thickness of Fe and Cr layers on the parameters measured by the Kerr method. The samples were obtained by vacuum condensation at room temperature with a thickness of separate layers of $2 \div 40$ nm.

In [1], it was shown that in the system based on Fe and Cr there is a significant mutual penetration of the atoms of the layers near the interface at the stage of condensation.

We investigated the magneto-optical properties of film systems based on Fe and Cr, taking into account the specific features of the diffusion.

It was established that single layer ferromagnetic films of Fe thickness range of 20-100 nm have a value of the coercive force BC_{Fe} 12 mT. In the study of Fe/Cr systems, it was established that the ratio of the concentration and thickness of the Cr layer essentially affects the values of the Kerr angle Θ and the coercivity value. It was found that when the thickness of the Cr layer is increased to 10, 15 and 20 nm, the coercivity of the samples linearly increases to Fe value.

Reducing the value of B_C double-layer films compared with single-layer Fe films is due to the formation of solid solutions on the boundary between the layers already in the process of condensation. These studies have shown that the magneto-optical Kerr effect can be used as an additional method for studying the composition of multilayer systems, granular alloys and spin-valve systems, using specific software methods.

References

[1] Fedchenko O., Protsenko S., Zukowski P., Marszalek M., *Vacuum* 86 (12) 1934 (2012).

Magnetoresistive properties of synthetic antiferromagnetic spin valves structures on the basis Co and Ru

Lohvynov A.¹⁾, Cheshko I.¹⁾, Protsenko S.¹⁾, Swic A.²⁾, Komsta H.³⁾ and Opielak M.³⁾

¹⁾*Sumy State University, Rymyskogo-Korsakova str. 2, 40007 Sumy, Ukraine*

²⁾*Institute of Technological Systems of Information, Lublin University of Technology, Nadbystrzycka 36, 20-618 Lublin, Poland*

³⁾*Institute of Transport, Combustion Engines and Ecology, Lublin University of Technology, Nadbystrzycka 36, 20-618 Lublin, Poland*

The synthetic antiferromagnetic functional (SAF) layers based on Ru and Co have become quite widely used in modern electronics and sensor technology. These structures are often used in the manufacture of magnetic field sensors with high sensitivity in the low-intensity field, where it is necessary to detect magnetic fields of non-significant magnitude (magnetic properties of nanoparticles) [1-2].

Thin three-layer film systems Co/Ru/Co/S (S-substrate) in the range of effective thicknesses of separate layers $d_{ef}=5-20$ nm were obtained by electron-beam formation in vacuum (residual gas pressure 10^{-4} Pa) on sittal substrate at a temperature $T_s = 400$ K with thickness control by a quartz resonator with an accuracy of ± 0.1 nm. In a single-layered sample Co(40)/S the magnitude of the magnetic resistivity (MR) at annealing temperature $T_a = 300$ K was about 0.02%. With an increase in T to 900 K, the value of MR increased to 0.05%. In the case of the sample Co(20)/Co(20)/S the magnitude of the MR at 300 K and 900 K was 0.04% and 0.08% respectively. Dividing the magnetic component Co with a nonmagnetic layer of Ru with a thickness of 5 nm (Co(20)/Ru(5)/Co(20)/S) there is an increase in the MR to 0.18% under the condition of heat up to $T_a=900$ K. By increasing the thickness of the nonmagnetic layer Ru $d = 10$ nm (at $T_a=900$ K) the value of MR = 0.2% was obtained. In the case of a three-layer system Co(20)/Ru (20)/Co(20)/S, under the condition of long-term heat-burning (about 30-40 minutes) up to 900 K, a significant increase value of MR is recorded to 0.45%.

Work was done as part of State Project № 0117U003925.

References

- [1] Tang X.L., Su H., Zhang H.W., J. Magn. Mag. Mater. 2017; 429: 65.
- [2] Yeo S., Choi S.-H., Park J.-Y., Thin Solid Films 2013; 546: 2.

Electrospinning process technology parameter influence on the properties of Polyamide-6 and Chitosan nanofibrous coatings for air filtration

Prokopchuk Nikolay¹⁾, Luhin Valery¹⁾, Shashok Zhanna¹⁾, Prishchepenko Dmitry¹⁾ and Komsta Henryk²⁾

¹⁾ Belarusian State Technological University, 13a, Sverdlov Str., 220006 Minsk, Belarus

²⁾ Lublin University of Technology, 38d, Nadbystrzycka Str., 20-618 Lublin, Poland

Electrospinning is a modern high-performance method for obtaining nanofibers from polymer solutions [1]. As a polymeric base for forming solutions were used chitosan and polyamide-6. They have necessary properties for obtaining nanofibers from them by electrospinning.

The purpose of this work was to determine the influence of technological parameters of the electroforming process on the density, average diameter and filtering capacity of nanofiberous coatings. Polyamide-6 was solved in mixture of formic and acetic acid in a ratio of 3: 1. For chitosan solving 70% acetic acid were used. The concentration of polymers in spinning solutions were: for polyamide-6 – 10.0% by weight, for chitosan – 10.0% by weight. The nanofibers were obtained on the NS LAB 500 S unit from ELMARCO (Czech Republic).

Dependences of changes in the average diameter of a nanofibrous coating on the technological parameters of electroforming are established. The smallest diameter of the fibers most of the samples shows at the maximum interelectrode distance and voltage. The obtained data show that the speed of rotation of the fiber-forming electrode does not significantly influence the average diameter of the resulting nanofibrous coating (changes in the range of 20-30 nm).

The filtering ability of the nanofibrous coatings obtained is determined. It is shown that the efficiency of the filtration process increases with increasing coating density and decreasing diameter of nanofibers. The best filtering ability is possessed by nanofibers of chitosan and polyamide-6.

References

[1] T. Spark, G Chase, Filter and Filtration Handbook, Elsevier, 2016.

Effects of nitrogen selective sputtering and flecking of nanostructured coating TiN, TiAlN, TiAlYN, TiCrN, (TiHfZrVNb)N under helium ion irradiation

Konstantinov S.V., Komarov F.F.

A.N. Sevchenko Institute of Applied Physical Problems of Belarusian State University, Kurchatov St., 7, 220045, Minsk, Belarus

Modeling of parameters of high-fluence ion irradiation of nanostructured TiN, TiAlN, TiAlYN, TiCrN, (TiHfZrVNb)N coatings by the Monte Carlo method was carried out. The obtained results and proposed mechanisms of processes were experimentally proved in studying the structure of the coatings after irradiation with 500 keV He⁺ ions in the fluence range from $5 \cdot 10^{16}$ ion/cm² to $3 \cdot 10^{17}$ ion/cm² [1]. The effect of depth localization of the maximum concentration of the implanted helium on nitrogen selective sputtering from coatings, as well as on partial flecking (exfoliation) of coatings was observed for ion fluences higher than $2 \cdot 10^{17}$ ion/cm² (figure 1). No phase segregation of the solid solution as the main phase in the nanostructured coatings was found after ion irradiations. There also was found no macro- or microblistering of coatings after ion irradiation, at least to a blister size approximating to nanoscale.

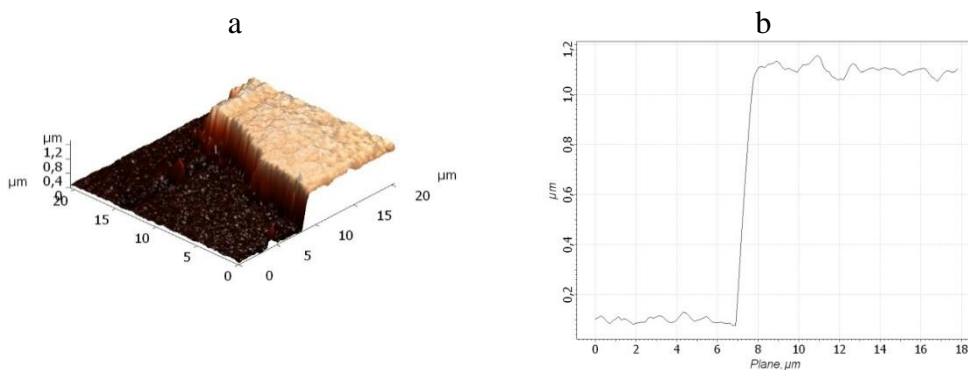


Figure 1 — The morphology of the cleavage on the surface (a) and profilogram (b) of the TiAlN coating after irradiation with He⁺ ions, fluence $2 \cdot 10^{17}$ ion/cm² and annealing at 500 °C for 15 min

References

- [1] Komarov F.F., Konstantinov S.V., Strel'nitskij V.E., Pilko V.V. Technical Physics 2016, Vol. 61, No. 5, pp. 696-702.

Development of multilayer condensates based on refractory compounds with a variable composition of the second layer in the bilayer

Kravchenko Ya.O.¹⁾, Bondar O.V.¹⁾, Pogrebnjak A.D.¹⁾ and Piotrowska K.²⁾

¹⁾*Sumy State University, 2, Rymkogo-Korsakova Str., 40007 Sumy, Ukraine*

²⁾*Lublin University of Technology, 38D, Nadbystrzycka Str., 20-618 Lublin, Poland*

Synthesis and fundamental research of nanoscale nitride coatings are an actual and in demand direction of nanotechnology development and material modification. Multilayered (TiAlSiY)N/CrN, (TiAlSiY)N/ZrN and (TiAlSiY)N/MoN coatings were fabricated by vacuum arc deposition in an “Bulat-6” device. SUS321 steel was used as the substrate material. The pressure of the working (nitrogen) atmosphere in the deposition chamber P_N was $4 \cdot 10^{-3}$ Torr. The constant negative bias potential $-U_b$ of -110 V was supplied to the substrates.

XRD analysis indicated the formation of a heterophasic composition in according to the bilayer composition. However, some inclusions of AlN phase were identified for multilayered (TiAlSiY)N/CrN coating. The predominant phase in the multielement layer was formed by means of isomorphous substitutions with doping atoms in the fcc-lattice of TiN.

The maximum values of nanohardness and elasticity modulus of 35.9 GPa and 406.8 GPa, respectively, at different depths of measurement, were obtained for (TiAlSiY)N/MoN system. These values for (TiAlSiY)N/CrN and (TiAlSiY)N/ZrN coatings were $H=23.4$ GPa and $E^*=300.2$ GPa, and $H=22.1$ GPa and $E^*=271$ GPa, correspondingly. Last parameters were much yield to the values obtained for (TiAlSiY)N/MoN coating, but they could be comparable. The difference in the mechanical properties of investigated coatings was determined to be varied in the phase-structural state, in particular, the change in the crystallographic grains size toward the coarsening.

Structure and phase composition of nanostructured functional coatings (TiAlSiY)N/MoN

Kravchenko Ya.O.¹⁾, Iatsunskiy I.¹⁾, Maksakova O.V.¹⁾, Pogrebnjak A.D.¹⁾, Kierczynski K.²⁾, Koltunowicz T.N.²⁾, Zukowski P.²⁾

¹⁾Sumy State University, 2, Rymasko-Korsakova Str., 40700 Sumy, Ukraine

²⁾Lublin University of Technology, 38d, Nadbystrzycka Str., 20-618 Lublin, Poland

In the paper it has been shown the possibilities of structural engineering during fabrication of the multielement and multilayer nanostructured coatings. The use of a vacuum-arc deposition method with evaporation of a cathode made possible obtaining of multilayer (TiAlSiY)N/MoN coating with high hardness (35.9 GPa). Produced multilayer coating was compared with a multielement (TiAlSiY)N coating for evaluation the influence of the interfaces on the phase-structure composition. Condensates investigation was made using a set of complementary methods: scanning electron microscopy (SEM) equipped with energy dispersive spectrum (EDS), Raman spectroscopy, X-ray diffraction (XRD) and hardness indicator. TiN phase with an advantageous orientation (111) is formed in (TiAlSiY)N coating, while the deposition of the multilayer composition results in the formation of an AlTiN phase with preferential orientation (200). The binary MoN layer has a weak degree of crystallization of the structure and forms a lattice of the B2-CsCl type. The size reduction of the crystallographic grains to medium sizes approximately 9.72 nm in the layered (TiAlSiY)N/MoN coating with small modulation periods ($\lambda \leq 10$ nm) is observed.

The calculation of small particles was made according to the Debye-Scherrer formula.

Radiation Effects on Single Crystal β -Ga₂O₃: Hydrogen vs. Optical Properties

Liu Chaoming^{1,2)}, Wang Mao²⁾, Berencén Yonder²⁾, Yang Jianqun¹⁾, Li Xingji¹⁾, Zhou Shengqiang²⁾

¹⁾Harbin Institute of Technology, School of Materials Science and Engineering, 150001, Harbin, China

²⁾Helmholtz-Zentrum Dresden-Rossendorf, D-01328, Dresden, Germany

³⁾Technische Universität Dresden, D-01062, Dresden, Germany

In this work, n-type single crystal β -Ga₂O₃ is irradiated by 6 MeV protons with different fluences to investigate the radiation effect of optical properties. The correlation between the injected hydrogen concentration and the optical properties is characterized by micro-Raman spectra and Photoluminescence (PL) spectrum. We demonstrate that the symmetric stretching modes and bending vibrations of GaO₄ and GaO₆ units are weakened to a certain extent upon increasing irradiation fluence. The intensity of luminescence increases significantly after irradiation. Moreover, the luminescence bands show a concentration quenching effect and a significant red-shift in the fluence which is higher than 1.25E12 cm⁻². The results envisage the possibility of obtaining pre-designed spectral behaviors by varying the irradiation fluence.

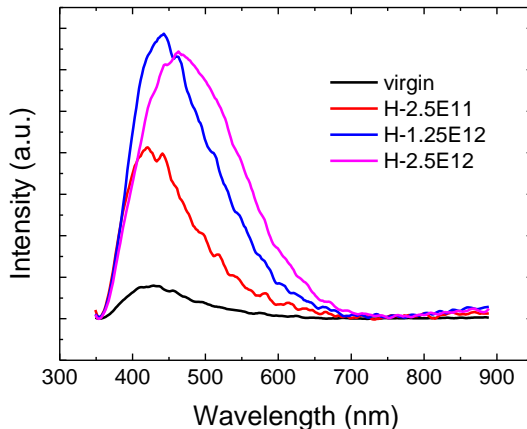


Figure 1. PL spectra from the non-irradiated and irradiated β -Ga₂O₃ samples

Soft-landing of organic molecules with mixed argon cluster on a metallic surface

Maciążek D., Postawa Z.

Smoluchowski Institute of Physics, Jagiellonian University, Lojasiewicza 11, 30-348 Krakow, Poland

One of the methods of controlled deposition of molecules onto the surfaces in the ultrahigh vacuum is a soft-landing technique [1]. In this technique, electro-sprayed molecules are deposited on the substrate with the kinetic energy of several eV. One of the limitations of this technique is a large beam spot size, which limits its capability for precise patterning. To overcome this limitation it is possible to embed molecules inside a large argon cluster projectile. It is known that ion beams of such projectiles can be focused into a spot of submicrometer diameter [2].

In this work, we investigate the feasibility of this approach using molecular dynamics computer simulations. The studied system is composed from beta-carotene molecules embedded inside argon cluster with various mass composition ratio, soft-landed on the Ag(100) substrate. A fraction of deposited molecules as a function of the cluster size and the cluster kinetic energy is measured.

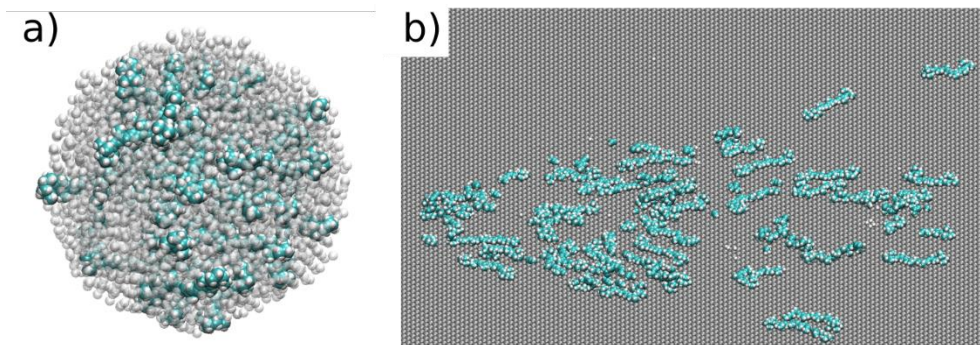


Figure 1: a) Argon cluster with 12% beta-carotene composition, b) Side view of beta-carotene molecules deposited on the Ag(100) surface

[1] V. Franchetti, B. H. Solka, W. E. Baitinger, J. W. Amy, and R. G. Cooks, *Int. J. Mass Spectrom.* 23, 29 (1977).

[2] J.C. Vickerman, N. Winograd, *International Journal of Mass Spectrometry*, 377 (2015) 568.

Influence of noble gases irradiation on the formation of transient layers in multilayer systems

Madadzada Afag I.^{1,2)}, Kulik M.^{1,3)}, Kolodynska D.⁴⁾, Kobzev A.P.¹⁾ and Asgerov E.B.^{1,2)}

¹⁾Joint Institute for Nuclear Research, 141980 Dubna, Russia

²⁾National Nuclear Research Center JSC, 370143, Baku, Azerbaijan

³⁾Institute of Physics, Maria Curie-Skłodowska University, Lublin Poland

⁴⁾Faculty of Chemistry, Maria Curie-Skłodowska University, Lublin Poland

Multilayer systems such as SiO₂/TiO₂/Si and TiO₂/SiO₂/Si have important physical properties, including high dielectric constants, adjustable wide refractive index range, and electro-optic effects. They have been widely used in chemical sensors, in optics, microelectronics, and other fields.

In this study, multilayer systems were subjected to surface **irradiation with ions of noble gases, and the** atomic and chemical compositions and optical properties of the near-surface regions were investigated.

The surfaces of the samples SiO₂/TiO₂/Si, SiO₂/TiO₂/SiO₂/Si and SiO₂/TiO₂/SiO₂/TiO₂/Si were implanted with Ne⁺ and Xe⁺ ions. Atomic concentrations and depth profiles of the elements were obtained on the basis of RBS measurements.

It was found that transient layers were formed in the systems after ion implantation. Their atomic composition changed with the change of the energy and the mass of the implanted ions. Dielectric function spectra of the examined layers were determined in the energy range from 1 eV to 5 eV at room temperature. The measurements were made using the SE method. The dielectric function of the transient layers was determined using EMA approximation. The thickness of the layers determined by the SE method was in good agreement with the estimated values, obtained on the basis of measurements by RBS methods.

XPS measurement results collected for the samples implanted with Xe ions showed that the near-surface SiO concentration increases as ion energy decreases. These changes were not observed within the error limits for samples implanted with Ne ions. These differences can be explained and attributed to radiation damage, which depends on the mass of incoming ions.

The use of piezoelectric phenomena to assess the moisture content of rape seeds

Majcher J. and Boguta A.

Lublin University of Technology, Nadbystrzycka 38 D Str., 20-618 Lublin, Poland

The article discusses the method of seed moisture assessment using a piezoelectric plate. Rape seeds were dropped from a fixed height onto a piezoelectric plate which generated an electric signal under the influence of mechanical stresses caused by the impact. The signal waveform was recorded using an oscilloscope. Then the signal was analysed and a coefficient was calculated. At the same time, seed humidity was tested for each measurement. The size of the calculated coefficient can be correlated with the moisture of seeds. The proposed system allows to determine the moisture content of individual rape seeds.

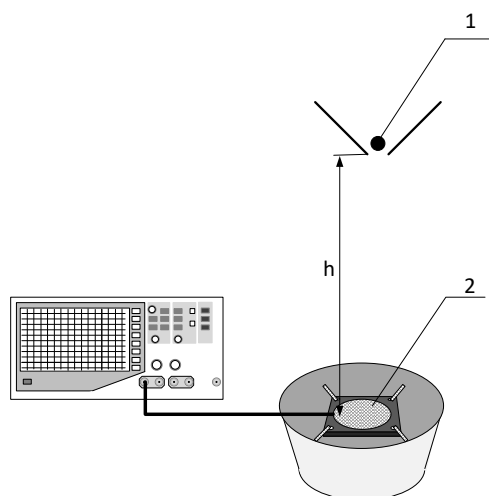


Figure 1: A system for determining seed moisture using a piezoelectric plate: 1 – rape seed, 2 – piezoelectric plate [1]

References

- [1] Boguta A., Majcher J., Using the physical parameters of rape seeds to assess germination force. 2017 International Conference on Electromagnetic Devices and Processes in Environment Protection with Seminar Applications of Superconductors (ELMECO & AoS), IEEE Conferences, 2017 Pages: 1-4.

Modification of MIS Devices by Radio-Frequency Plasma Treatment

*Andreev Dmitrii V.¹⁾, Bondarenko Gennady G.²⁾, Andreev Vladimir V.¹⁾,
Maslovsky Vladimir M.³⁾ and Stolyarov Alexander A.¹⁾*

¹⁾*Bauman Moscow State Technical University, the Kaluga Branch, Bazhenov St. 2, 248000 Kaluga, Russia*

²⁾*National Research University Higher School of Economics, Myasntiskaya ul. 20, 101000 Moscow, Russia*

³⁾*Moscow Institute of Physics and Technology (State University), Institutskii per. 9, 141700 Dolgoprudnyi, Moscow region, Russia*

The paper considers an influence of different kinds of Radio-Frequency (RF) plasma treatment intended for an improvement of electrophysical characteristics of MIS devices with a thermal SiO₂ film. We ascertain that for the modification of MIS structures it is better to use oxygen RF plasma treatment performed by a setup with the parallel-plate-type reactor due to the setup allows to have lesser degradation of charge characteristics of the gate dielectric in comparison with a setup with the cylindrical quartz reactor. Under certain modes of RF plasma treatment performed by a setup with the parallel-plate-type reactor it is possible to get a required density of electron traps with cross-section of 10⁻¹⁷-10⁻¹⁶ cm² in the bulk of the SiO₂ film. As a result, at an initial stage of Fowler-Nordheim tunnel electron injection from silicon in high-fields the dominant process of charge state change is the capture of electrons in the SiO₂ film in contrary to unmodified structures for which the dominant process is the generation of positive charge. This lowers possibility of sample breakdown and raises injection and radiation hardness of samples [1,2].

References

- [1] Andreev V.V., Bondarenko G.G., Maslovsky V.M., Stolyarov A.A., Acta Phys. Pol. A 2015;128;5:887–890.
- [2] Andreev V.V., Bondarenko G.G., Maslovsky V.M., Stolyarov A.A., Andreev D.V., Phys. Status Solidi C 2015;12;1–2:126–130.

Intrinsic gettering in silicon at complex influence of radiation and pulsed magnetic fields

Andreev D.V.¹⁾, Levin M.N.²⁾, and Maslovsky V.M.³⁾

¹⁾*Bauman Moscow State Technical University, the Kaluga Branch, Bazhenov st. 2, 248000 Kaluga, Russia*

²⁾*Innovation Center Biruch, Belaya Vezha st. 1, 309927 Belgorod obl., Malobykovo, Russia*

³⁾*Moscow Institute of Physics and Technology (State University), Institutskii per. 9, 141700 Dolgoprudnyi, Moscow region, Russia*

At present time, a significant amount of experimental data indicates an influence of weak magnetic fields (< 0.2 T) onto structure and properties of materials of solid-state electronics including silicon [1], III-V semiconductors, etc. A possible mechanism of the influence of pulsed magnetic fields (PMF) onto silicon crystals grown by Czochralski process consists in excitation of Si-O bond of interstitial oxygen, a raising of population of excited triplet states due to singlet-triplet transition in radical pairs, decay of nonequilibrium impurity-defective complexes, formation of migrating O-V centers (V-vacancies), long-term multistep cluster formation. An increasing of radical pair concentration in excited triplet state is caused by relaxation of polarization of ^{29}Si kernel spins because of hyperfine interaction after abruption of exposure by pulsed magnetic fields.

In the paper we consider a method of high-temperature gettering in silicon of MIS structure. An importance of irradiation of the crystals by α -particles with energy of 5 MeV consists in formation of defective layer in the end of particle path at a depth of 25 μm that exceeds depth used for formation of device structures. Radiation defects act as centers of precipitation of oxide phases at PMF induced decay of oversaturated oxygen solution. These centers are effective intrinsic heterodynes in silicon. As a result, one observes decreasing of concentration of heterodyne centers at surface layer what results in increasing of generation lifetime of minor charge carriers and decreasing of reverse current of p-n junctions.

References

- [1] Levin M.N, Maslovsky V.M, Solid State Communications 1994;90;12:813-816.

Heavy ion induced subthreshold upsets modeling in memory devices

Galimov A.M.¹⁾, Zebrev G.I.¹⁾, and Maslovsky V.M.²⁾

¹⁾National Research Nuclear University MEPhI, Kashirskoe shosse 31, 115409 Moscow, Russia

²⁾Moscow Institute of Physics and Technology (State University), Institutskii per. 9, 141700 Dolgoprudnyi, Moscow region, Russia

The aim of this work is to demonstrate a simple procedure for simulation of the subthreshold upset cross section of memory devices, that is the topical problem of radiation effects community. The calculation procedure uses only experimental heavy ions (HI) cross section data in above-threshold LET region $\sigma(\Lambda)$ and the differential LET-spectrum of the secondary particles $p(\Lambda|\varepsilon_{HI})$ simulated by Monte Carlo technique in Geant4:

$$\sigma_{sub}(\varepsilon_{HI}) = \int_{\Lambda_c} \sigma(\Lambda) p(\Lambda|\varepsilon_{HI}) d\Lambda, \quad (1)$$

where $\sigma_{sub}(\varepsilon_{HI})$ is the subthreshold cross section as function of HI energy ε_{HI} , Λ_c is the threshold LET.

Fig. 1 shows the comparison of the experimental and simulated $\sigma_{sub}(\varepsilon_{HI})$ for 0.25 um Atmel AT60142F memory device. As can be seen, a procedure shows good correlation to the experimental data.

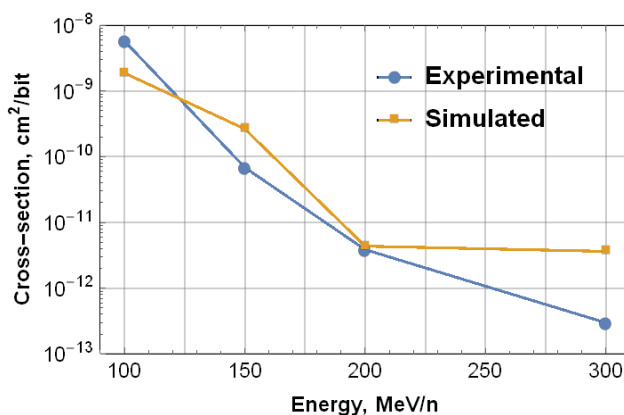


Figure 1: Experimental [1] and simulated $\sigma_{sub}(\varepsilon_{HI})$ for ⁵⁸Ni ion for AT60142F.

References

[1] Hoeffgen, Stefan K. et al., IEEE TNS 2012;59;4:1161-1166.

Lifetime control of silicon devices by proton and carbon implantation

Lagov P.B.^{1,2)}, Kulevoi T.V.³⁾, Maslovsky V.M.⁴⁾, Andreev D.V.⁵⁾, and Volkov A.N.⁶⁾

¹⁾National University of Science and Technology "MISiS" (NUST "MISiS"), Leninskiy prospekt 2, 119049 Moscow, Russia

²⁾A.N. Frumkin Institute of Physical Chemistry and Electrochemistry Russian Academy of Sciences (IPCE RAS), Leninsky prospekt 31, 119071 Moscow, Russia

³⁾Institute for Theoretical and Experimental Physics, Bol'shaya Cheryomushkinskaya st. 25, 117218 Moscow, Russia

⁴⁾Moscow Institute of Physics and Technology (State University), Institutskii per. 9, 141700 Dolgoprudnyi, Moscow region, Russia

⁵⁾Bauman Moscow State Technical University, the Kaluga Branch, Bazhenov st. 2, 248000 Kaluga, Russia

⁶⁾Zelenograd Research Institute of Physical Problems, Georgievskiy prospekt 5, 124460 Zelenograd, Russia

Many silicon devices, including high-power MOS transistors, require to apply technologies to control the lifetime of minor charge carriers (t_r). As a result, one utilizes thermodiffusion, radiation, and combined methods. In practice the most widely utilized method is a treatment by accelerated electrons and protons. The accelerated electrons allow to form electrically active defects at the treatment of few wafers, located as few layers, relatively uniformly. The protons allow to implement a local formation of hidden recombinational layers inside of device layers at significant depth which is especially important for deep diffusion structures [1].

However, for a great number of device structures, especially for epitaxial structures, it is required to form hidden recombinational layers with thickness of 1-2 μm at depth of no more than 20 μm . As a result, in the paper we research a possibility to utilize carbon ions for such aims. As advantages of the carbon implantation one considers the following: carbon in high concentrations is presented in silicon ($\sim 10^{16} \text{ cm}^{-3}$) and, thus, low dose implantation does not affect on dopant profile of the initial material; at the same time high-vacancy complexes are characterized by higher thermal stability. The results indicate higher thermal stability of recombination centers formed at the carbon implantation.

References

[1] Lagov P.B, Drenin A.S, Zinoviev M.A., Journal of Physics 2017;830:012152.

High-rate high-density ICP etching of germanium

Lagov P.B.^{1,2)}, Maslovsky V.M.³⁾, Pavlov Yu.S.²⁾, Rogovsky E.S.¹⁾, Drenin A.S.¹⁾, Skryleva E.A.¹⁾, and Lednev A.M.¹⁾

¹⁾National University of Science and Technology "MISIS" (NUST "MISIS"), Leninskiy prospekt 2, 119049 Moscow, Russia

²⁾A.N. Frumkin Institute of Physical Chemistry and Electrochemistry Russian Academy of Sciences (IPCE RAS), Leninsky prospect 31, 119071 Moscow, Russia

³⁾Moscow Institute of Physics and Technology (State University), Institutskii per. 9, 141700 Dolgoprudnyi, Moscow region, Russia

Nowadays Ge is one of the main substrate materials for multijunction III-V compound solar cells (MJ SC). Usually, Ge substrate thickness is about 150 ± 20 μm , while total thickness of multijunction part is about 5 μm . MJ SC are used to power spacecraft and in concentrator photovoltaic (CPV) systems. Generally space SC has an area of about 30 cm^2 . MJ SC for CPV receiver has an area of 0.1 to 1 cm^2 . Anyway MJ SC operates in severe conditions accompanied by intensive solar irradiation and variations in temperature over a wide range.

MJ SC could be improved by substrate thinning at the post-growth stage of fabrication. As it is known, the thermal conductivity of Ge decreases with temperature and with vacancy concentration increasing. Therefore, reducing the thickness of the substrate will decrease thermal resistance and provide more comfortable thermal conditions for operation and improve the energy/mass ratio of MJ SC. The most promising dry process for this purpose is high-rate inductively coupled plasma (ICP) etching.

As it was found the etch rate of Ge increases linearly from 11.9 to 19.4 $\mu\text{m}/\text{min}$ and surface roughness decreases as the ICP power level increases from 400 to 650 W at SF_6 flow rate of 300 sccm. Also, etch rate of Ge increases by a power law from 8.0 to 16.7 $\mu\text{m}/\text{min}$ as the SF_6 flow rate increase from 50 to 300 sccm at ICP power of 570 W. OES and XPS studies were carried out using NIST databases. Some experimentally observed by OES lines fit to calculated (Ritz) lines. The more clear and good conformity with sufficient amplitude show lines: for sulfur (415.63 \pm), (703.5 \pm), (726.9 \pm)/(727.1 \pm) and fluorine (794.8).

Simulation of silicon device structures operating in radiation environment

*Miskiewicz Siarhiej¹⁾, Komarov Fadei¹⁾, Komarov Alexander¹⁾, Yuvchenko Vera¹⁾,
Bozhatkin Vitali²⁾, Zayats Galina³⁾*

¹⁾*Institute of Applied Physics Problems, BSU, Kurchtov str. 7, Minsk, Belarus*

²⁾*OJSC Integral, Kazintsa str. 121A, Minsk, Belarus*

³⁾*Academy of Sciences of Belarus, 11 Surganov Street, Minsk, Belarus*

Currently, the semiconductors are widely used in the electronics including the space and military equipment operating in radiation environment. To forecast possible failure of these devices the numerical simulation of the radiation-induced effects should be implemented. The aim of this work is to develop an efficient model describing the processes in silicon structures under the radiation exposure.

The developed model based on [1, 2] is used to calculate the radiation-induced variations in the characteristics of bipolar transistors operating under the 1.2 MeV gamma-rays. Figure 1a shows the correlation between the simulated and experimental results [3] of radiation changes in the current gain. Figure 1b shows the calculated dependence of the current gain changes on the base thickness for the base current $I_b=1 \times 10^{-5}$ A.

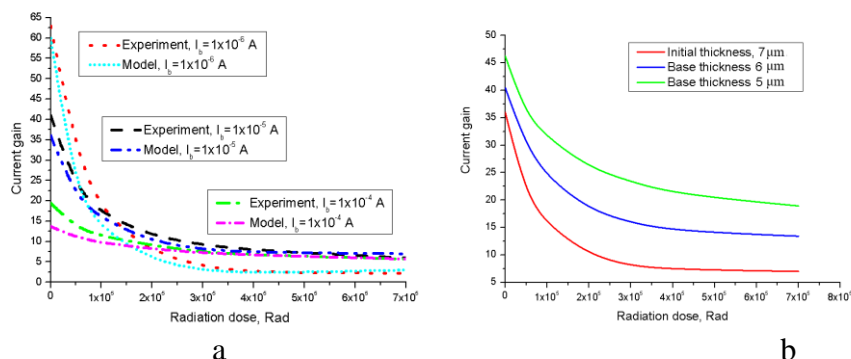


Figure 1: Changes in the current gain of bipolar transistor due to 1.2 MeV gamma-rays

Thus, the changes in the current gain are significant and depend on the operating mode and the size of work regions. The developed model describing the radiation changes in transistor characteristics provides appropriate accuracy of calculations and can be used to predict and minimize possible device malfunctions.

References

- [1] Vologdin E., Lysenko A. Radiation resistance of bipolar transistors. Moscow, 1999.
- [2] Miskiewicz S., Komarov F., Komarov A., Zhukowski P., Michailov V., Przegląd Elektrotechniczny 92, 11, 2016
- [3] Belous A., Solodukha V. Space electronics, Moscow, Technosphaera, 2015.

Diffusion and structural changes of ion implanted glassy carbon after thermal annealing

Njoroge E.¹⁾, Odutemowo O.S.¹⁾, Mlambo M.¹⁾, Hlatshwayo T.¹⁾, Wendler E.²⁾,
Malherbe J.¹⁾

¹⁾*Physics Department, University of Pretoria, Pretoria, South Africa*

²⁾*Institut für Festkörperphysik, Friedrich-Schiller University, Jena, Germany*

The structural changes, migration behaviour of glassy carbon (GC) implanted with 200 – 360 keV Xe, In, Cd, Sr and Cs ions at room temperature and high temperatures have been investigated. The effect of annealing on radiation damage introduced by ion implantation have been investigated. The glassy carbon structure consists of graphitic crystallites with nanopores. Ion bombardment causes the destruction of these nanopores leading to an amorphized structure with higher density. The damage caused by ion bombardment and recrystallization due to annealing at different temperatures has been investigated mostly by Raman spectroscopy and Rutherford backscattering spectrometry (RBS). Annealing of the RT implanted samples resulted in some recrystallization which increased with temperature and the diffusion behaviour of implanted ions. Fickian diffusion of implanted ions has been investigated and the diffusion coefficients of the different ionic species compared. These results were interpreted in terms of trapping and de-trapping of implanted ions by radiation damage.

The influence of PET film morphology on the ion transport properties of asymmetric track-etched single nanopores

Olejniczak K.^{1,2)}, Apel P.Y.^{2,3)}

¹⁾*Faculty of Chemistry, Nicolaus Copernicus University, Gagarina str. 7, 87-100 Torun, Poland*

²⁾*Flerov Laboratory of Nuclear Reactions, Joint Institute for Nuclear Research, Joliot-Curie str. 6, 141980 Dubna, Russia*

³⁾*Dubna State University, Universitetskaya str. 19, 141980 Dubna, Russia*

In this work the uniformity of the electrical characteristics of asymmetric bullet-like single nanochannels prepared in two types of Hostaphan polyester films (RN and RNK) was studied. Both films were irradiated with Au ions at the UNILAC accelerator (GSI, Darmstadt). The RNK samples were also bombarded with Xe ions at the IC-100 cyclotron (FLNR, Dubna). The Au and Xe ion beam energies were 11.4 and 1.2 MeV/u, respectively. Single-ion tracks in samples were obtained by using appropriate diaphragms placed in front of the irradiated film. The ion-irradiated samples were subjected to ultraviolet radiation and then to chemical etching in sodium hydroxide solution. The desired asymmetric shape of pores was obtained by adding an anionic surfactant to the etchant. The registration of the current-voltage characteristics of single pores in KCl solutions allowed us to conclude that the investigated nanoscale objects exhibit high ion current rectification (ICR). Nanopore parameters such as effective pore diameter and rectification ratio were calculated from the electrical current measured

at a voltage ranged from -1 V to + 1 V. It was found that individual single nanopores differ from one another in both effective pore diameters and ICR ratios. These differences presumably result from variations in the tip size and the shape of nanopores and are related to the difference in morphology of investigated films.

Crystalline structure and physical properties of multicomponent (high-entropy) film alloys

Bereznyak Yu.¹⁾, Opielak M.²⁾, Poduremne D.¹⁾, Protsenko I.¹⁾, Shabelnyk Yu.¹⁾

¹⁾Sumy State University, 2, Rymyskyi-Korsakov Str., 40007 Sumy, Ukraine

²⁾Lublin University of Technology, 38 D, Nadbystrzycka Str., 20-618 Lublin, Poland

A new class of materials – high-entropy alloys (HEA) proposed in [1] demonstrate the unique physical-mechanical and magnetic properties in a bulk state. At the same time, the study of the physical properties of film HEA has only been initiated [2]. We investigated on the electrophysical properties of non-eqiatomic HEA films based on Fe, Co, Ni, Cu, Cr or Al, which were formed by simultaneous or layer condensation of separate metals. The component concentration was calculated on the basis of the value of the final thickness of the separate components layers and clarified by the energy-dispersion analysis method.

The phase state and crystalline structure were investigated by electron diffraction and electron microscope methods. The calculation of entropy of mixing (ΔS_{mix}), as a criterion HEA performed on ratio [3]:

$$\Delta S_{mix} = -R \sum_{i=1}^n c_i \ln c_i,$$

where i and c_i – the number and atomic (molar) concentrations of i -components.

The samples of a total thickness $d \cong 30-80$ nm were obtained in a vacuum 10^{-4} Pa by layer-condensation method with subsequent annealing up to 600 K. In both the output and the annealed HEA samples has a fcc lattice ($a=0.3604$ nm) with traces of bcc phase, the parameter of which is close to the α -Fe lattice parameters of α -Fe or bcc Cr, and the solid solution α -Fe(Cr).

The value of magnetoresistance (MR) calculated on the basis of field dependence $R(B)$ based on ratio $MR=(R(B)-R(0))/R(0)$. To measure $R(T)$, $R(B)$ and calculate β and MR used appropriate computerized complex.

Research of MR was performed in geometry CIP (current j in the film plane) at the three relative orientation of the magnetic field: longitudinal (\parallel), transverse ($+$) and perpendicular (\perp) at an current intensity from 0.5 to 1 mA. The effect of annealing to 800 K leads to some increase in the amplitude of the MR , while in the case with the amplitude of the MR virtually unchanged. The relatively small size of the amplitude (maximum is 0.15 %) explained small thickness (40 nm) and very small value of the working current. Splitting the maximum on the dependence of MR due with to domain structure fcc s.s. HEA. The character dependence of MR on magnetic field indicates to realization of anisotropic magnetoresistance.

References

- [1] Yeh J.W., Chen S.K., Lin S.J., et al., *Advanced Engineering Materials* 2004; 6(5): 299.
- [2] Vorobiov S.I., Kondrakhova D.M., Nepijko S.A., et. al., *J. Nano- Electron. Phys.* 2016; 8(3): 03026-1.
- [3] Zhang Y., Zhou Y., *Mater. Sci. Forum* 2007; 561-565: 1337.

Swift heavy ion modification in "Silica+Zn nanocomposite"

*Komarov F.F.¹⁾, Vlasukova L.A.²⁾, Milchanin O.V.¹⁾, Makhavikou M.A.¹⁾,
Skuratov V.A.³⁾, Vuuren A. Janse⁴⁾, Neethling J.N.⁴⁾, Žuk J.⁵⁾, Dauletbekova A.K.⁶⁾,
Parkhomenko I.N.²⁾, Yuvchenko V.N.¹⁾*

¹⁾*A.N. Sevchenko Institute of Applied Physical Problems, Belarusian State University, Kurchatova Str. 7,
220045 Minsk, Belarus*

²⁾*Belarusian State University, Nezavisimosti Ave. 4, 220030 Minsk, Belarus*

³⁾*Joint Institute for Nuclear Research, 141980 Dubna, Russia*

⁴⁾*Centre for High Resolution Transmission Electron Microscopy, Nelson Mandela Metropolitan
University, Port Elizabeth, 6031 South Africa*

⁵⁾*Maria Curie-Skłodowska University, pl. M. Curie-Skłodowskiej 1, 20-031 Lublin, Poland*

⁶⁾*L.N. Gumilyov Eurasian National University, 5, Munaipassov St., 010008 Astana, Kazakhstan*

The process of metal and oxide nanoparticles (NPs) formation with controllable size and shape is investigated due to possible application in optoelectronics, microelectronics and spintronics. Recently several new techniques have been proposed to control the NPs morphology in SiO₂ matrix. One of them suggests using swift heavy ion beams. In this study, Zn-based nanoclusters were synthesized in SiO₂ via ion implantation followed by annealing and/or irradiation with Xe ions (200 MeV, 2×10^{14} cm⁻²). SiO₂ layers (600 nm) thermally grown on Si were implanted with Zn ions (150 keV, 7.5×10^{16} cm⁻²). Afterwards, a part of the samples was annealed in air (700°C, 60 min). The RBS, XTEM, HRTEM and PL techniques were used for diagnostics. It was shown that Xe irradiation resulted in ordering and elongation of Zn-based nanoclusters along the direction of the ion beam. The double-peaked band in visual range with maxima at 425 and 570 nm was observed in PL spectrum of "SiO₂ + Zn-based NPs" composite after Xe ion irradiation. The effects of annealing and Xe irradiation on Zn nanoparticle's modification and a nature of the registered PL are discussed.

Changes of Ti-Cr-N coatings structure and hardness under the impact of xenon ions and annealing

Satpaev D.A.¹⁾, Poltavtseva V.P.¹⁾, Degtyaryova V.P.¹⁾, Partyka J.²⁾

¹⁾*Institute of Nuclear Physics ME RK, Almaty, Kazakhstan*

²⁾*Lublin University of Technology, Lublin, Poland*

This article reports experimental studies of the patterns of changes in the structure and microhardness of Ti-Cr-N coatings on carbon steel as a function of irradiation with $^{132}\text{Xe}^{20+}$ ions at 200 MeV and post-radiation annealing up to 600°C. It is shown that interaction of $^{132}\text{Xe}^{20+}$ ions with the Ti-Cr-N coating surface leads to formation of the globules filled with the inert gas of xenon. It is established that softening of the coatings by 11% is associated with stress relief and structural change.

References

- [1] Van Vuuren A., Skuratov V., Uglov D., Sohatsky A., Swift heavy ion irradiation effects on He agglomeration in ZrN and TiZrN ceramics // Proc. 11th Intern. Confer.: Interaction of radiation with solids, Minsk, 2015, P. 91–92.
- [2] Uglov V.V., Rusalski D.P., Zlotski S.V. e. a., Stability of Ti-Zr-N coatings under Xe-ion irradiation, Surface & Coatings Technologies, 2010, V. 204, P. 2095–2098.
- [3] Uglov V.V., Barkovskaya M.M., Khodasevich V.V. e. a., Thermal stability of nitride coatings by ion-plasma deposition, Vacuum, 2007, V. 81, P. 1345-1347.
- [4] Poltavtseva V., Larionov A., Satpaev D., Gyngazova M., Radiation hardening of Ni-Ti alloy under implantation of inert gases heavy ions, IOP Conf. Series: Materials Science and Engineering, 2016, V.110, P.012011.

Effect of the fluence of high-energy krypton ions irradiation on Ni-Ti alloy hardening

Satpaev D.A.¹⁾, Poltavtseva V.P.¹⁾, Partyka J.²⁾

¹⁾*Institute of Nuclear Physics ME RK, Almaty, Kazakhstan*

²⁾*Lublin University of Technology, Lublin, Poland*

The patterns of changes in microhardness and phase composition of Ni-Ti alloy in the austenitic structural-phase state have been experimentally studied depending on the fluence of irradiation with ${}_{84}\text{Kr}^{15+}$ ions with the energy of 147 MeV. It was established that hardening with a maximum in the region of the projected range R_p and in the out-of-range region ($h > R_p$) increases with the growth of the irradiation fluence up to 5×10^{19} ion/m². It was shown that the reason of hardening is formation of the radiation-introduced hardened defective structures. The formation of nano-sized particles of the martensitic R-phase and the decrease in NiTi phase content with the B2 structure are also characteristic in the process of irradiation up to maximum fluence due to radiation effects.

References

- [1] Poltavtseva V., Larionov A., Satpaev D., Peculiarities of structure and hardening of Ni-Ti alloy surface layers formed by ${}_{84}\text{Kr}^{15+}$ ions irradiation at 147 MeV energy at high temperatures, IOP Conf. Series: Materials Science and Engineering, 2017, V.168, P.012032.
- [2] Poltavtseva V., Larionov A., Satpaev D., Gyngazova M., Radiation hardening of Ni-Ti alloy under implantation of inert gases heavy ions, IOP Conf. Series: Materials Science and Engineering, 2016, V.110., P.012011.
- [3] Poltavtseva, V.P., Kislitsin S.B., Satpaev D.A., Mylnikova T.S., Chernyavskii A.V., Feature of radiation damage of Ni-Ti alloy under exposure to heavy ions of gaseous elements, IOP Conf. Series: Materials Science and Engineering, 2015, V.81, P.01234.

Structure and hardness evolution of silicon carbide epitaxial layers irradiated with He⁺ ions

Pilko Vladimir¹⁾, Komarov Fadei¹⁾, Budzyński Piotr²⁾

¹⁾*A.N.Sevchenko Institute of Applied Physics Problems, Kurchatov St. 7, 220045 Minsk, Belarus*

²⁾*Lublin University of Technology, Nadbystrzycka St. 38 D, 20-618, Lublin, Poland*

Silicon carbide is a material of vital importance in several applications such as nuclear fission and fusion reactor projects, reliable radiation-resistant diagnostic sensors

and radiation detectors. All these applications suppose harsh influence of radiation that drastically changes intrinsic physical properties of materials. Particularly fission and transmutation reaction products such as He induced volumetric and tribomechanical properties deterioration that can lead to crucial consequences in such an environmental sensitive field as nuclear energetics. In our study, the 4H polytype SiC epitaxy

layers of ~ 3 μm thickness on SiC substrates were implanted with 500 keV He⁺ ions with fluences in the range from 5×10¹⁴ ion/cm² to 1×10¹⁷ ion/cm². Induced defects distributions were studied by means of Rutherford Backscattering technique in the channeling regime. Structure changes were identified via characteristic phonons intensity deviations registered by Raman Spectroscopy technique. Evolution of hardness for all irradiated samples were investigated by the means of conventional Vickers measurements and via dynamic nanoindentation with the Oliver-Pharr method results processing. For all samples, the normal indentation size effect [1] was observed.

References

[1] Nix W. D., Gao H., J.Mech.phys.Solids 1998, Vol.46, No3, pp. 411-425.

Continuous ultrasound assisted sonoelectrochemical synthesis of W-Co alloy nanoparticles

Plaipaitė-Nalivaiko Rita¹⁾, Griškonis Egidijus²⁾, Adlienė Diana³⁾

¹⁾*Kaunas University of Applied Engineering Sciences, Tvirtovės al. 35, LT-50155, Kaunas, Lithuania*

²⁾*Kaunas University of Technology, Department of Physical and Inorganic Chemistry, Radvilėnų road 19, LT-50254 Kaunas, Lithuania*

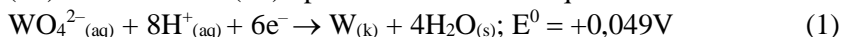
³⁾*Kaunas University of Technology, Department of Physics, Studentų str. 50, LT-51368 Kaunas, Lithuania*

The overwhelming attention towards nanostructured materials containing nanoparticles is increasing day-to-day. The successful application of nanoparticles depends upon both the synthesis and the surface modification of particles [1]. Surface modification can improve the intrinsic characteristics of nanoparticles and allows the fabrication of nanocomposites and other structures also inexistent in nature [2]. Specific interest is paid to synthesis of heavy metal and alloy nanoparticles exhibiting exceptional structural, magnetic and mechanical properties [3].

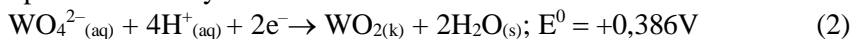
The main purpose of this work was to synthesize W-Co alloy nanoparticles from aqueous tungstate (VI) – cobalt (II) electrolyte by sonoelectrochemical method applying continuous ultrasound and pulsed potential mode and to analyze and discuss the formation mechanism of nanoparticles under continuous ultrasound irradiation.

W-Co alloy nanoparticles have been synthesized from aqueous electrolyte by sonoelectrochemical method applying pulsed potential mode and continuous ultrasound irradiation. Electrochemical synthesis technique with integrated ultrasonic bath as the ultrasound source was used for this purpose. For the electrochemical reduction

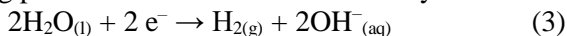
of tungstate (VI) to metallic W (IV) up to 6 electrons are required:



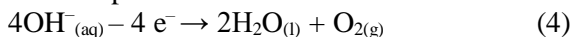
The first stage of electrochemical reduction of tungstate to tungsten (IV) oxide occurs in the presence of only two electrons:



The further tungstate reduction to metallic W is aggravated due to ongoing unfavorable electrochemical process - the release of gaseous hydrogen by reduction of H⁺ ions and/or H₂O molecules. W and Co atoms deposited on the cathode in this way are forming W-Co alloy. Free hydrogen is also formed at the cathode due to the side reactions taking place in the weak alkaline electrolyte:



The following reaction is present at the insoluble anode too:



The shape and surface morphology of the synthesized W-Co nanoparticles has been determined by transmission and scanning electron microscopy, as well as composition of W-Co NPs was assessed by energy dispersive X-ray spectroscopy. The size of

synthesized W-Co nanoparticles has been investigated in details by photon correlation spectroscopy.

It was found that the size of produced spherical W-Co nanoparticles varied from 100 to 500 nm, and the average atomic ratio of W and Co was 23:4 correspondingly. The non-uniformity of synthesized particles in size and the reasons for that are discussed on the basis of the obtained results.

References:

- [1] Gedanken A., *Ultrason. Sonochem.* 2004, 11, 47-55;
- [2] Sáez V., Mason T.J., *Molecules* 2009, 14, 4284-4299;
- [3] Tsyntaru N., Cesiulis H., Budreika A., Ye X., Juskenas R., Celis J.-P., *Surf. Coat. Tech.* 2012, 206, 4262-4269.

Combined multilayered coatings based on alternative triple nitride and binary metallic layers, their structure and physical-mechanical properties

Bondar O.V.^{1,2)}, Pogrebnjak A.D.¹⁾, Takeda Y.²⁾, Zukowski P.³⁾

¹⁾*Sumy State University, Department of Nanoelectronics, 40007 Sumy, Ukraine*

²⁾*National Institute for Material Science, 305-0047, Tsukuba, Ibaraki Prefecture, Japan*

³⁾*Lublin University of Technology, 20-618 Lublin, Poland*

The nitride coatings based on transition metals are widely used in modern materials science because of their exceptional physical and tribological properties. The most typical areas of application of such materials are wear protection, as well as corrosion and abrasive protection. The most extensively studied single-layer coatings are TiN, CrN, MoN and ZrN, but their properties are not good enough for modern demands in materials science. It has already been proved that the multilayer coatings demonstrates better properties in comparison with the single layered ones. The combination

of alternative layers made of binary or even triple nitrides of different refractory metals can provide superior performance and productivity of various tool components.

Combined multilayered coatings based on alternative triple nitride and binary metallic layers were deposited using vacuum-arc evaporation of a cathode. (TiMo)N/TiMo, (CrMo)N/CrMo, (CrZr)N/CrZr, (TiCr)N/TiCr and (MoZr)N/MoZr multilayer coatings were fabricated under the same deposition conditions, while bias potential was -200 V. Total thickness of the coatings was around 54 micrometers, while bilayer thickness was 900 nm and we had 60 bilayers in each coating. Thicknesses of triple nitride and binary metallic layers were 750 nm and 150 nm respectively. Vickers hardness HV0.1, HV0.5 and HV1 of the coatings varied from 2347 to 2912, 2077 to 2584 and from 1369 to 2327 respectively, which makes them perspective for application as protective ones.

This work was done under the aegis of Ukrainian state budget program №0116U006816.

Comparative analysis of structural disorder of surface layers of Yttrium Iron Garnet Films as a result of implantation by Si⁺ and P⁺ ions

Pylypiv V.M., Garpul O.Z., Khrushch L.Z.

Vasyl Stefanyk Precarpathian National University, 57 Shevchenko Str., Ivano-Frankivsk, 76025, Ukraine

For the study of the peculiarities of the formation of radiation defects and their distribution in the damaged layer at depth, the implantation of films of YIG by P⁺ with E = 65 keV and Si⁺ with energy of 90 keV with different doses, was performed. The simulation were executed using the program SRIM-2008. According to the results of modeling, the projective range of P⁺ to 46±2 nm, and the processes of elastic defect formation reach a depth of 100±3 nm, the total energy losses of the P⁺ implant are ≈800 eV per 1 nm of run [1]. The most effective radiation disorder occurs in the anion substrate, where the amount of mixing ions reaches 4.5 on 1 nm in the implant process, which is almost triple it increases the similar index for sublattices of Fe, and the maximum of defects distribution falls on the depth 35±5 nm. For the obtained model of low doses of implantation ($D \leq 1 \cdot 10^{14} \text{ cm}^{-2}$), the degree of disorder of the crystalline lattice for depths of 0-40 nm lies in the range of 60-70% [1]. In the case of implantation by Si⁺ ions, the projective range in the structure of YIG is 80 ± 5 nm, and the maximum depth of their penetration reaches 170 ± 6 nm, the energy losses of the implant reach 800 eV/nm, nuclear energy losses - make up 56% of all losses. Calculated profiles of structural damage of Si⁺ implanted with different doses and E = 90 keV of the film, have shown maxima at a depth of 25 ± 5 nm, for doses of implantation 1·10¹³, 6·10¹³ and 2·10¹⁴ (cm⁻²), the relative of disorder of the area surface of YIG film is 3%, 19% and 50%, respectively.

As result of modeling, in the implantation of the film YIG by the P⁺ ions the elastic type of stopping dominates. It was found that at a dose of 5 10¹⁴ cm⁻² the degree of decomposition of the lattice in the surface layer up to 40 nm is up to 70%, when the YIG film is implanted by the Si⁺ ions at a dose of 2 10¹⁴ cm⁻², the degree of structural disorder is 50%, with the initial thickness of the amorphous layer of about 30-40 nm.

References

- [1] H. Donnerberg, C. R. A. Catlow. Atomistic computer simulations of yttrium iron garnet (YIG) as an approach to materials defect chemistry. I. Intrinsic defects // J. Phys.: Condens. Matter. – 1993. – 5, No. 18. – P. 2947-2960.

Studies on transformation of magnetron sputtered and pulse electron beam melted zirconium silicide coatings deposited on zirconium alloy

Starosta W.¹⁾, Barlak M.²⁾, Smolik J.³⁾, Waliś L.¹⁾ and Sartowska B.¹⁾

¹⁾*Institute of Nuclear Chemistry and Technology, 16 Dorodna St., 03-195 Warsaw, Poland*

²⁾*National Center for Nuclear Research, 7 Andrzeja Sołtana St., 05-400 Otwock, Poland*

³⁾*Institute for Sustainable Technologies, 6/10 K.Pułaskiego St., 26-600 Radom, Poland*

Zirconium alloys are widely used in nuclear reactors for fuel element claddings. High oxidation rate of exothermic oxidation reaction in steam environment at elevated temperatures may severely compromise safety of nuclear reactor in the cases when cooling ability is lost (LOCA accident). The replacing of zirconium fuel claddings with ones made of SiC or FeCrAl alloy or applying external coatings made of much less oxidation prone materials e.g. MAX ceramic, chromium, zirconium silicides are considered [1-2]. We have conducted recently research works on oxidation properties of coatings deposited by magnetron sputtering from two independent Zr and Si targets or from one ZrSi₂ target. We have found that admixture of Cr at 15% level was necessary for getting coatings stable in autoclave test in water.

In searching for the methods best suited for the conditioning of deposited layer in order to make them compact and firmly bonded to the zirconium alloy support we performed preliminary experiments with pulsed electron beam. The coatings deposited from two independent targets ZrSi₂ and Cr with the chromium content of around 5, 10 and 15% were irradiated with electron beam. The used device was a source of low-energy high current electron beams of microsecond duration, which generates a fairly homogeneous wide-aperture electron beam up to 10 cm in diameter [3]. The main parameters of the modification processes were: energy density of pulses about 5 J/cm², pulse duration about 2 μs, number of pulses 3 or 5.

The results of X-ray diffraction, SEM observations of the surfaces and the cross-sections, the depth profiles of selected elements in the transformed surface layers will be presented.

References:

- [1] Zinkle S.J et al., J. Nucl. Mat. 2014; 448:374
- [2] Tang, C et al., Corrosion Reviews 2017; 35:141
- [3] http://www.microalloy.ru/html/Oborudovanie_en.htm

Microstructure and physical-mechanical properties of nanosized ZrN/CrN coatings under different deposition conditions

Maksakova O.V.¹⁾, Pogrebnjak A.D.¹⁾, Bondar O.V.¹⁾, Świć A.²⁾

¹⁾ Sumy State University, 2, Rymasko-Korsakova Str., 40007 Sumy, Ukraine

²⁾ Lublin University of Technology, 38D, Nadbystrzycka Str., 20-618 Lublin, Poland

The industrial application of thin coatings based on ZrN in machine building and other industries is limited by satisfactory combination of their tribological (wear-resistant

and antifriction) and physical-mechanical properties. Enhancement of properties and enlargement of applications of such films are possible due to the deposition of multilayered structures using CrN as the second alternating layer.

Multilayered ZrN/CrN coatings were deposited onto AISI321 stainless steel substrates by a cathodic arc technique. Two single-component cathodes of zirconium and chromium of 99.5% purity were used during deposition. The main process parameters were: the arc current (I_d) was 100 A, the nitrogen pressure (P_N) varied from 0.029 to 0.43 Pa, the substrate temperature (T_S) was 250°C, the constant negative bias potential ($-U_S$) was in the range of -70 and -150 V.

Fabricated multilayers had an alveolar surface structure. A significant amount of the microdroplet fractions were observed with the average size of 6 μm . Transition layer of 0.3-0.45 μm in width provided a good adhesion between the coating and the substrate. X-ray diffraction spectra analysis showed the presence of ZrN and CrN phases. The formation of predominant texture [200] was observed independently of applied deposition parameters. It was established that the negative bias potential and working pressure effected complexly on the mechanical properties of the investigated coatings. The maximum microhardness 4685HV0.025 was observed for the coating deposited

at high $P_N = 0.43$ and low $U_S = -70$ V.

Ion Implantation in the Technology of Metal-Oxide Memristive Devices

*Tetelbaum D.I.¹⁾, Mikhaylov A.N.¹⁾, Belov A.I.¹⁾, Korolev D.S.¹⁾, Okulich E.V.¹⁾,
Okulich V.I.²⁾, Shuisky R.A.¹⁾, Guseinov D.V.¹⁾, Gryaznov E.G.¹⁾, Stepanov A.V.¹⁾,
Gorshkov O.N.¹⁾*

¹⁾*Lobachevsky University, Prospect Gagarina, 23/3, Nizhny Novgorod, Russia*

²⁾*Nizhny Novgorod Institute of Management – a branch of Russian Presidential Academy of National Economy and Public Administration, Prospect Gagarina, 46, Nizhny Novgorod, Russia*

Memristive devices (MD) are among the “hot points” of modern electronic engineering due to potential applications in resistive memory (RRAM), logic and neuromorphic systems. The memristive effect is revealed in the change of resistance under electrical stress as a result of local modification of atomic structure or composition of a dielectric film deposited between two conductive electrodes. In the present report, it will be shown how ion implantation can be employed in the technology of the Au/SiO₂/TiN and Au/ZrO₂(Y)/TiN MD. In the first example, the dielectric film is ion-modified in order to improve the MD performance by reducing the role of uncontrollable factors responsible for the variation of resistive switching parameters. The low-energy Xe⁺ ions were used with ion ranges much lower than the film thickness. The ion fluences were chosen in such a way that the average distance between the ion incidence points were higher than the average lateral size of displacement cascade. The ion-induced defect regions play the role of nuclei for conductive filaments formed in dielectric film during electroforming. Such treatment lowers the device-to-device variation of electroforming parameters and also improves the high-to-low resistance ratio in the switching mode. The second implementation of ion implantation is the simulation of high-energy (space) proton and fission neutron irradiation. The medium-energy (150 keV) ions are used to reproduce the ionization and displacement damage and to predict the radiation hardness of MD. It is concluded that the described applications open new and prospective area for science and technology of ion implantation.

The study was supported by the Ministry of Education and Science of the Russian Federation (RFMEFI58717X0042).

Synthesis of hexagonal silicon by ion implantation

Tetelbaum D.I., Nikolskaya A.A., Korolev D.S., Mikhaylov A.N., Belov A.I., Sushkov A.A., Pavlov D.A.

Lobachevsky University, Prospekt Gagarina 23-3, 603950 Nizhny Novgorod, Russia

The search and development of light-emitting semiconductors which are compatible with traditional silicon technology for a new generation of optoelectronic integrated circuits is one of the most prominent goals of modern electronics. It is expected that hexagonal phases of silicon would have better light-emitting properties compared to diamond-like (C-phase) silicon. Here we report on the formation of hexagonal (9R) Si by using ion synthesis method and on the photoluminescence spectra of the corresponding samples.

Two kinds of procedures were carried out. The first one was as follows. The Si (100) samples were implanted by N_2^+ (20 keV, $2.6 \cdot 10^{17}$ at/cm²) with 1100 °C post-implantation annealing to synthesize thin Si_3N_4 layer. Then Ga^+ ($5 \cdot 10^{16}$ cm⁻²) and N_2^+ ($5 \cdot 10^{16}$ at/cm²) ions were co-implanted with energies of 80 and 40 keV, respectively. In the second procedure, the Kr^+ (80 keV, $5 \cdot 10^{16}$ cm⁻²) ions were implanted into the SiO_2/Si samples with SiO_2 thermal oxide thicknesses of 160 and 120 nm. For both procedures, the final annealing was performed at 800 °C (30 min).

The X-TEM data for these samples reveal the buried nanoregions which are identified (by using high-resolution image and its Fourier analysis) as nanocrystalline inclusions of 9R-Si phase. For the Kr^+ -implanted samples, the photoluminescence spectra measured at 78 K demonstrate the emission band at 1240 nm.

The 9R-Si formation is promoted by the relaxation of stresses induced by implantation (and/or annealing) at the interface layers with Si substrate: implanted layer/substrate and SiO_2 /substrate for the first and second procedures, respectively.

The study was supported by the Ministry of Education and Science of the Russian Federation (State Assignment № 16.2737.2017/4.6). A.A. Nikolskaya acknowledges the support in the framework of UMNIK program.

Thermal desorption of He implanted into Ge

Turek Marcin¹⁾, Drożdżiel Andrzej¹⁾, Pyszniak Krzysztof¹⁾, Prucnal Sławomir¹⁾, Żuk Jerzy¹⁾, Yuschkevich Yuriy²⁾, Węgierek Paweł³⁾

¹⁾*Institute of Physics, Maria Curie Skłodowska University in Lublin, Pl. M. Curie-Skłodowskiej 1, 20-031 Lublin, Poland*

²⁾*Joint Institute for Nuclear Research, Joliot-Curie 6, Dubna, Russia*

³⁾*Technical University in Lublin, Nadbystrzycka 38 A 20-618 Lublin, Poland*

After years of standstill germanium attracts attention as a possible semiconductor of the future, mostly due to its high carrier mobility, as well as similarities to „her brother” [1] silicon, what gives a chance for integration with contemporary CMOS technology. Formation of inert gas bubbles in this material could be especially important for fabrication of GeOI (germanium on insulator) wafers in a process resembling the Smart-cut. Investigations of He bubbles formation in Ge as well as of helium release due to electron impact were presented in [2]. It was shown that high-fluence ($5 \cdot 10^{16} \text{ cm}^{-2}$) irradiation with 30 keV He⁺ ions leads to formation of bubbles having diameter of 1-2 nm. Surface blistering was also observed after 60 keV H implantation (fluences up to 10^{17} cm^{-2}) followed by the annealing at temperatures in the range 200-350°C.

The paper presents results of TDS measurements of He⁺ implanted (100 and 80 keV) germanium samples with smaller fluences ($1 \cdot 10^{16} \text{ cm}^{-2}$), still large enough to lead to bubble formation in the case of Si. The TDS spectra collected for both implantation energies using heating ramp rates in the range 0.45 K/s up to 1.5 K/s are presented and discussed. Desorption activation energies are calculated from the peak shifts using the Redhead method. A brief presentation of the experimental setup and procedures is also given for completeness.

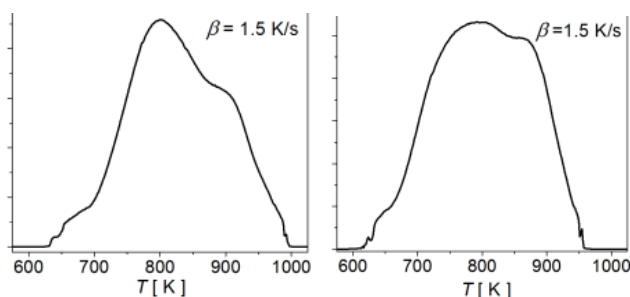


Fig 1. TDS spectra of He implanted into Ge at 100 keV (left) and 80 keV (right)

Acknowledgement: This work was partially supported by the National Science Centre, Poland, under Grant No. 2016/23/B/ST7/03451.

References

- [1] Vanhellefont J., Simoen E. *Journal of The Electrochemical Society*, 2007;154;H572
 [2] David M-L., Alix K., Pailloux F., Mauchamp V., Couillard M., Botton G. A., and Pizzagalli L. *Journal of Applied Physics* 2014;115:123508

Ion beam emittance for an ion source with a conical hot cavity

Turek Marcin

*Institute of Physics, Maria Curie Skłodowska University in Lublin Pl. M. Curie-Skłodowskiej 1,
20-031 Lublin, Poland*

Hot cavity ion sources are used in different ISOL (Isotope Separation On- Line) facilities [1] over decades mainly due to their advantages as high ionisation efficiency, excellent beam purity and low energy spread of produced beam. The short time atoms stay in the ioniser is crucial in the case of short-lived isotopes. Recently [2] the hot cavity having a shape of a truncated cone has been proposed. The conical cavity is by far easier to produce than a spherical one, as refractory metals are very hard to machine. The advantage of elongated cavity shapes over the compact ones was proven for stable isotopes, the twofold increase of ionisation efficiency is especially important for hard-to-ionise substances. Compact shape prevails for very short-lived isotopes as the average time a particle stays in the compact cavity is shorter.

The brief description of the numerical model and results of emittance calculations for different elongations of the cavity in the case of stable isotopes are presented and discussed. Dependences of beam emittance on ionization probability, half-life period and average sticking time obtained for different cavity shapes are also considered. Influence of the extraction opening geometry i.e. the extraction opening radius and the length of the extraction channel is studied. A concept of scaled efficiency is used to compare beam quality for different extraction opening configurations as well as isotope half-lives.

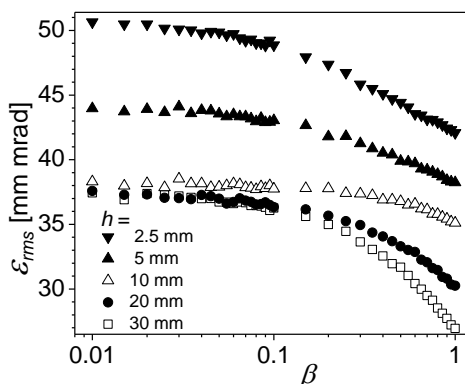


Fig 1. The rms emittance for different cavity elongations in the case of stable isotopes

References

- [1] Panteleev V N, Rev. Sci. Instrum. 2004;75:1602
 [2] Turek M, Acta Phys. Pol. A 2017;132:259

Negative ion beam production in an ion source with chamfered extraction opening

Turek Marcin

Institute of Physics, Maria Curie Skłodowska University in Lublin Pl. M. Curie-Skłodowskiej 1,
20-031 Lublin, Poland

Neutral beam injection (NBI) systems making use of neutralisation of negative ion beams are crucial for plasma heating in future nuclear fusion devices like ITER [1].

The paper presents a 2D Particle-in-Cell model of H⁻ ion transport and extraction in a single aperture system. The improved model not only enables more accurate calculations using a finer numerical mesh compared to the previous paper [2] but it assumes that negative ions can be created not only at caesiated plasma grid parts facing the chamber but also at the chamfered surfaces of the extraction opening. The presented results were obtained using a self-consistent electrostatic code taking also into account some particle-particle collisions.

Besides the concise model description, the paper presents results of the calculations of charge density and potential distributions as well as H⁻ extracted currents. The influence of the chamfered walls inclination angle on H⁻ yield and charge distribution is discussed. Impact of the H⁻ flux outgoing from the chamber wall on the extracted current is also considered for different extraction channel geometries. Current-voltage curves obtained for different chamfering angles are compared. Evolution of the beam profiles with the change of extraction voltage due to the change of the place the beam is emerging from is demonstrated and discussed in details.

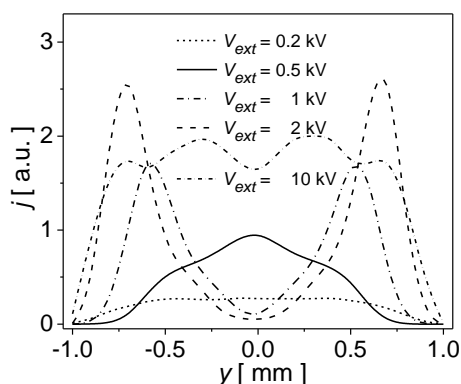


Fig 1. H⁻ ion current density profiles obtained for different V_{ext}

References

- [1] Hemsworth R., Tanga A., Antoni V., Rev. Sci. Instrum. 2008;79:02C109
- [2] Turek M, Acta Phys. Pol. A 2017;132:254

Properties and scratch resistance of PVD coatings on Ti6Al4V alloy

Walczak M. and Pasierbiewicz K.

University of Technology, Faculty of Mechanical Engineering, Department of Materials Engineering, Lublin, Nadbystrzycka St. 36, 20-618 Lublin, Poland

According to literature data abrasive wear is one of the most frequent causes of damage to biomaterials. This mechanism of wear leads to reduced implant life and increased number of necessary revision treatments. Abrasive wear products lead to decreased mechanical properties, particularly on the contact of a tribological pair. Moreover, they intensify pain and the negative biological response of tissues, which leads to local irritation and inflammation, and, consequently, to implant failure. Titanium and its alloys are very popular in medicine. Unfortunately, titanium alloys have insufficient abrasion resistance. In recent years, there has been a trend related to the modification of the surface layer of titanium materials. This trend, among others is related to the application of nitride coatings using the PVD method. PVD coatings enable to obtain a gradient diffusion layer of sufficient thickness and adhesion, which ensures long-lasting abrasion-resistant surface.

In this research, it was decided to study the usefulness of AlTiN and TiAlN coatings on Ti6Al4V alloy to improve its abrasion resistance. Coatings were placed physically from the gas phase PVD in the magnetron sputtering process. The substrate was Ti6Al4V titanium alloy. The titanium substrate have been fabricated in direct selective laser melting (DSLM) process by means of 3D printer for metals - EOSINT M280 supplied by EOS. The roughness of specimens was examined using a Dektak 150 profilometer (Veeco Instruments Inc., USA). The mechanical properties (hardness, Young's modulus) of nitride coating and the substrate were studied by an Ultra Nanoindentation Tester (Anton Paar GmbH, Germany). The hardness and elastic modulus were calculated from the load-displacement curves according to the Oliver Pharr method. The adhesion of the coatings was determined by the scratch test and Rockwell test. Scratch tests were performed on a Micro Combi Tester (Anton Paar GmbH, Germany) according to the ASTM C1624 – 05(2015) standard for ceramic coatings scratch testing.

Analysis of the influence of annealing temperature on mechanisms of charge carrier transfer in GaAs in the aspect of possible applications in photovoltaics

Węgierek P., Billewicz P., Pietraszek J.

Lublin University of Technology, ul. Nadbystrzycka 38 D, 20-618 Lublin, Poland

In our previous work [1] we investigated probability of the occurrence of jump mechanism of electric charge transfer in gallium arsenide irradiated with H^+ ions. This article presents some correlations between electron's jump probability and annealing temperature in GaAs structure dedicated to applications in photovoltaic. It allows to conclude that observed value of probability is strictly connected with type of the radiation defects. Disappearance of every single defect during the process of annealing causes rapid changes of the value of both conductivity and electron's jump probability as well.

References

[1] Węgierek P., Billewicz P., Przegląd Elektrotechniczny 2012;11b:364.

Magnetoresistive properties of nanostructured thin film systems based on Ni₈₀Fe₂₀ and Ag

Żukowski P.¹⁾, Pazukha I.²⁾, Shuliarenko D.²⁾ and Protsenko S.²⁾

¹⁾Lublin University of Technology, 38 D, Nadbystrzycka Str., 20-618 Lublin, Poland

²⁾Sumy State University, 2, Rymskyi-Korsakov Str., 40007 Sumy, Ukraine

Nanostructured thin film systems based on permalloy Ni₈₀Fe₂₀ (Py) and Ag exhibit giant magnetoresistance, so their electric resistance can change highly by applying of magnetic field.

Thin film structures based on permalloy and silver of 55 nm thickness were deposited by electron-beam co-evaporation technique using Py and Ag independent sources in HV chamber with a base pressure 10⁻⁴ Pa. As a result, the series of samples with concentration $c_{\text{Ag}} = 15-75$ at.% were obtained in one deposition run.

The study of field dependences of magnetoresistance that were measured using software-hardware complex with current-in-plane geometries in an external magnetic field from 0 to 500 mT at room temperature allows to conclude that a value of MR of nanostructured thin films based on Py and Ag strongly depends on component concentration. For the films with $c_{\text{Ag}} = 15$ at.% the magnitude of magnetoresistance is small (less than 0.2%). At the increasing of the concentration of Ag atoms the MR value gradually increases and reaches maximum 1.5% at the $c_{\text{Ag}} = 60$ at.%. A future increase of the non-magnetic component concentration leads to the reduction of magnetoresistive effect. A peculiarity of field dependences for samples after deposition for the entire concentration range is the absence of the saturation of MR in fields as high as 500 mT. The annealing up to 500 K does not change the field dependences shape in all geometries within the range $c_{\text{Ag}} = 15-75$ at.% with maximum value 1.8% at the $c_{\text{Ag}} = 60$ at.%. At the same time high-temperature annealing up to 600 and 700 K leads to the fall of effect amplitude and to the change MR curve shape.

Constant current hopping conductivity in percolation channel

Żukowski Paweł and Rogalski Przemysław

Lublin University of Technology, Nadbystrzycka 38D, 20-618 Lublin, Poland

As is known, in many heterogeneous systems with relatively high resistivity, there may occur hopping conductivity, involving electron tunneling between potential wells. This phenomenon occurs in semiconductors compensated with shallow admixtures at helium temperatures, semiconductors irradiated with neutrons, ions or electrons, in metal-dielectric nanocomposites produced by ion spraying, and even in insulating oil impregnated electrotechnical pressboard, containing water nanodrops. At low contents of the potential wells, hopping exchange of charge on a direct current can only occur when a percolation channel connecting both measuring contacts is created. In percolation channel there is a hopping change of electrons between neighboring neutral potential wells. In the paper, based on equations describing the hopping conductivity caused by the electron tunneling between neighboring potential wells, a computer simulation

of a single percolation channel resistance was made. This situation occurs at relatively low content of potential wells. The number of potential wells that made the percolation channel is very large. It must be assumed that the potentials wells in the percolation channel are arranged in a random manner. Based on a computer simulation, it was found that the random distribution of potential wells in the percolation channel causes its resistance to be higher than if the wells were arranged regularly in the chain. The simulation also shows that the higher the standard deviation in probability distribution of distances between wells in percolation channel is, the higher is the resistance of such channel.

Electrical conduction properties of DC magnetron sputtered indium oxide thin films

Pochtenny A.¹⁾, Luhn V.¹⁾, Volobuev V.¹⁾, Shikanov S.¹⁾ and Żukowski P.²⁾

¹⁾ Belarussian State University of Technology, Sverdlova st., 13a, 220006 Minsk, Republic of Belarus

²⁾ Lublin University of Technology, 20-618 Lublin, Poland

Thin In_2O_3 films with thickness 30-50 nm have been received by a thermal oxidation of thin indium films, formed on the muscovite mica substrates by a DC magnetron sputtering method in the vacuum universal post VUP-5M [1].

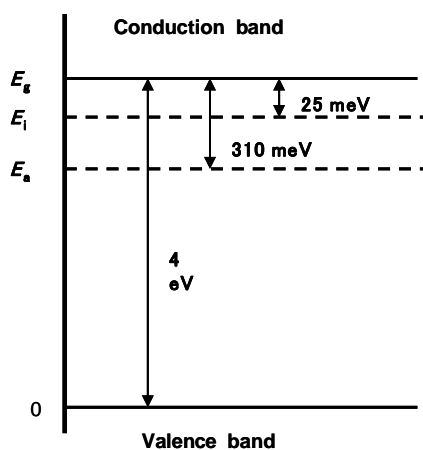


Fig. 1. Band structure of In_2O_3 in presence of adsorbed oxygen

In_2O_3 formation of films was established using the electron diffraction. The XPS-study of films with thickness 30-50 nm shows that these films contain oxygen in two forms: direct in crystalline lattice and as adsorbed molecules.

The DC conductivity of In_2O_3 films and the temperature dependences of conductivity in temperature range of 300-440 K were measured in a vacuum of 10^{-2} Pa with the aid of a V7E-42 electrometer. The investigation was performed by method of cyclic thermal desorption [2]. A family of the temperature dependences of conductivity corresponding to various concentrations of adsorbed oxygen on the same sample was measured.

The comparison of experimental data with theoretical modeling allows determining the isobar of oxygen in In_2O_3 films and numerical value E_a (310 meV) of adsorbed oxygen in gap of In_2O_3 film band structure (Fig. 1).

References

- [1] Luhn V., Zharsky I., Zukovski P., Acta Physica Polonica A, vol. 123 n. 5, 2013, pp. 837-839.
 [2] Pochtenny A., Misevich A., JTP Lett., vol. 29, 2003, p. 56

Authors Index

A	
Adlienė Diana	116
Akylbekov A.....	34
Aldabergenova T.....	73
Alontseva D.L.....	39
Andreev D.V.....	104, 106
Andreev Dmitrii V.....	103
Andreev Vladimir V.....	103
Ape P.....	85
Apel P.Y.....	110
Asgerov E.B.....	101
Ażgin J.....	42
B	
Barcz A.....	60
Barcz Adam.....	15
Barlak M.....	31, 120
Baydin A.....	24
Belov A.I.....	122, 123
Berencén Y.....	55, 69
Berencén Yonder.....	99
Bereznyak Yu.....	111
Bezdidko O.....	93
Billewicz P.....	74, 75, 128
Boguta A.....	102
Boiko O.....	76
Bondar O.V.....	97, 118, 121
Bondarenko G.G.....	78
Bondarenko Gennady G.....	103
Bondariiev V.....	79, 90
Borkovska L.....	51
Borovitskaya I.V.....	78
Böttger R.....	55, 69, 70
Bozhatkin Vitali.....	108
Budzyński P.....	16
Budzyński Piotr.....	115
C	
Celler G.K.....	60
Chartier Alain.....	21
Cheshko I.....	93, 94
Chmiel Jarosław.....	48
Cieślík I.....	80
Csík A.....	63
Czarnacka Karolina.....	57, 81
Czarnewicz S.....	80
D	
Dauletbekova A.....	34
Dauletbekova A.K.....	112
Degtyaryova V.P.....	113
Dorosh Orest.....	21
Dosbolayev M.K.....	82
Drenin A.S.....	107
Droździel A.....	51, 83
Droździel Andrzej.....	49, 124
Duchna M.....	80
Dudek Agata.....	48
Duk M.....	84, 89
E	
Erbe A.....	55
Evtukh A.A.....	18, 86
F	
Fedoriv V.D.....	87
Fedotov A.K.....	18, 76, 85, 86
Fedotov A.S.....	58, 85
Fedotov Aleksander K.....	81
Fedotova J.....	76
Fedotova J.A.....	18, 58
Fedotova Julia A.....	81
Fedotova V.V.....	86
Feldman L.C.....	24
Fortuna E.....	30
G	
Gaidar A.I.....	78
Gaiduk P.I.....	20
Galimov A.M.....	105
García-Hemme E.....	69
Garpul O.Z.....	87
Garpul O.Z.....	119
Georgiev Y.M.....	55
Glaser M.....	55
Gluba L.....	51
Gorshkov O.N.....	122
Griškonis Egidijus.....	116
Grudniewski T.....	74, 75
Grudziński W.....	51
Grudziński Wojciech.....	49
Gryaznov E.G.....	122
Guseinov D.V.....	122
H	
Haase Felix.....	23
Häberlein Sven.....	32
Heinemann B.....	32
Heller R.....	69
Helm M.....	55, 69, 70
Hlatshwayo T.....	109
Horodek P.....	26, 40, 88
Hubicki Z.....	43
Hübner R.....	55, 69
Huseynov E.....	67

Huseynov N. 67

I

Iatsunskiy I. 98
Ibraeva Anel 50
Ivanov I. 41
Ivlev G.D. 64
Ivlev Gennady..... 92

J

Jagielski Jacek 21
Jakięła R. 60
Janse van Vuuren A..... 28
Jozwik Iwona 21

K

Kalinin Yu.E. 18, 86
Kamiński M. 16
Kasiuk J.V. 58
Kerékgyártó R. 63
Khiem L.H. 66
Khilinov V. 26
Khrushch L.Z. 119
Kierczynski K. 98
Kirilkin N. 34
Kislitsin S. 41, 73
Kobets A. 26
Kobets A.G. 88
Kobzev A.P. 66, 101
Kociubiński A. 84, 89
Kolodynska D. 66
Kolomys O. 51
Koltunowicz T.N. 58, 86, 98
Kołodynska D. 101
Kołodynska D.E. 43
Kołtunowicz T.N. 18, 90, 91
Kołtunowicz Tomasz N. 57, 81
Komarov Alexander 92, 108
Komarov F.F. 22, 64, 96, 112
Komarov Fadei 57, 62, 92, 108, 115
Komsta H. 93, 94
Komsta Henryk 95
Konarski P. 31, 42
Konstantinov S.V. 22, 96
Korolev D.S. 122, 123
Kozubal M. 60
Kravchenko Ya.O. 97, 98
Krawczynska A. 30
Krügener Jan 23
Krzyżanowska Halina..... 24
Kuchinsky Peter 62
Kulevoi T.V. 106
Kulik M. 43, 45, 66, 67, 101
Kurovets V.V. 87
Kurpaska Ł. 80

L

Lagov P.B. 106, 107
Larionov A. 41
Lednev A.M. 107
Lee M.E. 44
Lenke T. 32
Lerch Wilfried..... 25
Levin M.N. 104
Li Xingji 99
Liu Chaoming 99
Lizak T. 84, 89
Lohvynov A. 94
Luchowski Rafał 49
Lugstein A. 55
Luhin V. 131
Luhin V.G. 91
Luhin Valery 95

Ł

Łatka L. 61

M

Maciążek D. 100
Madadzada Afag I. 101
Majcher J. 102
Makhavikou M.A. 112
Makhavikou Maksim..... 62
Makhavikou Maxim 57
Maksakova O.V. 98, 121
Malherbe J. 109
Małecka-Massalska T. 84, 89
Mamykin S. 51
Maruszczczyk Andrzej..... 48
Maslovsky V.M. 104, 105, 106, 107
Maslovsky Vladimir M. 103
Meshkov I. 26
Michalak M. 61
Mieszczynski Cyprian 21
Mikhailova A.B. 78
Mikhaylov A.N. 122, 123
Milchanin O.V. 112
Milchanin Oleg 62
Miskiewicz Siarhiej..... 92, 108
Miśnik M. 42
Mlambo M. 109
Möller W. 55
Moon S.W. 30
Muzyka K. 84, 89

N

Nagy Gy. 63
Najafov A. 67
Nebogatikova N.A. 45
Nechaev N.S. 64
Nechayev Nikita..... 92

Neethling J.H.	28
Neethling J.N.	112
Niess Jürgen	25
Nikolskaya A.A.	123
Nikulin V.Ya.	78
Njoroge E.	109
Novikov A.	85

O

O'Connell J.H.	44, 65
Odnodvoretz L.	79, 90
Odutemowo O.S.	109
Okulich E.V.	122
Okulich V.I.	122
Olejniczak A.	45, 67
Olejniczak K.	110
Olivier E.J.	28
Opielak M.	93, 94, 111
Orlov O.	26
Osten H.-J.	23

P

Paramonova V.V.	78
Parkhomenko I.N.	64, 112
Parkhomenko Irina	57, 62
Partyka J.	113, 114
Pasierbiewicz K.	127
Pavlov D.A.	123
Pavlov Yu.S.	107
Pazukha I.	129
Pągowska K.	60
Peibst Robby	23
Pelc Andrzej	46
Peregudova E.N.	78
Petterson P.	30
Phuc T.V.	66
Pieńkos Tomasz	46
Pietraszek J.	128
Pilko V.V.	22
Pilko Vladimir	115
Piotrowska K.	97
Plaipaité-Nalivaiko Rita	116
Pochtenny A.	131
Poduremne D.	111
Pogrebnyak A.D.	22, 97, 98, 118, 121
Poltavtseva V.P.	113, 114
Poplavsky V.V.	91
Postawa Z.	100
Predecka M.	84, 89
Prishchepenko Dmitry	95
Prokopchuk Nikolay	95
Protsenko I.	79, 111
Protsenko S.	90, 93, 94, 129
Prucnal S.	55, 69, 83

Prucnal Sławomir	29
Prucnal Sławomir	124
Przewłocki H.M.	43
Pylypiv V.M.	119
Pyszniak K.	16, 43, 67, 83
Pyszniak Krzysztof	49, 124

R

Raiymkhanov Zh.	82
Rajta I.	63
Ramazanov T.S.	82
Ratajczak J.	60
Rebohle L.	32, 69
Rebohle R.	55
Rogalski Przemysław	130
Rogovsky E.S.	107
Romanov I.A.	64
Romanov Ivan	62
Ronassi Ali Arash	58, 86
Rubel M.	30
Rücker H.	32
Rusak D.	58

S

Sadowski J.	51
Samadov O.	67
Samadov S.	67
Sartowska B.	31, 120
Satpaev D.A.	113, 114
Scheit A.	32
Schneider H.	69
Schönherr T.	55
Schumann T.	32
Seitbayev A.	34
Shabelnyk Yu.	111
Shashok Zhanna	95
Shikanov S.	131
Shuisky R.A.	122
Shuliarenko D.	129
Shumakova M.	90
Shumakova N.	79
Shvetsov V.N.	33
Sidorin A.A.	26
Siemek K.	26, 88
Silin P.V.	78
Sitek R.	80
Sitnikov A.V.	86
Skorupa W.	32, 55, 69
Skryleva E.A.	107
Skuratov V.A.	34, 44, 45, 65, 88, 112
Skuratov Vladimir	50
Słowiński B.	47
Smolik J.	120
Sokołowski P.	61

Starosta W.	120
Stepanov A.V.....	122
Stolyarov Alexander A.	103
Streltsov E.A.....	18
Sushkov A.A.....	123
Svito I.....	85
Swic A.....	93, 94
Szala M.....	61
Szala Mirosław	48
Szypulski M.....	84, 89

Ś

Świć A.....	121
-------------	-----

T

Takeda Y.	118
Tan Yang.....	35
Tataryn N.....	51
Taube A.....	60
Tazhen A.B.....	82
Tetelbaum D.I.....	122, 123
Teterev Yu.G.	34
Thomé Lionel.....	21
Tkach O.....	90
Tolk N.H.....	24
Tooski Sahib Babae.....	68
Turek M.....	51, 66, 83
Turek Marcin	49, 124, 125, 126
Tyschenko K.....	79

U

Utegenov A.U.	82
--------------------	----

V

Vlasukova L.A.	64, 112
Vlasukova Ludmila.....	62
Volkov A.N.	106
Volobuev V.....	131
Vuuren A. Janse.....	112
Vuuren Arno Janse.....	50

W

Walczak M.....	127
Walczak Mariusz	48
Waliś L.	120
Wang M.....	55
Wang Mao	69, 70, 99
Wendler E.....	64, 109
Wendler Elke	62, 92
Węgierek P.	74, 75, 128
Węgierek Paweł	124
Widdowson A.	30
Wieleba W.	73
Wiertel M.	16
Wojciechowski T.	60
Wolansky D.	32

X

Xu Chi	69, 70
--------------	--------

Y

Yang Jianqun	99
Yaremiy S.I.....	87
Yastrubchak O.....	51
Yuan Y.....	55
Yuan Ye.....	69, 70
Yurasov D.....	85
Yuschkevich Yuriy.....	124
Yuvchenko V.N.....	112
Yuvchenko Vera.....	108

Z

Zarzeczny D.....	84, 89
Zawada A.....	42
Zayats Galina	92, 108
Zdorovets M.....	34, 41
Zdorovets Maxim	50
Zebrev G.I.....	105
Zhou S.	55
Zhou Shengqiang.....	69, 70, 99
Zimek Z.	36
Zukowski P.	58, 85, 86, 98, 118

Ż

Żuk J.....	43, 51, 66, 83, 112
Żuk Jerzy	62, 124
Żukowski P.	18, 129, 131
Żukowski Paweł	130

